2-AMINO-1, 3-PROPANEDIOL AS A BIOGLYCEROL-DERIVED SOLVENT FOR CO_2 CAPTURE

NURUL FATIN NABILAH BINTI ABDUL SAMAT

FACULTY OF ENGINEERING
UNIVERSITY OF MALAYA
KUALA LUMPUR

2019

2-AMINO-1, 3-PROPANEDIOL AS A BIOGLYCEROL-DERIVED SOLVENT FOR CO_2 CAPTURE

NURUL FATIN NABILAH BINTI ABDUL SAMAT

DISSERTATION SUBMITTED IN FULFILMENT OF THE REQUIREMENTS FOR THE DEGREE OF MASTER OF ENGINEERING SCIENCE

FACULTY OF ENGINEERING
UNIVERSITY OF MALAYA
KUALA LUMPUR

2019

UNIVERSITY OF MALAYA

ORIGINAL LITERARY WORK DECLARATION

Name of Candidate: **NURUL FATIN NABILAH BINTI ABDUL SAMAT**

Matric No: **KGA140071**

Name of Degree: **MASTER OF ENGINEERING SCIENCE**

Title of Project Paper/Research Report/Dissertation/Thesis ("this Work"):

2-AMINO-1, 3-PROPANEDIOL AS A BIOGLYCEROL-DERIVED SOLVENT FOR CO_2 CAPTURE

Field of Study: **PURIFICATION AND SEPARATION PROCESSES**

I do solemnly and sincerely declare that:

(1) I am the sole author/writer of this Work;
(2) This Work is original;
(3) Any use of any work in which copyright exists was done by way of fair dealing and for permitted purposes and any excerpt or extract from, or reference to or reproduction of any copyright work has been disclosed expressly and sufficiently and the title of the Work and its authorship have been acknowledged in this Work;
(4) I do not have any actual knowledge nor do I ought reasonably to know that the making of this work constitutes an infringement of any copyright work;
(5) I hereby assign all and every rights in the copyright to this Work to the University of Malaya ("UM"), who henceforth shall be owner of the copyright in this Work and that any reproduction or use in any form or by any means whatsoever is prohibited without the written consent of UM having been first had and obtained;
(6) I am fully aware that if in the course of making this Work I have infringed any copyright whether intentionally or otherwise, I may be subject to legal action or any other action as may be determined by UM.

Candidate's Signature Date:

Subscribed and solemnly declared before,

Witness's Signature Date:

Name:

Designation:

2-AMINO-1, 3-PROPANEDIOL AS A BIOGLYCEROL-DERIVED SOLVENT FOR CO_2 CAPTURE

ABSTRACT

In this work, aqueous 2-amino-1, 3-propanediol solution (serinol) was investigated as a potential solvent for CO_2 capture. For this purpose, the solubility of CO_2 in serinol were carried out at various concentration, pressure and temperature. Prior to CO_2 solubility experiments, qualitative prediction using COSMO-RS approach based on quantum chemistry calculation was performed on serinol to confirm its potentiality as CO_2 capture solvent. Based on this approach, serinol shows good affinity towards hydrogen –bond donors which is beneficial to develop intermolecular interaction between serinol and CO_2. The solubility of CO_2 in serinol were conducted at serinol molar concentration ranging from 1M to 3M, temperature ranging from 313.15 K to 353.15 K and CO_2 pressures ranging from 1034.31 kPa to 2068.43 kPa. The solubility of CO_2 achieved the highest value of 1.64 mol of CO_2/mol of serinol in 1M serinol solution at 313.15 K and 2068.43kPa. The physical properties (densities and viscosities) of serinol at various concentration (1 - 3M), and temperature (298.15 - 333.15 K) were also conducted at atmospheric pressure. The results showed that the density and viscosity of serinol increase with increase in concentration and decrease in temperature. In addition, Henry's law constants of CO_2 in serinol were calculated using N_2O analogy due to the chemical reaction between the amine group in serinol and CO_2. Henry's law constant were measured at temperature 313.15 K and 333.15 K for molar concentration 1M and 3M of serinol. The physical solubility of serinol increases as the temperature and the concentration of solution decreases. A 599.4 kPa.m^3/kmol was the lowest Henry's law constant of CO_2 for 1M of serinol at temperature of 313.15 K. Furthermore, the recyclability of 3M of serinol was carried out to investigate the stability of the solvent. The regeneration experiment was conducted at temperature of 313.15 K and partial

pressure ranging from 1034.31 kPa to 2068.43 kPa. The maximum decreases of the regeneration efficiency after three regeneration cycles is 41.41%.

Keywords: bioglycerol, serinol, COSMO-RS, CO_2 capture, regeneration.

2-AMINO-1, 3-PROPANEDIOL SEBAGAI PELARUT DARIPADA BIOGLISEROL UNTUK PENANGKAPAN CO_2

ABSTRAK

Kajian telah dijalankan ke atas larutan akuas 2-amino-1, 3-propanediol (serinol) sebagai pelarut yang berpotensi untuk menangkap CO_2. Untuk tujuan ini, kelarutan CO_2 dalam serinol telah dijalankan pada pelbagai kadar kepekatan, tekanan dan suhu. Sebelum kajian tentang kelarutan CO_2, ramalan kualitatif menggunakan pendekatan COSMO-RS yang berdasarkan pengiraan kuantum kimia telah dilakukan pada serinol untuk memastikan potentisinya sebagai pelarut untuk menangkap CO_2. Berdasarkan pendekatan ini, serinol mempunyai kedorongan yang baik terhadap ikatan hidrogen penderma yang bermanfaat untuk membina interaksi intermolekul di antara serinol dan CO_2. Kelarutan CO_2 dalam serinol telah dijalankan pada kepekatan serinol dari 1M hingga 3M, suhu dari 313.15 K hingga 353.15 K dan tekanan CO_2 dari 1034.31 kPa to 2068.43 kPa. Kelarutan CO_2 telah mencapai nilai tertinggi 1.64 mol CO_2/mol serinol dalam 1M serinol pada 313.15 K dan 2068.43 kPa. Ciri-ciri fizikal (ketumpatan dan kelikatan) untuk serinol juga telah dijalankan pada pelbagai kadar kepekatan (1-3M) dan suhu (298.15 -333.15 K) pada tekanan atmosfera. Hasil kajian menunjukkan ketumpatan dan kelikatan serinol meningkat apabila kadar kepekatan meningkat dan suhu menurun. Di samping itu, pemalar undang-undang Henry untuk CO_2 dalam serinol dikira dengan menggunakan analogi N_2O disebabkan reaksi kimia antara kumpulan amina dalam serinol dan CO_2. Pemalar undang-undang Henry diukur pada suhu 313.15 K dan 333.15K untuk kepekatan 1M dan 3M serinol. Kelarutan fizikal dalam serinol meningkat apabila suhu dan kepekatan larutan menurun. 599.4 kPa.m^3/kmol ialah nilai terendah pemalar undang- undang Henry untuk CO_2 dalam 1M serinol pada suhu 313.15 K. Selain itu, kajian penggunaan semula 3M serinol telah dijalankan untuk menyiasat kestabilan pelarut. Kajian penggunaan semula telah dilakukan pada suhu 313.15 K dan tekanan

separa dari 1034.31 kPa hingga 2068.43 kPa. Pengurangan maksimum sebanyak 41.41% selepas 3 kitaran penggunaan semula.

Kata kunci: biogliserol, serinol, COSMO-RS, penyerapan CO_2, penggunaan semula.

ACKNOWLEDGEMENTS

Foremost, I thank to Allah the Mighty for the wisdom he granted upon me, the determination, good health and strength to complete my studies at master level.

I would like to express my special gratitude to my supervisors, Assoc. Prof. Ir Dr. Rozita Binti Yusoff and Prof. Mohamed Kheireddine Aroua for their continuous support, great motivation, inspiration, guidance and patience.

Special thanks to my beloved parents, Abdul Samat bin Sungot and Khadijah binti Selamat, my siblings, Nurul Hidayah and Nur Syafiqah and my best friends, Nur Ain Amirah and Mira Edora who are always encourage me through thick or thin along this journey.

I thank my fellow thermodynamic labmates: Nurul Ain Ramli, Mohd Azlan Kassim, Hawaiah Maarof, Mook Tze Wei, Farihah Husna, Pei San and Mahsa for sharing their knowledge and cooperative response to all the question related to this research. In addition, I would like to thank to all staff of Department of Chemical Engineering especially Cik Fazizah, Encik Jalaluddin and Encik Kamaruddin who help me in making the research run smoothly.

TABLE OF CONTENTS

LIST OF FIGURES

LIST OF TABLES

LIST OF ABBREVIATIONS

CO_2	Carbon dioxide
CCS	Carbon capture and storage
AMP	2-amino-2-methyl -1-propanol
MeOH	Methanol
MEA	Monoethanolamine
O_2	Oxygen
SO_X	Sulfur oxides
NO_X	Nitrogen oxides
COSMO-RS	COnductor like Screening MOdel in combination with Real Solvent
ppm	Part per million
IPCC	Intergovernmental Panel on Climate Change
WBCSD	World Business Council for Sustainable Development
IEA	International Energy Agency
WRI	World Resources Institute
SO_2	Sulfur dioxide
NO_2	Nitrogen dioxide
DFT	Density functional theory
H_2S	Hydrogen Sulfide
VSA	Vacuum swing adsorption
PEBA	Poly (ether blockamide)
PSF	Polysulfone
IGCC	Integrated Gasification Combined Cycle
DEA	Diethanolamine

MDEA	Methyl ethanolamine
DETA	Diethylenetriamine
DEPG	Dimethyl Ether of Polyethylene Glycol
PC	Propylene Carbonate
NGCC	Natural Gas Combined Cycle
EPA	Environmental Protection Agency
QM	Quantum chemical method
vdW	Van der Waals
BP/TZVP	Becke-Perdew /Triple zeta valence potential
HOMO-LUMO	Highest occupied and lowest unoccupied molecular orbital
HB	Hydrogen bond
HSS	Heat stable salts
[bmim][Ac]	1-butyl-3-methylimidazolium acetate
[emim][TF_2N]	1-ethyl-3-methylimidazolium bis[(trifluoromethyl)sulfonyl]imide
[bmim][TF_2N]	1-butyl-3-methylimidazolium bis[(trifluoromethyl)sulfonyl]imide
[emim][Ac]	1-ethyl-3-methylimidazolium acetate
[bmim][BF_4]	1-butyl-3-methylimidazolium tetrafluoroborate
[bmim][DCA]	1-butyl-3-methylimidazolium dicyanamide
[bmim][PF_6]	1-butyl-3-methylimidazolium hexafluorophosphate

LIST OF SYMBOLS

E_{misfit}	electrostatic misfit energy(kJ/mol/A^2)
E_{hb}	hydrogen bond interaction(kJ/mol/A^2)
E_{vdw}	van der Waals interaction(kJ/mol/A^2)
α_{eff}	effective contact area(A^2)
σ, σ'	Polarization charge density
σ_{hb}	polarization charge density threshold for hydrogen bond (e/A^2)
c_{hb}	strength of hydrogen bond (kJ/mol/A^2)
α'	Interaction parameter (kJ/mol/A^2)
$\sigma_{acceptor}$	Polarization charge density acceptor(kJ/mol/A^2)
σ_{donor}	Polarization charge density donor(kJ/mol/A^2)
τ_{vdw} , τ'_{vdw}	element- specific van der Walls parameter(kJ/mol/A^2)
$p_s(\sigma)$	σ-profile
$\mu_s(\sigma)$	Chemical potential of a surface segment(kcal/mol A^2)
α	CO_2 loading in mol of CO_2/total mol of absorbent(mol/mol)
χ	CO_2 loading in mol of CO_2/ total mass of absorbent(mol/kg)
P_T	total pressure(kPa)
P_V	vapor pressure(kPa)
V_{gc}	volume of gas container(L)
V_{sol}	volume of solution(L)
V_{cell}	volume of cell(L)
i	initial condition
f	final condition
n_{total}	total moles of absorbent in the liquid phase (mol)
mt_{otal}	total mass of absorbent in the liquid phase (kg)

R	Gas constant, 8.314 (kPa. L / mol. K)
T	Temperature (K)
M	Molarity (mol/L)
K	Kelvin
kg	Kilogram
MPa	Megapascal
kPa	Kilopascal
ρ	Density (g/cm^3)
$H_{N2O,solution}$	Henry's law constant of N_2O in the aqueous amine
$H_{CO2,solution}$	Henry's law constant of CO_2 in the aqueous amine
$H_{N2O,water}$	Henry's law constant of N_2O in water
$H_{CO2,water}$	Henry's law constant of CO_2 in water
μ	Viscosity (mPa.s)
μ_∞	Viscosity at infinite temperature (mPa.s)
Ea	Activation energy (kJ/mol)
η	Regeneration efficiency (%)

LIST OF APPENDICES

CHAPTER 1: INTRODUCTION

1.1 Background

Increasing anthropogenic emissions of greenhouse gases to the atmosphere may cause climate change and harmful towards the health of human being as they can worsen the condition of respiratory disease which might then cause cancer. About 21% of global greenhouse gas emissions from industry sector and 25% from electricity and heat production. Industry sector involve fossil fuels fired power plants as they release flue gas stream containing CO_2 to the atmosphere, thus contribute to the continuous increase in the atmospheric concentration of CO_2 (Gielen, Moriguchi, & Yagita, 2002; Torralba-Calleja, Skinner, & Gutiérrez-Tauste, 2013). Without main policy or technology changes, future concentrations of CO_2 will increase. As a result, any major emission reduction involves also an emission reduction of the industry. Nevertheless the reduction of industrial CO_2 emissions is a challenging task.

There are three main process of capturing CO_2 which are, (1) post-combustion: CO_2 is separated from the flue gases using a liquid solvent; (2) pre-combustion: fuel is pretreated and converted into a mix of hydrogen and CO_2 and (3) oxyfuel combustion: the fuel is combusted using oxygen which produced the flue stream of water vapor and CO_2 (Durmaz, 2018). Post-combustion capture is the most mature technology as compared to other processes of CO_2 capture (Figueroa, Fout, Plasynski, McIlvried, & Srivastava, 2008). The most commonly used solvent for post-combustion of CO_2 capture with chemical absorption is monoethanolamine (MEA). MEA has the greatest attention scientifically and commercially (Chong, Eljack, Atilhan, Foo, & Chemmangattuvalappil, 2014). This is due to MEA has a low molecular weight, low solvent cost, low rate of thermal degradation and high reactivity (McCann, Maeder, & Attalla, 2008). This solvent has proven to be able to remove CO_2 from some of gas mixture such as natural gas, synthesis gas and refinery streams as it remained the benchmark for current industrial

standard solvent due to its fast reaction with CO_2 and simplicity of operation (Rivera-Tinoco & Bouallou, 2010). Nonetheless several problems exist such as degradation of MEA in the presence of O_2, SO_2 and NO_2 whereas limitation of concentration to ~30% w/w in the absence of corrosion inhibitors (Aroonwilas & Veawab, 2004; Conway et al., 2015).

CO_2 emission is a worldwide problem to be solved. Fast development of world biodiesel industry has brought about an oversupply of bioglycerol. This turn into a weight until new markets are made for bioglycerol by the improvement of new products. Studies have demonstrated that some high value chemicals could be created by utilizing bioglycerol as crude material such as lactic acid, dihydroxyacetone, ethanol and citric acid. Thus, it is a mandatory to find innovative and flexible ways to utilize the bioglycerol and simultaneously reduce the CO_2 emission. One possibility is to transform bioglycerol into bioglycerol-based solvent with addition of amine group. It is a great opportunity to make this transformation as it is able to capture CO_2 with the presence of amine group and can be one of the alternative uses for glycerol.

1.2 Problem statement and significant of study

CO_2 capture by chemical absorption using aqueous alkanolamines is a well-developed system practice. The prominent aqueous alkanolamines which are employed in processes of industry are monoethanolamine (MEA), diethanolamine (DEA) and methyl ethanolamine (MDEA). However, these solvents have environmental and economic disadvantages such as corrosive solvents which need special and expensive construction materials therefore increased capital costs, likely to degrade under high temperature particularly in the process of regeneration and solvent loss through process of evaporation (Kothandaraman, 2010).

Besides, the remarkable increased for clean chemicals from renewable resources has directed towards comprehensive research to grow industrial applications of biomass.

Bioglycerol is a very favorable cheap raw material for manufacturing a range of value-added chemicals. Even though there are various creation of new chemical products using bioglycerol as a feedstock, there are less publish work discussing on the implementation of bioglycerol-derived solvent to capture CO_2. The transformation of bioglycerol into chemical solvents to capture CO_2 will help in reducing the atmospheric concentration of CO_2 which consequently avoid environmental problems and health hazards. Other than this, the economical utilization of bioglycerol is one of the key challenging issues for sustainability biodiesel industry.

The efficiency of CO_2 capture solvents greatly depends on the performance of the solvent. However, it is impractical to conduct preliminary experiments to evaluate suitable products of bioglycerol which are able to capture CO_2 due to time consuming and high cost consumption. Thus, a method of prediction is compulsory to evaluate bioglycerol-based solvent. On top of that, density and viscosity of bioglycerol-based solvent are also important to provide a full characterization of solvent in designing treatment equipment. Therefore, the thermophysical properties of potential solvent are also obtained.

1.3 Research objectives

This research aims to systematically evaluate aqueous serinol as a potential solvent to capture CO_2. Serinol is one of the bioglycerol-based solvents to be used in CO_2 absorption towards the utilization the bioglycerol and simultaneously reduce the CO_2 emission. Thus, to achieve this aim, the objectives of this research are as follows.

i. To evaluate aqueous serinol as a potential solvent to capture CO_2 using COSMO-RS.
ii. To investigate the CO_2 absorption of aqueous serinol at different concentrations and temperatures particularly at high pressure.

iii. To determine the densities and viscosities of aqueous serinol at different concentrations and temperatures.

iv. To determine Henry's law constant of CO_2 in aqueous serinol solutions.

v. To evaluate the reusability of aqueous serinol for CO_2 absorption.

1.4 Outline of the thesis

This thesis comprises of the following main chapters:

Chapter 1 includes a brief introduction to the related research, problem statements to justify this work and research objectives.

Chapter 2 encompasses of a review on CO_2 absorption process including carbon capture technologies and process chemistry. A broad literature review on biodiesel and bioglycerol were also summarized. In addition, the applications of COSMO-RS are reported in this chapter. The thermo physical properties such as viscosity and density were also discussed. The regeneration of alkanolamines and Henry's law constant were also detailed.

Chapter 3 demonstrates details of the materials, experimental setup and method used for the experiments.

Chapter 4 discusses the results of this thesis as follows:

i. COSMO-RS

This sub-chapter reports on qualitative prediction of serinol, MDEA, water and CO_2 using σ – profiles and σ – potentials generated by the COSMO-RS model.

ii. CO_2 absorption at high pressure

This sub-chapter reports on the experimental data of CO_2 solubility of aqueous serinol at concentrations ranging from 1M to 3M, temperatures ranging from 313.15 K to 353.15 K and CO_2 partial pressures ranging from 1034.31 kPa to 2068.43 kPa.

iii. Thermo physical properties

This sub-chapter discusses on the density and viscosity of aqueous serinol at temperatures ranging from 298.15 K to 333.15 K and concentrations ranging from 1M to 3M at constant atmospheric pressure.

iv. Physical solubility of N_2O and CO_2

This sub-chapter discusses on physical solubility and Henry's law constants of N_2O and CO_2 in aqueous serinol at 313.15 K and 333.15 K for molar concentration of 1M and 3M of aqueous serinol.

v. Regeneration of CO_2 absorption

This sub-chapter reports on three regeneration cycle and regeneration efficiency of 3M aqueous serinol from CO_2 partial pressure range 1034.31kPa to 2068.43 kPa at temperature 313.15 K.

Chapter 5 concludes all the findings of this research work and also the recommendations for future work.

CHAPTER 2: LITERATURE REVIEW

2.1 Anthropogenic emission of carbon dioxide

Numbers of engineering studies have been committed to control greenhouse gas emissions which became the number one contributor of the global warming scenario. Greenhouse gases are those that captivate and release infrared radiation within the range of wavelength emitted by Earth (Cleary, Roulet, & Moore, 2005). CO_2 is a significant contributor among these greenhouse gases to increase in the average global earth temperature, environmental and humanitarian concerns such as flooding, shortage of food, acid rain and health problem (Bernard, Samet, Grambsch, Ebi, & Romieu, 2001). Arrhenius was first proposed the existence of the greenhouse effect in 1896. Based on his hypothesis, specific gases in the atmosphere of the earth which are CO_2, methane, ozone, dinitrogen oxide and halogenated hydrocarbons permit the transmission of the sun radiation reflected by the earth surface. This natural greenhouse effect is useful but where it is too strong, this warming might lead to a nun-sustainable development of the earth (Kessel, 2000).

Cement production, steel production and fossil fuel fired power plants release flue gas stream containing CO_2 to the atmosphere, thus contribute to the continuous increased in the atmospheric concentration of CO_2. The gases emission by these human activity creates the so-called anthropogenic greenhouse effect (Lin & Lei, 2015; Maul, Metcalfe, Pearce, Savage, & West, 2007; Notz, Tonnies, McCann, Scheffknecht, & Hasse, 2011). Ludwig et al. reported the cement production contributes 5% of the global CO_2 emission which is 0.95 tons of CO_2 per ton of Portland cement (Ludwig & Zhang, 2015). Purification of fuel gas streams is needed in oil and gas industries and these processes generate streams of CO_2 that generally vented to the atmosphere (Meerman et al., 2012). The huge emission amount of CO_2 contributes more than 60% to global warming. The concentration of atmospheric CO_2 has increased vigorously from 280 ppm in 1750 to 367 ppm in 2005.

The CO_2 abundance in the atmosphere increased substantially during this period as the average rate of CO_2 increased is measured by direct instrumental measurements over the year of 1960 to 2005 is 1.4 ppm per year (P. Luis, Van Gerven, & Van der Bruggen, 2012).

In order to avoid the global average temperature rise of 2 – 2.5℃ by the year 2050, the United Nations Intergovernmental Panel on Climate Change (IPCC) which is the most authoritative body on the subject of climate change claims that the requirement of reduction by 50% of current carbon dioxide emissions (Andirova, Cogswell, Lei, & Choi, 2016). IPCC has developed strategies for creating emission portfolios for the six major greenhouse gases (Leung & Lee, 2000). World Business Council for Sustainable Development (WBCSD) and World Resources Institute (WRI) gives guidance and a standard for organizations regarding how to classify, measure and report greenhouse gas emissions (Supekar & Skerlos, 2014). International agreements and policies has been implemented to decrease CO_2 emissions. China, United States and India are the countries that have been targeted in discussion concerning efforts to curb CO_2 emission (Levitt, Pedersen, & Sorensen, 2015).

The Kyoto protocol of 1997 sets emission target of total CO_2 emission for a country beyond the year 2000 (Centi, Perathoner, & Rak, 2003). In 2005, the Greenhouse Gas Emission Trading Act was established which implying a system of quota for greenhouse gases like CO_2. There are three key policy instruments to reduce the CO_2 emission in Norway, which are the Pollution Control Act in 1981, the CO_2 Tax Act in 1990 and the Green Gas Emission Trading Act in 2004. Besides, Norway implemented the EU's Emission Trading Directive in the Greenhouse Gas Emission Trading Act in 2009 (Norstebo, Midthun, & Bjorkvoll, 2012). Hence, an urgent need for the worldwide

implementation technologies to reduce greenhouse gas emissions is an evidence of the international community's growing awareness on climate changed.

Besides, CO_2 is one of the major contaminants present in natural gas. In the presence of water, CO_2 becomes acidic, which has the capability to corrode the equipment and pipelines. Moreover, Liquefied Natural Gas (LNG) is considered to be an alternative option for the transportation of natural gas. In the process of cooling the natural gas to a very low temperature, the CO_2 will freeze and block the pipeline. This will cause disadvantage for transportation (Rufford et al., 2012). In addition, attention has been given to the production and purification of biogas as a renewable fuel. In order to produce methane-rich biogas, CO_2 must be removed from the mixture of gas. In terms of combustion, CO_2 is an inert gas. The presence of CO_2 in biogas decreased its heating value (Ravagnani, Ligero, & Suslick, 2009). Therefore, the removal of CO_2 from biogas and natural gas through processes of purification is important to improve the quality of the product.

2.2 Carbon capture technology

Two major approaches have been implemented as CO_2 separation technology, which are carbon capture and storage (CCS) and the sustainable utilization of captured CO_2 as a raw material (Kamimura, Shimomura, & Endo, 2014). The second option will play an important role within the next decade as CO_2 is a non-toxic, cheap, thermodynamically and kinetically stable, easily available and renewable carbon resource which can be transformed into a variety of chemical products (L. Li, Zhao, Wei, & Sun, 2013).The utilization of CO_2 as a raw material in the synthesis of chemicals including synthesis of dimethyl carbonate from CO_2 and methanol, hydrogenation of CO_2 to methanol, synthesis of cyclic carbonate from CO_2 and epoxide and producing synthesis gas as one of the vital feedstock in the industry of chemical (Choi, Park, Han, & Yoon, 2008; Ma et al., 2009;

Patil, Tambade, Jagtap, & Bhanage, 2010; Wambach, Baiker, & Wokaun, 1999). However only small amount of CO_2 can be fixed for utilization method and the typical lifetime of the CO_2 currently used in chemical applications is only days to months (B. Y. Li, Duan, Luebke, & Morreale, 2013). So, reformation of the current setup of chemicals and fundamental research of new CO_2 reactions to synthesize value-added chemicals are necessary.

CCS is a technology focusing at separating, transporting and storing CO_2 underground to prevent its emission into the atmosphere. CCS can be applied to both industrial production and generation of power. Particularly, when replacement of material or process is not economically or technically feasible for the sector of industry, CCS is the merely technology capable to reduce carbon emissions (Budinis, Krevor, Dowell, Brandon, & Hawkes, 2018). In both the pre-combustion and post-combustion, the rates of carbon captured can achieved up to 85 – 95% (Durmaz, 2018). The International Energy Agency (IEA) emphasized that CCS will contribute to 14% of the accumulated reduction in emission of CO_2 by 2060 in the 2℃ scenario and 32% of the reduction in the beyond 2℃ scenario by 2060. Furthermore, IPCC also affirmed that the cost to achieve the atmospheric concentration of 450 ppm CO_2 equivalent by 2100 might be 138% more costly without the technology of CCS (Fan, Xu, Li, Yang, & Zhang, 2018).

For these justifications, there are a number of technologies to capture CO_2 which are post- combustion capture, pre-combustion capture and oxyfuel combustion as illustrated in Figure 2.1.The characteristics of all the three processes are different and yield different conditions for CO_2 capture (Mores, Rodriguez, Scenna, & Mussati, 2012). Table 2.1 discusses the advantages and disadvantages of these three CO_2 capture technologies. Each of the proposed method will be reviewed in order to compare their mechanism and difficulties that might be faced if it were to be implement at an industrial scale.

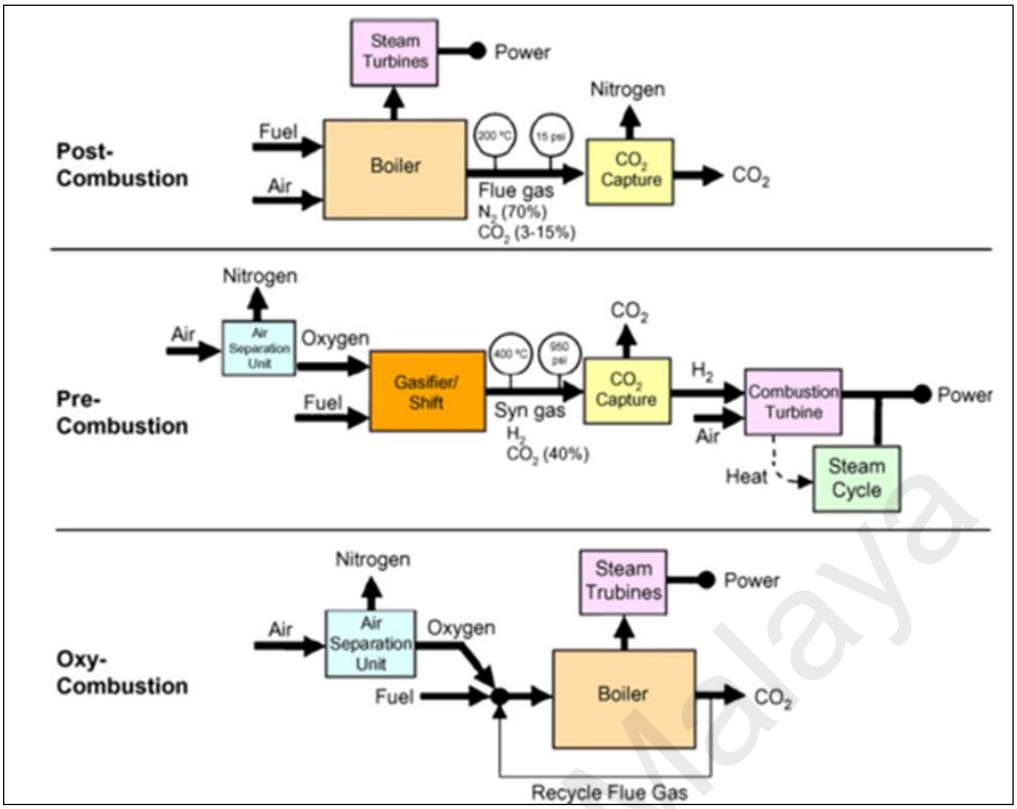

Figure 2.1: Diagram of post- combustion capture, pre-combustion capture and oxyfuel combustion (Figueroa et al., 2008)

Table 2.1: The advantages and disadvantages of pre-combustion, oxyfuel combustion and post-combustion (Ramdin, de Loos, & Vlugt, 2012)

Technology	Advantages	Disadvantages
Pre-combustion	• High concentrated CO_2 present in the synthesis gas. • Suitable for high pressure system. • Lower water consumption	• Applicable mainly to new plants, a few gasification plants are currently in operation • High cost of equipment
Oxyfuel combustion	• High CO_2 concentration in flue gas • Retrofit and repowering technology option	• High cryogenic O_2 production requirement may be cost prohibitive.
Post-combustion	• Applicable to the majority of existing coal-fired power plants • Retrofit technology option	• Low CO_2 partial pressure due to low concentration of CO_2 present in flue gas (at ambient pressure)

2.2.1 Pre-combustion capture

Pre-combustion is a process of converting the fuel into mixture of CO_2 and hydrogen at high pressure which CO_2 can be removed (Feron, 2010). The tendency for high efficiency conversion of energy is marked to be highest for the route of the pre-combustion capture. This is due to the energy contained in the intermediate product of hydrogen can be converted into electricity at high efficiency by using present technology which is gas turbine combined cycle (Jansen, Gazzani, Manzolini, Dijk, & Carbo, 2015). The pre-combustion capture is suitable for process stream that operated at high temperature within 200 to 400℃, elevated pressure within 2-7 MPa and higher concentration of CO_2 which is 15-60% by dry volume basis. This technology is promising for future high efficiency power stations with integrated CO_2 capture but the technology is not well explored (Olajire, 2010). An important advantage is the higher concentration of CO_2 and pressure achieved in the output stream, lower water consumption and generation of hydrogen gas which can be used as alternative fuel while the main disadvantage is the high costs of investments and high auxiliary system requirement by Integrated Gasification Combined Cycle (IGCC) technology (Pires, Martins, Alvim-Ferraz, & Simoes, 2011).

Pre-combustion CO_2 capture process starts with gasification of fuel in order to produce syngas enriched with hydrogen and carbon monoxide. Syngas is processed in water gas shift reformer after removing particulate by cyclone separation unit. In here, carbon monoxide reacts with steam to produce hydrogen and carbon dioxide and sent for desulphurization and separation of CO_2. The carbon capture system generates hydrogen fuel stream for many power generation applications such as fuel cell and gas turbine with minimum generation of sulphur dioxide. This will increase the value of fuel by reduction of carbon content. CO_2 separation unit led by water gas shift and autothermal reforming in natural gas power plant (Romano, Chiesa, & Lozza, 2010).

2.2.2 Oxyfuel combustion capture

During oxyfuel combustion, pure oxygen as the oxidant instead of air. The flue gas is mainly consist of highly concentrated CO_2 and steam. The process combustion is carried out in the presence of oxygen to mitigate the dilution of the flue gases due to nitrogen. Oxyfuel combustion is also called as the O_2/CO_2 combustion. There are many advantages of the oxyfuel combustion such as the CO_2 concentrations can achieve up to 95% in the dry flue gas, the volume of flue gas can be reduced, lesser gas energy loss and reduce amount of NO_x and SO_x. However the necessity for pure oxygen is its major challenge and constraint. Significant decreased in the oxygen production cost is an important prerequisite in order to make the power plant of oxyfuel combustion a possible future option as CO_2 capture becomes an essential (Z. S. Li, Zhang, & Cai, 2008).

Scheffknecht et al. provided a comprehensive overview on the oxyfuel coal combustion process primarily concentrating on pulverized coal combustion and its related development and research (Scheffknecht, Al-Makhadmeh, Schnell, & Maier, 2011). The oxyfuel combustion technology is expected to undergo development towards commercialization. Wall and Yu reported an overview of the oxyfuel CCS technology, including the most recent demonstration project and developments in pilot plants worldwide. Park et al., Zanganeh and Shafeen, Amato et al. and Wang et al. investigated the use of oxyfuel combustion technology are one of the near-zero emission clean coal technologies (Amato et al., 2011; Park et al., 2007; Wang, Zhang, Liu, & Che, 2012; Zanganeh & Shafeen, 2007). It provides an elegant approach to CO_2 capture as both cost effective and practical to implement for large-scale oxyfired coal power plants by integrating oxyfuel system components and the overall process of operating conditions are optimized.

2.2.3 Post-combustion capture

Post-combustion capture is a CO_2 capture from flue gas as the flue gas flow from the power generation step. Post combustion capture is the most reported method for CO_2 capture in the literature (Schreiber, Zapp, & Kuckshinrichs, 2009). It has the greatest near-term potential to reduce greenhouse gas emissions. Post –combustion technology is able to capture low concentration of CO_2 from 3% to 15% from flue gas and produce 99% of CO_2 stream for the next industrial processes (Abu-Zahra, Abbas, Singh, & Feron, 2013). Moreover, with only minor modifications or without, the existing power plants can be retrofitted, commercially available, established technology which has a low technology risk and it is practical to be implemented in the manufacturing industry such as steel and cement industry to capture CO_2 (H. Yu, 2018). Four technologies has been developed for the post-combustion process which are solvent absorption, adsorption using solid sorbent, membrane separation and cryogenic fractionation (Figueroa et al., 2008).

2.2.3.1 Adsorption using solid sorbents

Adsorption takes place at the surface of the material (Feng, Liu, Li, & An, 2006). Common adsorbents are activated carbons, metal oxides, zeolites, silica gel and ion-exchange resins. Activated carbon is a popular adsorbent because of its good characteristics which includes large distribution of pore size and pore structure and very active surface area. For economically feasible, the ideal adsorbents must have these characteristics such as easily regenerated, high capacity of adsorption and high selectivity for CO_2. However, adsorbent affinity for CO_2 should not be too high due to the step of regeneration will adversely affect process economy (Dantas, Luna, Silva, de Azevedo, et al., 2011). Adsorption process takes place as the flue gas is put in contact with a bed of adsorbent where the CO_2 from other gases passes through. As the bed is saturated with CO_2, the flue gas is directed to a clean bed while the saturated bed is regenerated.

Huck et al., Soares et al., Pan et al., Kamimura et al. and Dantas et al. studied various sorts of adsorbent in order to capture CO_2 (Dantas, Luna, Silva, Torres, et al., 2011; Huck et al., 2014; Kamimura et al., 2014; Pan & Connell, 2009; Soares, Oberziner, Jose, Rodrigues, & Moreira, 2007). Li et al. reported approximately 350 patents belonged to solid adsorbent since the year 2000 (B. Y. Li et al., 2013). Several functional groups can be attached to the adsorbents by modification of surface. This affects the behavior of adsorption as the chemical functionalization influences the physiochemical properties of the adsorbent surface. Different amine-enriched carbon based adsorbents such as activated carbon, carbon nanotube and carbon molecular sieve have been introduced. Maroto-Valer et al. showed enhancement of the CO_2 adsorption capacity is achieved by impregnation with amine molecules (Hong, Kim, & Lee, 2013).

2.2.3.2 Cryogenic fractionation

Cryogenic fractionation process operates at extremely high pressure and low temperature in order to separate CO_2 and other components based on different boiling point temperatures. It is a well-established technique for purification of natural gas from CO_2. The newest improvement made is the CryoCell Technology which is implemented at the Cool Energy demonstration site in Australia (Amin, Jackson, & Kennaird, 2005). When this technology was first presented, broad studies have been conducted on separation of hydrocarbon mixtures containing 5-95 mol% CO_2 and abundant enhancement has been achieved. Plenty of research data are tabulated and schemed on graphs displaying phase envelopes of CO_2-hydrocarbons mixtures. However there is inadequate information on this process for large-scale separation of CO_2-hydrocarbons.

Cryogenic process is suitable only for concentrated stream of CO_2. This method is not economical for dilute stream as it required high consumption of energy to provide cooling process, especially for low concentration gas stream. Column choking and solid

formation are operating problems that are need to be solved particularly at lower and higher pressure ranges in the colder top part of the distillation column. In order to prevent plugging by ice or high rise in pressure drop during operation, moisture has to be removed before channeling the flue gas to the cooling unit (McGlashan & Marquis, 2008).

2.2.3.3 Membrane separation

Membrane separation technology is an interaction of specific gases with the material of the membrane by chemical or physical interaction. The rate of the gases passes through can be controlled by modifying the material. Membrane separation compromised a high driving force and high selectivity at low concentration and can easily be adapted to the particular strains of an individual plant. The membrane provides a modular, energy efficient, flexible device with a high specific surface area (Kim & Harriott, 1987). Membrane separation process is based on a gas-liquid contact through a hydrophobic micro porous membrane. This membrane forms a permeable barrier between the gas and liquid phase. It allows mass transfer between the two phases without scattering one phase into the other. The gas fills the hydrophobic membrane pores and in contacts with the liquid at the opposite side of the membrane. In order to prevent dispersion of gas bubble into the liquid, the pressure of liquid phase must be slightly higher than the gas phase (Mavroudi, Kaldis, & Sakellaropoulos, 2003).

Early work by Mavroudi and coworkers studied about the absorption of a variety of gases in a medium of alkaline or acidic by using a hollow fibre module membrane (Mavroudi et al., 2003). Liu et al. prepared a composite membrane of hollow fibre poly (ether blockamide) (PEBA) /polysulfone (PSF) for separation of CO_2/N_2. It was found that PEBA 2533 copolymer is a good per selective membrane material for CO_2/N_2 separation (L. Liu, Chakma, & Feng, 2004). Powell et al. provide a comprehensive review on polymeric gas separation membrane which covers review on fabrication, synthesis,

possible design strategies of membrane (Powell & Qiao, 2006). High CO_2/N_2 selectivity, high CO_2 permeability, thermally and chemically robust, resistant to aging and plastication and able to manufacture into different membrane modules with lower cost are characteristics of membrane that make it valuable in capturing CO_2 (Ku, Kulkarni, Shisler, & Wei, 2011).

2.2.3.4 Solvent absorption

The absorption process occurs within the bulk of the material via a physical or chemical interaction. The gas absorption occurs at low temperatures which is at or above room temperature and high pressures up to 4 MPa or more. The desorption of gas occurs at elevated temperatures up to 390 K or more and low pressures (G. Puxty et al., 2009). Physical absorption captures CO_2 without undergoing chemical reaction. Kanniche et al. reported that Selexol (dimethylether of polyethylene glycol) is known for their chemical stability and for a non-induced corrosion effect (Kanniche & Bouallou, 2007).

Absorption via chemical reaction has been long considered the most practicable route to post combustion CO_2 capture and developed over 60 years ago as nonselective solvent such as alkanolamines to remove acidic gas impurities from natural gas streams (Svendsen, Hessen, & Mejdell, 2011; Y. S. Yu, Li, Lu, Yan, & Zhang, 2011). Figure 2.2 explained the CO_2 gas loading performance of several solvents. The curves show linear relations between the partial pressure and CO_2 loading for physical solvents (water, N-methyl-2-pyrrolidone and methanol) and non-linear relations for chemical solvents (Hot potassium carbonate solution, sulfinol solution, diethanolamine solution and Amisol DETA solution). Details for absorption process were comprehensively discussed in later sub-chapter.

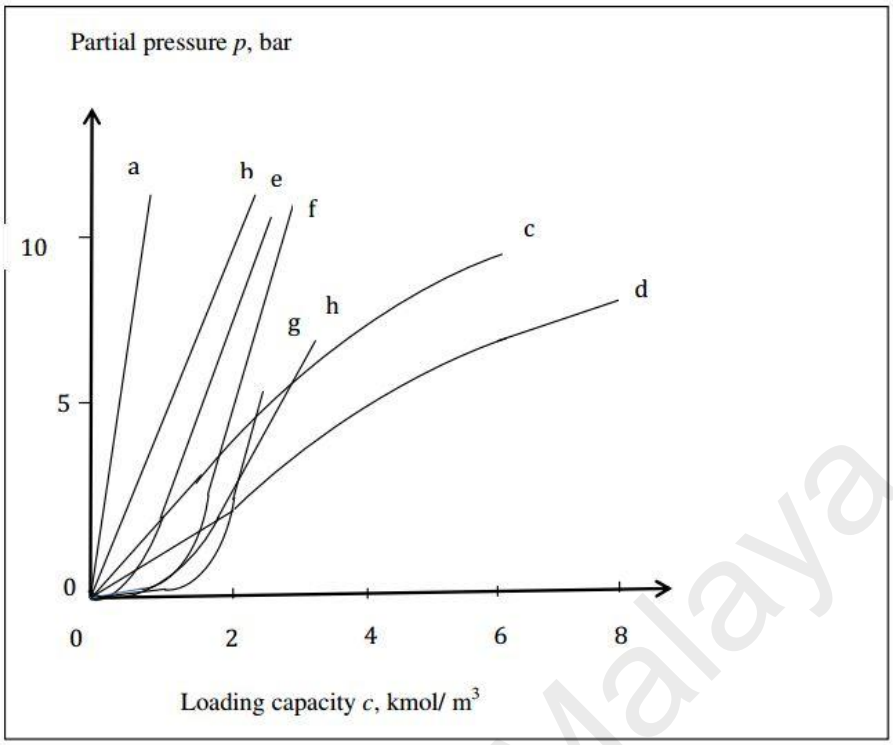

Figure 2.2: Comparison of CO_2 gas loading performance of a) Water (30℃);b) N-methyl-2-pyrrolidone (110℃); c) Methanol (-15℃); d) Methanol (-30℃); e) Hot potassium carbonate solution (110℃); f) Sulfinol solution (50℃); g) 2.5 M Diethanolamine solution (50℃); h) 3M Amisol DETA solution(Kemper, Ewert, & Grunewald, 2011)

2.3 Solvents for CO_2 capture

Previously mentioned, there are techniques to reduce the emission of greenhouse gas such as absorption, membranes separation, adsorption using solid sorbent and cryogenic fractionation. CO_2 absorption is the most preferred method to reduce CO_2 emissions (Irani, Maleki, & Tavasoli, 2019). Absorption processes for CO_2 capture are characterized as chemical or physical processes based on types of gas components that dissolved physically or chemically to the solvent. Sometimes in certain processes, mixing both solvents can fully utilize beneficial characteristics of both chemical and physical solvents. As illustrated in Figure 2.3, the capacity for low partial pressure absorption of chemical

solvents is higher than the capacity of absorption in physical solvents. However physical solvents give higher capacity of absorption at high partial pressure.

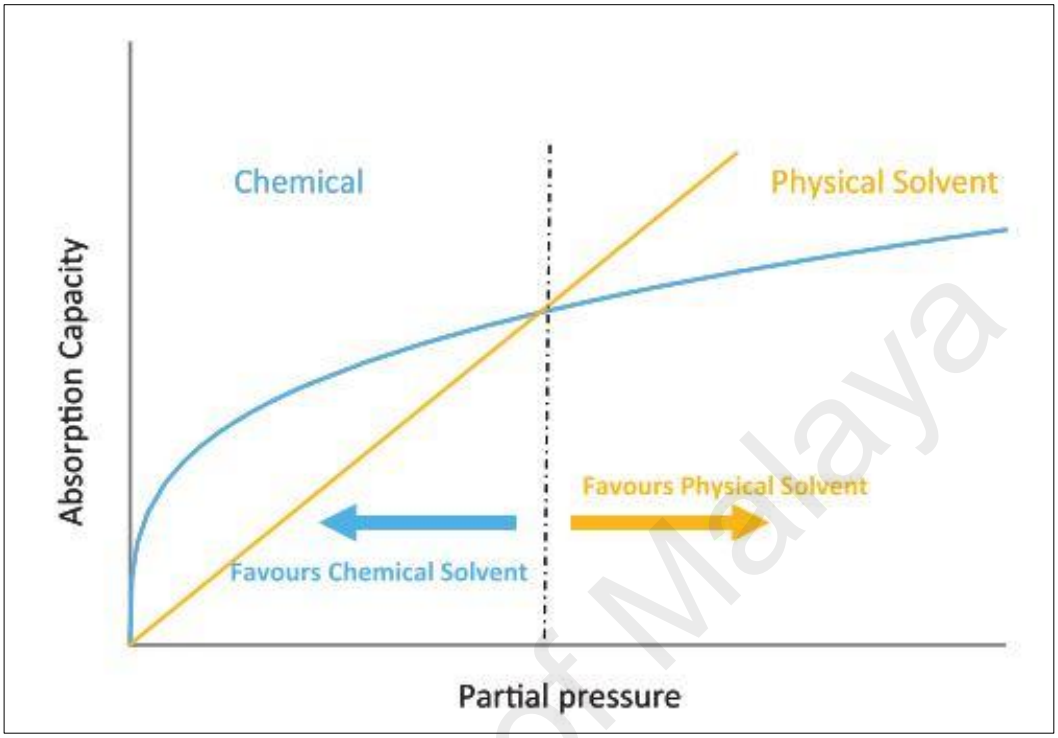

Figure 2.3: Absorption capacity for chemical and physical solvents as a function of partial pressure (Laboratory, 2011)

2.3.1 Physical absorption solvent

Physical absorption is controlled by the thermodynamic equilibrium between aqueous phases and CO_2 gas molecule. Low temperature and CO_2 partial pressures more than 2 MPa accelerates the physical absorption (Yuan & Rochelle, 2018). Besides, simple regeneration of solvent can occur by reducing the pressure. This is favorable when bulk removal at high operating pressures and higher purities of product are targeted. Typically, physical solvents have larger capacity of absorption which reduce recirculation rate of solvent (Olajire, 2010). However by using physical solvents, it is difficult to meet specifications of gas as this absorption process is less selective than chemical solvents. Other than this, it is very sensitive to acid gas partial pressure (Knudsen, Andersen, Jensen, & Biede, 2011).

MeOH (Methanol), DEPG (Dimethyl Ether of Polyethylene Glycol) and PC (Propylene Carbonate) are commercially used as physical solvents (Koytsoumpa, Bergins, & Kakaras, 2018). One of the state of the art processes is Selexol which the major components are dimethyl ether of polyethylene glycol. It exhibits the highest solubility of CO_2 and no requirement of water wash because of very low vapor pressure. The operating temperature is from 0℃ to 175℃. For sequestering step, Selexol is less costly than Rectisol. However, it is more viscous than other physical solvents especially at low temperature which required high packing and lower mass transfer (Gainar & Anitescu, 1995). The major component for Fluor process is propylene carbonate. It has higher vapor pressure than Selexol even though low loses of solvent and unstable operated at high temperature which makes it operating temperature not more than 65℃. It is not recommended to use if higher trace level of H_2S are present. Lastly, Rectisol process. For this process, methanol is used to separate acid gas. It required water wash for stream of effluent to avoid excessive loss of solvent due to higher vapor pressure at elevated temperature. However, it exhibits higher selectivity for H_2S over CO_2 (Bucklin & Schendel, 1984).

2.3.2 Chemical absorption solvent

Today, chemical absorption for CO_2 capture process is technically and economically validated in the oil gas industry for extraction of natural gas, for different power plants and cement industry (Dinca, Slavu, & Badea, 2018). The selectivity by chemical absorption is comparatively high. Moreover, a pure CO_2 stream could be formed. The reactions have to be reversible for regeneration of solvent (Graeme Puxty et al., 2014). Several researchers throughout the years used chemical absorption for CO_2 capture process. Figure 2.4 illustrates a process flow diagram for CO_2 capture from flue gas by chemical absorption (Metz, Davidson, Coninck, Loos, & Meyer, 2005).

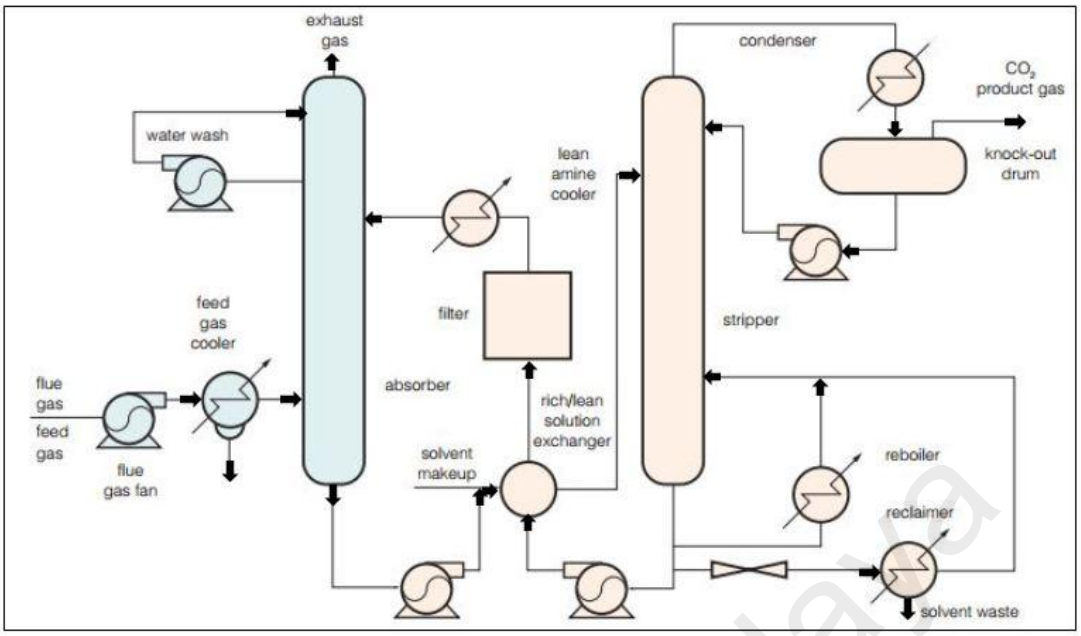

Figure 2.4: Process flow diagram for CO_2 capture from flue gas by chemical absorption (Metz et al., 2005)

As illustrated in Figure 2.4, the flue gas is cooling before it is brought into contact with the lean solvent in the absorber. The flue gas undergoes a water wash to remove any solvent vapor carried over and vented to the atmosphere. The lean solvent increasingly heats up as it absorbs CO_2. The absorbed temperature is usually between 40^{o}C and 60^{o}C. The rich solvent which chemically bound with CO_2 is pumped to the top of a stripper through a heat exchanger where the regeneration of the solvent is carried out at elevated pressure between 100^{o}C to 140^{o}C and pressure not much higher than atmospheric pressure. In order to maintain the regeneration conditions, heat is supplied to the reboiler. Steam is recovered in the condenser and return back to the stripper while the CO_2 product gas leaves the stripper. The lean solvent is pumped back to the absorber via the lean-rich heat exchanger and a cooler to reduce the absorber temperature. There are several chemical solvents that can be used in this process such as amine solvents, mixed amine-based solvents, ammonia based solvents and ionic liquids (Abu-Zahra et al., 2013).

2.3.2.1 Amine solvents

Generally, amine solvents can be categories into two which are alkanolamines and sterically hindered amines. Monoethanolamine (MEA), diethanolamine (DEA) and methyldiethanolamine (MDEA) solvents are among popular alkanolamine solvents. MEA acts as the benchmark for CO_2 capture solvent and it is a great and valuable solvent in research field and industry. Primary, secondary and tertiary amine solvents can be characterized by rate of corrosion, stability of product, capacity for CO_2 absorption, equilibrium of CO_2 absorption and reaction kinetics of CO_2 (Rivera-Tinoco & Bouallou, 2010). Primary and secondary amine are rapidly reacted with CO_2 because of the formation of carbamate. MEA is more likely to oxidize and degradation occurred when O_2 is present. High energy requirement of regeneration for CO_2 desorbing process from CO_2-rich MEA and CO_2-rich DEA because carbamate needed to be decomposed. These are corrosive solvents which need special and expensive construction materials. Tertiary amine solvent, MDEA has slow rate of reaction with CO_2 but required less energy of regeneration for CO_2 desorption process (Glasscock, Critchfield, & Rochelle, 1991).

Luis reviewed the consequences and alternative in using MEA for CO_2 capture. In this review, they reported the main consequences of utilizing MEA as absorption solvent for CO_2 capture and various ways to enhance the conventional process of absorption (Patricia Luis, 2015). DeMontigny et al. investigated the effect of operating parameters which are liquid flow rate, solution CO_2 loading and CO_2 partial pressure on the overall mass transfer coefficient in an MEA- CO_2 absorption system. They reported that the overall mass transfer coefficient increases as the liquid flow rate increases while the overall mass transfer coefficient value decreases as the solution CO_2 loading and the CO_2 partial pressure increases (deMontigny, Tontiwachwuthikul, & Chakma, 2001).

Sterically hindered amines have one or more group of methyl attached with the alpha carbon which is attached to the amino group as it is inhibited from reacting with CO_2 by the steric hindrance effect. The 2-amino-2-methyl -1-propanol (AMP) is a good steric hindered amine. AMP is capable to increase capacity of CO_2 absorption as it can stimulate hydrolyzing process to form bicarbonate and reduce energy of regeneration. Nevertheless, the reaction kinetics of AMP is slow like MDEA (Mandal, Guha, Biswas, & Bandyopadhyay, 2001). Mandal et al. investigated the CO_2 loading in AMP and MDEA. They observed the rate of reaction for AMP- CO_2 is higher than MDEA- CO_2. The costs for regeneration of energy may be lower when aqueous AMP solution is used to capture CO_2 because AMP does not able to form stable carbamate thus larger amount of carbonate and bicarbonate ions present in the solution (Mandal et al., 2001).

2.3.2.2 Mixed amine-based solvents

Mixed amine-based solvents are established to overcome some of the disadvantage of single amine solvents and also incorporated some of the advantages of single amine solvents. Blending amines at different proportions can give estimation of the solvent selectivity as it can optimize the performance of separation for a gas mixture. Higher reaction rates of primary and secondary amine can combine with higher capacity at equilibrium of tertiary amine. This combination may improves gas absorption process and reduce requirement of energy regeneration (Mandal et al., 2001). Nwaoha et al. discussed tri-solvent blends of MEA, piperazine and AMP for absorption and desorption of CO_2 process. The MEA-piperazine-AMP tri-solvent blends give positive results to cyclic capacities, initial rate of desorption and heat duties which is 50% compared to the 5 M of standard MEA (C. Nwaoha et al., 2016). Liao et al. reported the kinetic of CO_2 absorption into aqueous MDEA and MEA at temperature of 30^{o}C, 35^{o}C and 40^{o}C using a laboratory wetted wall column. They reported that small addition of MEA to aqueous MDEA give a significant improvement in rate absorption of CO_2 (Liao & Li, 2002).

2.3.2.3 Ammonia based solvents

Ammonia based solvents have chemical and thermal stability, high capacity of CO_2 absorption and lower cost of production. In order to avoid excessive losses of ammonia throughout the process, it has to operate below 25^oC. Even though ammonia based solvents can tolerate the oxidative degradation, they required large amount of energy consumption to sustain the operating temperature below 10^oC. Besides, the crystalline products are found in the CO_2 scrubber. Yeh et al. compared ammonia and MEA solvent to capture CO_2. Among the solvents, they reported that ammonia solvent gave better CO_2 removal efficiency and CO_2 capacity than MEA solvent. The ammonia solvent achieves 99% of CO_2 removal efficiency and 1.20 kg CO_2/kg ammonia of CO_2 absorption capacity (Yeh & Bai, 1999). A comprehensive review on the use of aqueous ammonia for post combustion CO_2 capture in general has been done by Zhao et al. where they presented the process chemistry of aqueous ammonia, effects of parameters on efficiency of absorption, methodologies to improve absorption and simultaneous CO_2 capture with other pollutants (B. T. Zhao, Su, Tao, Li, & Peng, 2012).

2.3.2.4 Ionic liquids

Ionic liquids have become attractive in CO_2 absorption applications both in academia and industry due to their low vapor pressures and thermally stable properties. The lower vapor pressure reduced the consumption of energy in the stripping of CO_2 and regeneration of solvent. Estimation by simulation showed that CO_2 capture with ionic liquid, [bmim][Ac] can decrease 16% of energy losses compared to a MEA process and 12% in equipment of footprint. The anion and cation group are features of ionic liquids that give impact to the absorption capacity. A large amount of CO_2 can be dissolved in a typical ionic liquid such as [emim][TF_2N] (X. P. Zhang et al., 2012). Ramdin and co-workers reviewed CO_2 capture with ionic liquids. This review included the experimental data of CO_2 solubility, diffusivity and selectivity in different ionic liquids, the effects of

functional groups, anions and cations in CO_2 absorption, toxicity and biodegradability of the ionic liquids (Ramdin et al., 2012). Zareie et al. evaluated the CO_2 capture from flue gas by MEA, aqueous potassium carbonate and [emim][Ac] in a packed column. It was reported that [emim][Ac] gives 7% more CO_2 absorption capacity that the MEA solution and 26% more than aqueous potassium carbonate (Zareie-kordshouli, Lashani-zadehgan, & Darvishi, 2016). Table 2.2 summarizes some reported solvents for CO_2 capture.

Table 2.2: Comparison of solvents performance

Absorbents	Parameters	CO_2 solubility	References
MEA+Potassium lysinate (PL) blend solution	C: 2M MEA +0.5M PL T: 303 K P: 5.34 – 44.16 kPa	0.641 – 0.784 mol CO_2/ mol blend solution	(Ramazani, Samsami, Jahanmiri, Van der Bruggen, & Mazinani, 2016)
1,5-diamino-2-methylpentane solution	C: 1M-2.5M T: 303.15 K- 323.15 K P: 4.5 kPa – 145.6 kPa	0.657 – 1.206 mol CO_2/mol solution	(Azhgan, Farsi, & Eslamloueyan, 2016; Pazuki, Pahlevanzadeh, & Mohseni Ahooei, 2006)
30 wt% aqueous MEA mixture with glycerol	C: 30 %wt MEA + (5-20%wt glycerol) T: 313.15 -333.15 K P: 500-1500 kPa	0.64-0.88 mol CO_2/ mol solution	(Shamiri et al., 2016)
[BMIM][NTf_2] +Sulfolane	C: 0.1-0.9% IL T: 323.15 K P: 400-2000 kPa	0.1-0.5 mol CO_2/ mol absorbent	(Kassim et al., 2016)
Glycerol	T: 353.15 – 423.15 K P: Up to 32 MPa	0.019 – 0.089 in mol fraction CO_2	(Nunes, Carrera, Najdanovic-Visak, & Nunes da Ponte, 2013)
Ammonia solution	C: 1.13-8.11 m T: 268.15-288.15 K P: 1.62-20.90 kPa	0.907-5.8 m	(Pazuki et al., 2006)

2.4 Process chemistry

The primary, secondary and tertiary amino group are generated from the first, second and third derivatives of ammonia which differ in reactivity and basicity. Amines with one, two or three amino groups are called mono, di, and triamine. Alkanolamines have

one or more groups of alcohol while sterically hindered amines have one or more group of methyl attached with the alpha carbon. Due to their properties such as relatively high thermal stability, high reactivity towards CO_2 and high absorbing capacity in terms of mass of CO_2, amines are so effective for CO_2 capture.

Primary and secondary amines such as monoethanolamine and diethanolamine have capability to react directly with CO_2 and form carbamic acid which then deprotonates to the carbamate by exchanging a proton with a second amine molecule. The chemical reaction is described in equation 2.1 and equation 2.2 and the overall reaction as in equation 2.3. The important advantage of the route of carbamate is the rapid rate of reaction of the amino groups with CO_2. Yet this advantage must be balanced with the carbamate's stability and requirement of energy for releasing CO_2 during the desorption process.

$$R_1R_2NH + CO_2(aq) \leftrightarrow R_1R_2NHCO_2 \quad (2.1)$$

$$R_1R_2NCO_2^- + H^+ \leftrightarrow R_1R_2NHCO_2 \quad (2.2)$$

$$2R_1R_2NHCO_2^- + CO_2(aq) \leftrightarrow R_1R_2NCO_2^- + R_1R_2NH^+ \quad (2.3)$$

Tertiary amine such as MDEA is not able to directly react with CO_2 and consequently cannot form carbamates which make formation of bicarbonate from the reaction of water with CO_2 is the only main reaction (Figueroa et al., 2008). The chemical reaction is described in equation 2.4 to equation 2.6 with overall reaction as in equation 2.7.

$$CO_2(aq) + H_2O \leftrightarrow H_2CO_3 \quad (2.4)$$

$$HCO_3^- + H^+ \leftrightarrow H_2CO_3 \quad (2.5)$$

$$R_1R_2R_3N + H^+ \leftrightarrow R_1R_2R_3NH^+ \quad (2.6)$$

$$R_1R_2R_3N + CO_2 + H_2O \leftrightarrow R_1R_2R_3NH^+ + HCO_3^- \quad (2.7)$$

R_1, R_2 and R_3 represent attached substituents by N-C bond in the above chemical reaction. The route from equation 2.4 to equation 2.7 increases the amount of absorbed CO_2 by the amine solution and provide less input of energy for process of desorption. However, this route is the slowest rate of reaction as compared to primary and secondary amines (Yang et al., 2016).

2.5 Biodiesel and bioglycerol

2.5.1 Biodiesel

Biodiesel is a renewable fuel which is produced from transesterification of animal fats or vegetable oils (El Doukkali et al., 2012). It can also be produced from inedible tallow, yellow grease and pork lard (Oner & Altun, 2009). Biodiesel consists of the mixtures of aliphatic alcohols and alkyl esters of fatty acids. When vegetable oil goes through the transesterification process to become biodiesel , glycerol is a byproduct of the chemical reaction (Melero, Iglesias, & Morales, 2009). For production of biodiesel, various sources of edible and non-edible oil, used and waste oil and also fats are the sources of triglyceride (El-Gendy, Hamdy, & Abu Amr, 2014). The discovery of suitability of crops can produce valuable chemical was in 1990 by Rudolph Diesel. In his work on diesel engines, methyl esters have been produced from fatty acids obtained from crops. However, during that time, attention has been more focused on the usage of mineral deposits of crude oil to produce diesel (Alaswad, Dassisti, Prescott, & Olabi, 2015).

Since 2000, biodiesel is now of interest as an alternative source as biodiesel production has been exponentially increased for environmental reasons and most importantly to meet the Kyoto protocol (Al-Lal, Garcia-Gonzalez, Llamas, Monjas, & Canoira, 2012). The valuable properties of biodiesel make it an option as the alternative and green fuel as the extinction of fossil fuel, the rising price of crude oil and the stringent regulations of

exhaust emission (El-Gendy et al., 2014) . Biodiesel has higher flash point, improved lubricity, close combustion of heat and viscosity. Other than this, biodiesel is less toxic and more biodegradable as compared with fossil diesel which makes it to be an environmental friendly fuel. It has lower exhaust emission of carbon monoxide, carbon dioxide, dust, smoke or hydrocarbon during the engines combustion (C. S. Lee et al., 2015).

Biodiesel is a fast growing product in Europe and United States. This is due to the development of renewable transportation fuel in their government policies (Mangas-Sánchez & Adlercreutz, 2015). Europe manufactured 10 million megatonnes of biodiesel in year 2010 but it has decreased in the year 2011 and increased of biodiesel imported from other countries such as Asia, Brazil, Argentina and US. However, as production of biodiesel is increasing, bioglycerol is also produced in large amounts. The bioglycerol coproduct yields 10 wt% of the total product from the transesterification reaction. Nowadays, two-third of the global glycerol supply is from biodiesel production (C. S. Lee et al., 2015). Therefore, in order to improve the profitability of biodiesel, consideration on one of promising alternatives is a bioglycerol conversion into higher added value products. Finding proper applications for bioglycerol became a research target of scientists from all over the world.

2.5.2 Bioglycerol

It is found that bioglycerol is useful in more than two thousand applications in several industries (Mallesham, Sudarsanam, & Reddy, 2014). Bioglycerol is a byproduct of production of biodiesel, production of fatty acid and microbial fermentation. Apart from this, it can be prepared by hydrogenolysis of glucose or saccharides from propylene. Due to high crude oil prices, this route is not economical to be used (Vijay, Prasad, & Devi, 2013). The EPA has mandated about the usage of 1.28 billion gallons of biodiesel in 2013.

Besides, production of biodiesel came from 112 plants of biodiesel with 2.2 billion gallons per year of capacity. According to experts' estimate, about 6 million tons of glycerol will be produced in the world annually by 2025(Lyadov & Khadzhiev, 2017). Increase in biodiesel demand will supply the glycerol continuously (Yadav & Chandan, 2014).

Glycerol with three hydroxyl groups can be converted to a variety of bulk chemicals. It has larger chemical advantages and should be considered as a versatile feedstock for the creation of new chemicals. Ramesh et al. and Karnakar et al. synthesed new bioglycerol-based carbon catalyst which acted as a readily available, reusable and an efficient catalyst (Karnakar et al., 2012; Ramesh et al., 2012). It was found that 91% bioglycerol-based carbon catalyst can be recovered and be used in other reaction. There are many products produced from bioglycerol especially in food, pharmaceutical, leather industry and cosmetic. Esterification of bioglycerol can yield three products which are monoacetin, diacetin and triacetin which is useful as precursors in the synthesis of polyesters. Acetalization of bioglycerol are versatile additive for diesel fuels (Mallesham et al., 2014). Dihydroxineacetone is a three carbon sugar that has been used in cosmetic industries as a tanning agent. Polyglycerol esters find their utilization as lubricants, plasticizers, antifogging and antistatic additives. Maleinization and methacrylation reactions from bioglycerol under mild condition can produce polyunsaturated resin(Gómez, Echeverri, Inciarte, & Rios, 2019).

Wang et al. reported that the global production of biodiesel has increased and expected to reach 37 billion gallons by 2016. As the global biodiesel production vigorously increased, bioglycerol has dramatically increased and become worthless. In year 2007, based on the report in United States, the crude bioglycerol's price dropped from $0.55/kg to $0.11/kg (C. S. Lee et al., 2015). Thus, it is necessary to develop new

uses for glycerol. One possibility is to transform it to bioglycerol-based solvent with the addition of amine group. It is great opportunity to make this transformation as it is able to capture CO_2 due to the presence of amine group and can be one of the alternative uses for glycerol.

2.5.2.1 Bioglycerol for CO_2 absorption

Recently, bioglycerol is introduced as a green solvent to capture CO_2. This application targets to lessen the usage of chemical solvents with the environmental friendly solvents. Bioglycerol is a stable, colorless, odorless, high boiling point (290℃), non-toxic, low vapor pressure and bio-degradable liquid. It exhibits as a physical solvent to capture CO_2. Aschenbrenner and coworkers have proven the solubility of CO_2 in glycerol solvent. The solubility of CO_2 in glycerol at 25℃ proves its capability to absorb CO_2 as the solubility of CO_2 in glycerol is higher than polymeric liquids, methanol and water (Aschenbrenner & Styring, 2010).

The solubility of CO_2 in blended amines with bioglycerol was investigated by Shamiri et al. (Shamiri et al., 2016). The solubility of CO_2 was investigated in aqueous mixtures of 30 wt% MEA with varying concentration of glycerol from 0 to 20 % at 3 different temperatures (313 K, 323 K and 333 K) and pressure up to 1500 kPa. The results showed that by adding 5 wt% of glycerol into MEA, it could increase the CO_2 solubility of MEA at low pressure and maintain the CO_2 absorption performance at high pressures. Moreover, Chiang et al. reported that by adding glycerol in the sodium hydroxide solution easily increased the efficiency of CO_2 absorption to be more than 90 %. This addition of glycerol gives affirmative effect of CO_2 absorption and enhanced performance of mass transfer (Chiang, Lee, & Liu, 2017).

2.5.2.2 Derivatives of bioglycerol in CO_2 capture

Although glycerol is considered a green solvent to capture CO_2, it has high viscosity in its pure form to be considered as a good solvent for CO_2 capture. Glycerol aqueous solutions can reduce the viscosity of pure glycerol but cause a detrimental effect on CO_2 absorption (Flowers et al., 2017). The 1, 2, 3-trimethoxypropane is a glycerol-derived physical solvent for absorption of CO_2 was reported by Flowers et al. The physical properties of 1, 2, 3-trimethoxypropane were investigated with respect to temperature. The solubility of CO_2 in this solvent was conducted at temperature from 30℃ to 75℃ at pressure up to 10 atm. As a result, 1, 2, 3- trimethoxypropane exhibits favorable properties and good solvents for CO_2 absorption.

The 2-amino-1, 3-propanediol (serinol) is one of the derivative of bioglycerol. It belongs to the amino alcohol group and is prochiral. It cannot be categorized as a primary sterically hindered alkanolamine as it has lower kinetics towards CO_2 as compared to sterically hindered alkanolamine (Bougie & Iliuta, 2014). Figure 2.5 shows the route synthesis of serinol which is catalytically derived from glycerol (Kimura & Tsuto, 1993). Glycerol undergo oxidation process to form dihydroxyacetone. Glycerol oxidation product was reduced to 2-amino-1, 2, 3- propanetriol in the presence of ammonia gas over Ru-Pd/C catalyst of glyceric acid. Then, serinol is prepared by undergoing process of hydrogenation and dehydration.

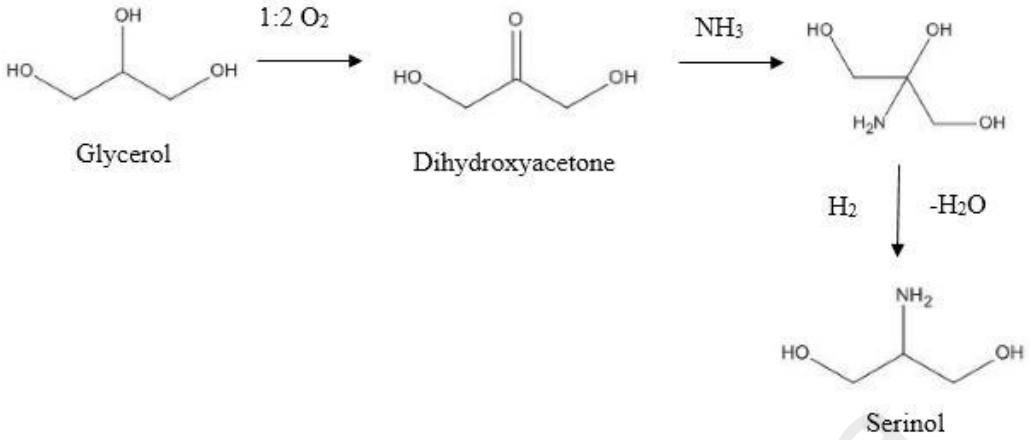

Figure 2.5: Route synthesis of serinol (Kimura & Tsuto, 1993)

There is very limited information regarding serinol aqueous solutions. Conway et al. reported there is no carbamate form for serinol in the experiment of kinetic (Conway et al., 2013). Bougie et al. proposed serinol aqueous solutions as a new potential solvent to capture CO_2. It was found that serinol solutions have higher surface tension than the conventional absorbents and serinol is applicable for CO_2 removal using membrane contactors at low pressure. Moreover, the formation of carbamates from the reaction of serinol with CO_2 can be more straightforward when compared to MEA carbamates. Bougie et al. characterized serinol aqueous solutions through viscosity, density and surface tension from temperature of 293.2 K to 313.2 K. Although researchers have revealed the supremacy of serinol, the CO_2 solubility of serinol at high pressure was not reported in the literature thus far.

2.5.2.3 Chemical reaction of serinol with CO_2

Serinol, a primary amine has the capability to react directly with CO_2 with or without the presence of water via zwitterion mechanism analogous to MEA reaction with CO_2 (Lv, Guo, Zhou, & Jing, 2015). Initially, serinol reacts reversibly with CO_2 to form a zwitterion molecule as shown by equation 2.8. Hydrolysis of the zwitterion molecule in the presence of second serinol molecule leads to the formation of serinol carbamates as shown in equation 2.9.

$$(CH_2OH)_2CHNH_2 + CO_2 \leftrightarrow (CH_2OH)_2CHNH_2^+COO^- \quad (2.8)$$

$$(CH_2OH)_2CHNH_2^+COO^- + (CH_2OH)_2CHNH_2 \rightarrow (CH_2OH)_2CHNHCOO^- + (CH_2OH)_2CHNH_3^+ \quad (2.9)$$

In the presence of water, CO_2 hydration reaction takes place, forming HCO_3^- (equation 2.10). Subsequently, some of the free serinol can also react with HCO_3^- forming another carbamate (equation 2.11).

$$CO_2 + H_2O \rightarrow HCO_3^- + H^+ \quad (2.10)$$

$$(CH_2OH)_2CHNH_2 + CO_2 + H_2O \leftrightarrow (CH_2OH)_2CHNH_2^+ + HCO_3^- \quad (2.11)$$

The important advantage of the route of carbamate is the rapid rate of reaction of the amino groups with CO_2. Yet this advantage must be balanced with the carbamate's stability and the energy requirement for releasing CO_2 during the desorption process. The chemical absorption of CO_2 by serinol is stoichiometrically limited by the amount of amine present in the solution despite being carried out under relatively high pressure. Upon completion of the chemical absorption of CO_2 by serinol, subsequent absorptions of CO_2 into the solution will occur via physical absorption by aqueous serinol-carbamate.

2.6 Computational method in screening solvents

Bioglycerol is expected to become the major platform chemical and the transformation of glycerol into valuable chemicals is highly desirable since the reactant is abundant and very cheap. However, in order to evaluate new potential solvent from bioglycerol, a systematic approach must be taken and knowledge of the reactivity of the system is important. The most practical approach to evaluate the potential bioglycerol based solvent is quantum chemical methods.

A thermodynamic model based on quantum chemical calculations was developed by Professor Andreas Klamt in 1999 (A. Klamt & Eckert, 2000). The name composed of Conductor like Screening Model in combination with Real Solvent (COSMO-RS) which is functioned as a connection between chemical engineering thermodynamic and quantum chemistry (A. Klamt & Eckert, 2004). COSMO-RS is a prediction method for thermodynamic properties of liquid and fluid mixtures using the approach of statistical thermodynamic framework which imports information of molecular level dissolved in a conductor (volume, cavity, energy and screening charges) obtained from COSMO model (A. Klamt, Eckert, & Hornig, 2001).

The approach is from the surface of the molecular as computed by quantum chemical methods (QM). COSMO-RS combines a methodology of statistical thermodynamics with an electrostatic theory of locally interacting molecular surface descriptors (Eckert & Klamt, 2003). Each molecule involves in a mixture has to be computed by quantum chemical COSMO-RS. The COSMO-RS calculation can predict the thermodynamic properties such as the activity coefficients, chemical potentials, solvent partition coefficient, vapor pressure, excess enthalpies and excess Gibbs free energy (Putnam, Taylor, Klamt, Eckert, & Schiller, 2003).

The main advantages of COSMO-RS is the lack of need for experimental data that can save time, cost and energy required to conduct experiments and reliable method for screening solvent based on prediction of thermodynamic behavior and properties (Burghoff, Goetheer, & de Haant, 2008). There is no thermodynamic experiments have to be conducted to expand the databank. The QM COSMO-RS considers the electrostatic interaction between solute and solvent in a fluid as local contact interactions of molecular surfaces. Moreover, COSMO-RS is based on COSMO model which is a quantum

chemical dielectric continuum model. So only computational calculations are required to create the desired.

2.6.1 COSMO-RS model

COSMO-RS is a two-step approach. In the first step, quantum chemical calculations have to be performed for potential solvents by using standard quantum chemical method which is density functional theory (DFT) (Andreas Klamt, 2003). For the second step, statistical thermodynamics of the molecular interactions are performed. The interaction energy in COSMO-RS is demonstrated in terms of its polarization charge density, σ and σ'. The molecular interactions represented in COSMO-RS are van der Waals interaction (E_{vdW}), hydrogen bond interaction (E_{hb}) and electrostatic misfit energy (E_{misfit}). This model can be used to compute the activity coefficient of any component in a mixture at infinite dilution or/and specific dilution. Henry's constant, the change in Gibbs free energy and others thermodynamic properties can also be predicted (Constantinescu, Rarey, & Gmehling, 2009).

The interactions of molecular surfaces in COSMO-RS are given in terms of σ and σ' by the following expression (Mu, Rarey, & Gmehling, 2007):

$$E_{misfit}(\sigma, \sigma') = \alpha_{eff} \frac{\alpha'}{2} (\sigma + \sigma')^2 \tag{2.12}$$

$$E_{hb} = \alpha_{eff} c_{hb} \min(0; \min(0; \sigma_{donor} + \sigma_{hb}) \max(0; \sigma_{acceptor} - \sigma_{hb})) \tag{2.13}$$

$$E_{vdw} = \alpha_{eff}(\tau_{vdw} + \tau'_{vdw}) \tag{2.14}$$

Based on the above expressions, there are five universal adjustable parameters which are α_{eff} is the effective contact area, α' is the interaction parameter, c_{hb} is the strength of hydrogen bond, σ_{hb} is the polarization charge density threshold for hydrogen

bond and τ_{vdw} is the element- specific van der Walls parameter (M. Diedenhofen & Klamt, 2010).

2.6.1.1 Statistical thermodynamics in COSMO-RS

COSMO-RS treats the solvent S as an ensemble of pair-wise interaction surface segments. The interaction energy in COSMO-RS is demonstrated in terms of its polarization charge density, σ and σ' of the respective surface segments. For the statistical thermodynamic of COSMO-RS, σ-profile $p^x(\sigma)$ which is the histogram of the screening charge density can be considered sufficient. It provides information about the relative amount of surface with polarity σ for a molecule X. Then the σ-profile of the system is given by the weighted sum of the σ-profile of the components (Michael Diedenhofen, Eckert, & Klamt, 2003),

$$p_s(\sigma) = \sum_{i \in S} x^i \, p^{X_i}(\sigma) \tag{2.15}$$

The σ-profiles of pure or mixed solvent S can be derived as weighted sum of mole fraction of the σ-profiles of its compound in combination with normalization of a surface,

$$p_s(\sigma) = \frac{p_s(\sigma)}{\sum_{i \in S} x_i A^{X_i}} \tag{2.16}$$

As the solvents interaction can be described by $p_s(\sigma)$, the chemical potential of the surface segments can be calculated by equation 2.17,

$$\mu_s(\sigma) = -\frac{RT}{a_{eff}} \ln \left[\int p_s(\sigma') exp\left(\frac{a_{eff}}{RT} (\mu_s(\sigma') - E_{misfit}(\sigma, \sigma') - E_{HB}(\sigma, \sigma')) d\sigma' \right] \right. \tag{2.17}$$

Where $\mu_s(\sigma)$is a measure for the affinity of the system S to a surface of polarity σ. It is a characteristic function of each system and is called σ-potential. The vdW energy can

be added in the reference energy in solution as it does not include in equation 2.17. Next, the pseudo-chemical potential of compound X_i in the system S can be calculated by integration of $\mu_s(\sigma)$ over the surface compound. An additional volume and area based on combinatorial term $\mu_{C,S}^{X}$ is added for consideration of differences in size and shape of the molecules of the system.

$$\mu_S^X = \mu_{C,S}^X + \int p^X(\sigma)\mu_S(\sigma)d\sigma \quad (2.18)$$

By using equation 2.18, chemical potential of all compounds in a mixture can be calculated and various properties of thermodynamic can be defined such as activity coefficient, solubility and henry's law constant.

2.6.2 Application of COSMO-RS for screening of solvents

Recently, the role of chemical structure in the prediction of thermodynamic properties, physical and transport properties and physicochemical properties has been the important subject of research. Reports on successful application of COSMO-RS model for screening of selection solvents in chemical engineering are tremendous. Mohanty et al. use selectivity at infinite dilution to predict the best extractant for phenol from aqueous solution among 416 possible ionic liquids. Activity coefficient at finite dilution approach was used to describe ionic liquids (Mohanty, Banerjee, & Mohanty, 2010). COSMO-RS is also applied to predict the basicity of aqueous amine solutions and the species distribution in the amine-H_2O-CO_2 system. Yamada et al. reported that the predictions of pKa values for 25 amines were compared at different density functional theory (DFT) levels for optimization of geometry and found that DFT-COSMO calculation at BP/TZVP give the best and accurate correlation with experimental values (Yamada et al., 2010).

Mustapha et al. screened more than 2000 solvents for CO_2 absorption technology using COSMO-RS method. The four group comprised of amine solvents, neutral solvents, ionic

liquids and mixed solvents. Several thermodynamic properties such as Henry's law constant, solubility in water, vapor pressure and octanol-water partition were used in selecting the best solvents for CO_2 capture (Mustapha, Okonkwo, & Waziri, 2013). Sumon et al. explained the effect of structure, properties and interactions of molecule on selectivity and solubility ionic liquids in CO_2 by using Henry's law constants, activity coefficient at infinite dilution, enthalpies and entropies of solvations using COSMO-RS. It was reported that sigma profiles and sigma-potentials of solvents are valuable tools for a priori solvent characterization (Sumon & Henni, 2011).

Anantharaj et al. studied properties of global scalar such as global hardness, chemical potential, electronegativity, chemical hardness, HOMO-LUMO energy gap and HOMO-LUMO energies for groups comprising ionic liquids with pyridine and thiophene. For validation purpose, the properties of global scalar give the same trend with the COSMO-RS predicted of activity coefficient in infinite dilution (Anantharaj & Banerjee, 2010). Freire et al. explored the capability of COSMO-RS predictive by utilizing predicted value of the molar Gibbs free energy and molar enthalpy of water solution for relating the water-perfluorocarbon molecular interactions. Based on their results, COSMO-RS is shown to be valuable model to give realistic predictions of the values of solubility and to define dependency of their structural modifications and temperature (Freire et al., 2010).

2.6.3 Quantum chemical method for the evaluating of solvent

Through quantum chemical calculation, σ-potential and σ-profile can be used to extract information regarding interacting species which is based on electron affinity and charge distribution. The σ- profile, p(σ) is the distribution of probability of surface area that has charge density σ. It is used to obtain the interaction energy on the surface between pairs of segments. The σ -profile can estimate the electronic interactions and the hydrogen bond of the COSMO-RS model. The ideal screening charge density of most of the

molecules is within -0.0025 e/Å^2 to 0.0025 e/Å^2. Therefore, the σ-profile is usually reported as a histogram of surface's segment in the charge density range of -0.0025 e/Å^2 to 0.0025 e/Å^2 (Y. S. Zhao, Huang, Zhang, & Zhang, 2015).The σ-potential, μ(σ) is a measure for the affinity of the solvent to a polarity of molecular surfaces. The σ-potential describes the solvent behavior regarding electrostatics, hydrogen bond affinity and hydrophobicity. The σ-potential is determined from an equation derived by Klamt for the chemical potentials of segments with charge density σ in the ensemble S (Lapkin et al., 2010).

Lapkin et al. used COSMO-RS approach in screening new solvents for extraction process of artemisinin (Lapkin et al., 2010). In this work, the screening charge density, distribution profile and surface chemical potential distribution were used as a parameter in the analysis for a solvent. Mohanty et al. reported that σ- profile and σ-potential give a good qualitative screening in terms of hydrogen bonding effect between phenol and ionic liquids interaction for extraction purpose (Mohanty et al., 2010). In another report by Schurer et al., σ-profile was used for preliminary screening of a series of fullerenes and polyhydroxylated C_{60}-fullerenes to characterize the adsorption behavior between small molecules and activated carbon (Schurer & Peukert, 2005). Palomar et al. stated that σ-profiles of the ion paired molecules provide qualitative prediction in analyzing the nature effect of anion and cation of ionic liquids on their properties of volumetric (Palomar, Ferro, Torrecilla, & Rodriguez, 2007).

COSMO-RS is a valuable tool especially as a tool for screening of solvents and the fact that it does not need experimental data to do predictions for systems with compounds. Although there are plenty of reports on the application of COSMO-RS to screen and to predict the thermodynamic properties of systems for ionic liquids, there is no report on

the use of COSMO-RS in evaluating and prediction for system of bioglycerol-based solvents containing amino group.

2.7 Thermophysical properties

Thermophysical properties such as density and viscosity of aqueous amines are important for designing treatment equipment and provide a full characterization of these solutions (Sobrino, Concepcion, Gomez-Hernandez, Martin, & Segovia, 2016). Density and viscosity are essential in the rate of mass transfer modelling of regenerators and absorbers as they affect the coefficient of liquid film in contact of mass transfer. Besides, designing heat exchangers and pumps are much easier with better knowledge of the thermophysical properties of the process solvents. From these experimental values, thermal expansion, excess molar volume, Gibbs free energy and activity coefficient can be calculated (Kassim et al., 2016).

2.7.1 Density

Density is defined as the mass of fluid per unit volume. For a solution, it is a summation of density for each components in that solution. In the SI system, the density unit is kg/m^3.

$$\rho = \frac{m}{v} = \sum_i \rho_i \tag{2.19}$$

Where;

m is mass, v is volume.

From 1992 to 2003, these period of time has been very rewarding for the experimental study of different thermophysical properties of aqueous alkanolamines especially blended-amine. This gives great interest for purification of sour gas streams (Rebolledo-Libreros & Trejo, 2006). Leo et al. discussed the density of aqueous mixtures of glycerol

and MDEA, glycerol and MEA, glycerol and piperazine, and glycerol and [bmim][DCA] at temperature of 313.15 K, 333.15 K and 353.15 K at atmospheric pressure. It was found that the density of the mixtures increased with increasing concentration of glycerol (Leo et al., 2016). Ahmady et al. presented the atmospheric pressure density of MDEA+[bmim][BF_4] solutions from 303.15 K to 333.15 K at concentration of 0-2 M [bmim][BF_4]. It was found that as the concentration of [bmim][BF_4] increases, the density of solution also increases while as the temperature of the system increases, the density of solution decreases (Ahmady, Hashim, & Aroua, 2011).

2.7.2 Viscosity

Viscosity can be defined as a resistance of the growth of shear deformation. This resistance is caused by intermolecular friction employed when the layers of fluids attempt to slide. This property is important especially for their practical applications related to heat transfer and fluid flow (Murshed & Estellé, 2017). Fluids in which shear stress is directly proportional to the rate of deformation are Newtonian fluids whereas non-Newtonian fluids are fluids in which shear stress is not directly proportional to shear rate. Generally, there are two types of viscosity which are dynamic and kinematic viscosity. Dynamic viscosity is a tangential force per unit area required to move one horizontal plane with respect to the other at unit velocity when maintained a unit distance apart by the fluid. In the SI system, the dynamic viscosity units are Pa.s or kg/m.s. Kinematic viscosity is the ratio of dynamic viscosity to density. In the SI system, the kinematic viscosity unit is m^2/s (Bashirnezhad et al., 2016).

Rebolledo et al. evaluated viscosity of aqueous blends of three alkanolamines composed of 32.5 mass % MDEA and 12.5 mass% DEA with 2, 4, 6, 8 and 10 mass% AMP in the temperature range of 303.15 K to 343.15 K. As the result, the values of viscosity increase as the concentration of AMP increase (Rebolledo-Libreros & Trejo,

2006) . Nookuea et al. measured the viscosity of MDEA-[bmim][BF_4] aqueous mixtures at various temperatures and concentrations. It was found that the viscosity increases with an increases in [bmim][BF_4] concentration but decreases with an increases in temperature. Besides, the impact of temperature on the viscosity is more significant at low temperature range (Nookuea et al., 2017).

2.8 Henry's law constant for alkanolamines solvent

Physical solubility data of CO_2 in aqueous alkanolamines plays important role in evaluating mass transfer and kinetic data, also in simulating and modelling the absorption of CO_2 into and desorption from aqueous amine. As CO_2 can chemically react with these solvents, a physical solubility of CO_2 in any aqueous amines cannot be measured directly and is generally evaluated by using the N_2O analogy. N_2O has similar mass, molecular interaction and structure as CO_2 but N_2O is inert when in contact with any aqueous amines (Monteiro & Svendsen, 2015). Therefore, the solubility of N_2O in aqueous amines can be determined experimentally and correlated to the solubility of CO_2 in the same aqueous amines using below equation 2.20 (Penttilä, Dell'Era, Uusi-Kyyny, & Alopaeus, 2011),

$$H_{CO_2,solution} = \frac{H_{CO_2,water}}{H_{N_2O,water}} H_{N_2O,solution} \quad (2.20)$$

Where, $H_{N2O,solution}$ is the Henry's law constant of N_2O in the aqueous amine, $H_{CO2,solution}$ is the Henry's law constant of CO_2 in the aqueous amine, $H_{N2O,water}$ is the Henry's law constant of N_2O in water and $H_{CO2,water}$ is the Henry's law constant of CO_2 in water.

Reports on application of N_2O analogy to evaluate the physical solubility of CO_2 in aqueous amines are remarkable. Saha et al. reported N_2O analogy was used to estimate the solubility and diffusivity of CO_2 in ranging concentration from 0.5M to 2M of 2-amino-2-methyl-1-propanol solution at atmospheric pressure and over a range of

temperature. The Henry's law constant of N_2O in aqueous 2-amino-2-methyl-1-propanol changes linearly with concentration and temperature (Saha, Bandyopadhyay, & Biswas, 1993). Lee et al. also investigated the physical solubility of N_2O and CO_2 in aqueous sodium glycinate of mass fraction from 0.1 to 0.5 at temperature from 303.15 K to 323.15 K by the well-known N_2O analogy. Based on his investigation, the physical solubility increases as the temperature and mass fraction decrease while the diffusivity increases with an increase in temperature and decreases in mass fraction (S. Lee et al., 2006).

2.9 Regeneration of alkanolamines solvent

Amine-based solvent for CO_2 chemical absorption is the most promising CO_2 capture solvent. However, regenerating the CO_2-rich solvent consumes high energy is still the main challenge as the heat input of reboiler to regenerate the rich solvent is crucial for the overall efficiency of this process. Therefore, it is important to develop new solvents which are capable to reduce the heat requirement for solvent regeneration. In recent years, some researchers expected that as the solute concentration of rich-CO_2 solvents increases, the energy cost for the regeneration can be reduced. Generally, an increase in concentration of solute for CO_2 rich solvent may increases the driving force of regeneration consequently increases the equilibrium partial pressure of CO_2 over the rich solvent at a given temperature and loading of CO_2. Therefore, the performance of regeneration can be improved. Nevertheless, high concentration can accelerate the corrosion of absorber, increase in solvent viscosity and reduce the driving force of CO_2 absorption (Yan, He, Ai, Wang, & Zhang, 2013).

Li et al. conducted experimental study of energy requirement for CO_2 desorption from rich solvent. In his study, there are 5 important parameters for regeneration process including flow rate of rich solvent, concentration of MEA, temperature of feeding solvent, loading of rich solvent and temperature of reboiler. The energy of regeneration was found

to reduce with increasing concentration of MEA, increasing temperature of the feeding solvent, increasing the loading of rich solvent, decreasing the temperature of reboiler and using a blended of aqueous MEA/MDEA (X. F. Li, Wang, & Chen, 2013). Nwaoha et al. discovered the contribution of heat of absorption, sensible heat and heat of vaporization towards the regeneration energy of AMP-MDEA-DETA tri-solvent blends. Results showed that the blend of tri-solvents have lower energy of regeneration than pure MEA due to a lower sensible heat of the blends. In addition, higher heat of absorption does not necessarily indicate higher energy of regeneration. The sensible heat and heat of vaporization can significantly affect the energy of regeneration (Chikezie Nwaoha et al., 2017).

Zhang et al. investigated the regeneration behavior of a sterically hindered amine of 2-amino-2-methyl-1-propanol (AMP). Based on this report, the regeneration efficiency increased from 86.2 % to 98.3 % within the temperature range from 358 K to 403 K and the most regeneration temperature for AMP was 383 K. The aqueous AMP was easier to regenerate than MEA, DEA, diethylenetriamine (DETA) and MDEA with the regeneration efficiency reduced from 98.3 % to 94.0 % (P. Zhang, Shi, Wei, Zhao, & Ye, 2008).

2.10 Summary

The percentage of greenhouse gases has remarkable increased since the Industrial Revolution in 1750 (Takht Ravanchi & Sahebdelfar, 2014) whilst the regulations are becoming stricter in setting the limits for global CO_2 concentration. Among the methods for CO_2 capture, absorption by chemical solvent (in particular alkanolamines) is a good approach because the selectivity by chemical absorption is comparatively high. Other solvents that were researched are mixed amine-based solvents, ammonia-based solvents and ionic liquids. In addition, bioglycerol has been researched as the CO_2 capture solvent.

However, the reported use of bioglycerol-derived solvent is very limited. Aqueous serinol is applicable for CO_2 removal at low pressure but there is no further research on aqueous serinol to capture CO_2 at high pressure. Based on previous researchers, carbamates formed from the reaction of serinol with CO_2 are straightforwardly regenerated (Bougie & Iliuta, 2014). This can reduce consumption of regeneration energy.

On the other hand, COSMO-RS model can be used to evaluate bioglycerol-based solvent as it can save time, cost and energy required to conduct experiments and a reliable method for screening solvent based on prediction of thermodynamic behavior and properties. Thus, in this work, the suitability of aqueous serinol as a potential solvent for CO_2 capture would be evaluated using COSMO-RS model. The solubility of CO_2 in aqueous serinol would be then investigated experimentally to confirm the COSMO-RS results. In addition, densities and viscosities of aqueous serinol would be measured to obtain the thermo physical properties of aqueous serinol. Then, Henry's law constant of CO_2 in aqueous serinol would be determined using N_2O analogy. Aqueous serinol would also undergo reusability evaluation to assess its recyclability.

CHAPTER 3: MATERIALS AND METHODOLOGY

3.1 Introduction

This chapter is divided into two parts which are materials and methodology. First part provides details of the materials involved and solvents preparation while the second part provides details of methodology of this work.

3.2 Materials

N-methyldiethanolamine (MDEA) with a minimum purity of 98.5% and glycerol was purchased from MERCK. The 2-amino-1, 3 propanediol with minimum purity of 98% was purchased from Sigma Adrich. Purified CO_2 and N_2O with a minimum purity of are 99.995% from Linde Malaysia Sdn Bhd.

3.2.1 Preparation of solvents

The aqueous amine with various compositions were prepared using distilled water and measured by analytical balance with accuracy of ±0.001mg. All prepared samples were stored in tightly sealed bottles to avoid any absorption of atmosphere moisture. All compositions for solvents were summarized in Table 3.1.

Table 3.1: Composition of solvents

Solvents	Composition
N-methyldiethanolamine	2M
2-amino-1, 3 propanediol	1M, 2M and 3M
Glycerol	3M

3.3 Methodology

3.3.1 COSMO-RS: Computational details

COSMO-RS is a two-step approach (A. Klamt, 2016). Firstly, geometry optimization of structure for solvents and CO_2 has been performed using the TURBOMOLE program

package. This program package was used to draw the initial structure of serinol, MDEA, water and CO_2. The optimized structure was obtained using Hartree-Fock level of theory and 6-31G* basis set. Level of theory Hatree-Fock was chosen because it gives accurate value for energy of orbital and 6-31G* basis set was used because it calculates effect of polarization of the species. After the step of geometry optimization, a calculation of single point was conducted with the generation of the *.cosmofile* using the density functional theory (DFT) level, utilizing the Becke-Perdew functional with TZVP (triple zeta valence potential) approximation and a basis set of 6-31G* (Hizaddin, Hashim, & Anantharaj, 2013; Kassim et al., 2016; Mortazavi-Manesh, Satyro, & Marriott, 2011). In here, TZVP was employed because it provides more useful value of hydrogen bond interaction which is important interaction between CO_2 and solvents. The generated *.cosmo* files were used for COSMO-RS calculation in the COSMOthermX software package to obtain statistical thermodynamics of the molecular interactions of serinol, MDEA, water and CO_2.

3.3.2 CO_2 absorption at high pressure

3.3.2.1 CO_2 absorption setup

The CO_2 absorption experiment was performed using experimental set up as in Figure 3.1. Parr Honeywell FPG high pressure reactor cell, Columbus can tolerate up to 373 K and 4000 kPa. For CO_2 absorption, the temperature was varied from 313.15 K, 333.15 K and 353.15 K and the pressure was set at 1034.31 kPa, 1378.95 kPa, 1723.69 kPa and 2068.43 kPa. The solubility experiment begun by removing the air out from the gas reservoir by adequately streaming CO_2 all through the system. The gas reservoir was loaded with purified CO_2 from the CO_2 gas cylinder and was heated and pressurized to the predetermined condition.

Once the temperature of the gas reservoir was steady, a 20 ml of aqueous amine was loaded in the high pressure reactor cell. The reactor was heated to a required temperature

and kept constant throughout the process. The pressure was automatically recorded during the process until equilibrium was reached. Equilibrium was assumed to be reached when the pressure was constant for 30 minutes. Three equilibrium samples were taken to ensure consistency at a given temperature and the values were reported as an average.

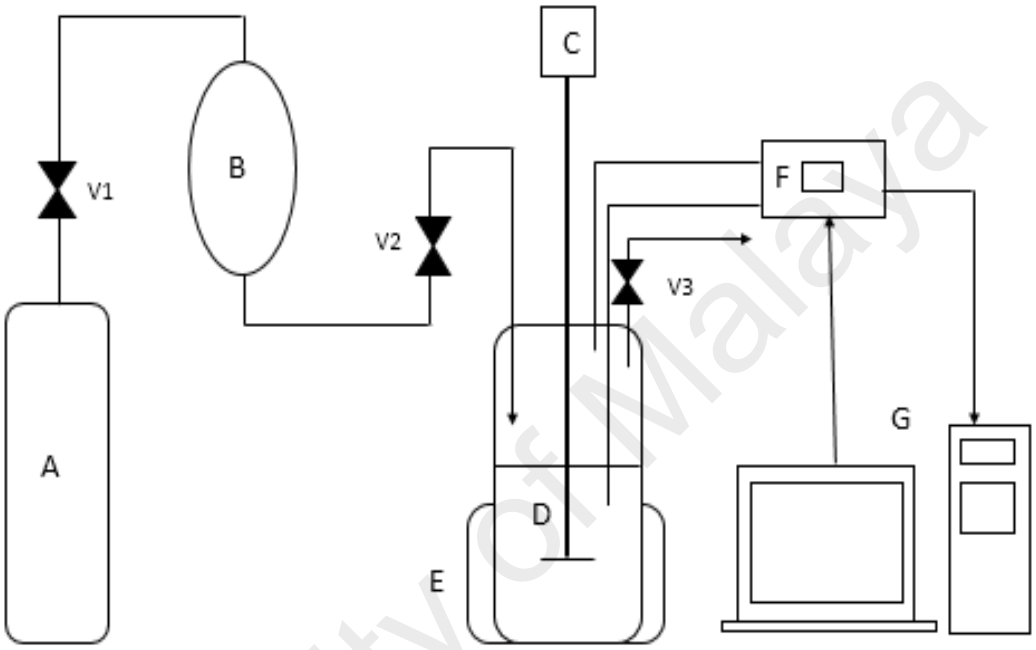

Figure 3.1:A diagram of the experimental set up: A, gas cylinder; B, gas reservoir; C, motor; D, high pressure reactor cell; E, heater; F, controller; G, computer; V1, control valve; V2, needle valve; V3, pressure relief valve

3.3.2.2 CO_2 loading calculation techniques

The differences in moles of CO_2 throughout the absorption were computed using initial and equilibrium pressures. The solubility was conveyed as mol CO_2 per mole of total absorbent or mass of absorbent. Three equilibrium samples were taken to check the consistency at a given temperature. The solubility was calculated using equation 3.1 and equation 3.2 as follows:

$$\alpha = \frac{\left[\frac{P_{Ti}-P_{Vi}xV_{gc}}{zRT}\right]-\left[\frac{\left(P_{Tf}-P_{Vf}\right)x\left(V_{gc}+\left(V_{cell}-V_{sol}\right)\right)}{zRT}\right]}{n_{total}} \quad (3.1)$$

$$\chi = \frac{\left[\frac{P_{Ti}-P_{Vi}xV_{gc}}{zRT}\right]-\left[\frac{\left(P_{Tf}-P_{Vf}\right)x\left(V_{gc}+(V_{cell}-V_{sol})\right)}{zRT}\right]}{m_{total}} \quad (3.2)$$

Where;

α = CO_2 loading in mol of CO_2/total mol of absorbent (mol/mol)

χ = CO_2 loading in mol of CO_2/ total mass of absorbent (mol/kg)

P_T = total pressure (kPa)

P_v = solution vapor pressure (kPa)

V_{gc} = volume of gas container (L)

V_{sol} = volume of solution (L)

V_{cell} = volume of cell (L)

R= Gas constant, 8.3145 (kPa. L/ mol. K)

T= Temperature of the system (K)

z = compressibility factor

i = initial condition

f = final condition

n_{total} = total moles of absorbent in the liquid phase (mol)

m_{total} = total mass of absorbent in the liquid phase (kg)

Based on temperatures (313.15 - 353.15 K) and pressures (1034.31- 2068.43 kPa) to determine CO_2 solubility, z, compressibility factor values are close to 1. Therefore, z value is chosen to be 1 for the ease of the calculation.

3.3.3 Density measurement

A digital density meter DM40 from Mettler Toledo was used to measure the densities of the aqueous serinol with accuracy of ±0.001g/cm^3. The measurements were made at temperature range of 298.15 K to 333.15 K with concentration 1M, 2M and 3M at constant atmospheric pressure. Each set of experiments was repeated three times in order to ensure accuracy and the values were reported as an average.

3.3.4 Viscosity measurement

Viscosities of aqueous serinol were measured using a BROOKFIELD LV DV-II+Pro EXTRA viscometer. Three measurements were made to obtain an average value of viscosity for each sample at each experimental concentrations of 1M, 2M and 3M while temperature of range of 298.15 K to 333.15 K at atmospheric pressure. Temperature of the aqueous serinol was maintained within ±0.1 K.

3.3.5 N_2O analogy experiment

The experimental setup to measure the N_2O solubility of aqueous serinol was using the same experimental setup to determine the CO_2 absorption aqueous amine (see Figure 3.1). For this part, N_2O gas was used instead of CO_2 gas. For N_2O absorption, temperature was varied from 313.15 K and 333.15 K while pressure was set to 1034.31 kPa, 1378.95kPa, 1723.69 kPa and 2068.43 kPa at concentrations of 1M and 3M aqueous serinol.

3.3.6 Solvent regeneration

For regeneration process, the rich aqueous serinol was heated at temperature of 363.15K for 60 minutes. The regeneration of aqueous serinol was conducted at temperature 313.15 K for a concentration of 3M aqueous serinol and the pressure were set to 1034.31 kPa, 1378.95 kPa, 1723.69 kPa and 2068.43 kPa using similar experimental set up as CO_2 absorption experiment. This process was performed three (3) cycles to investigate the stability of the solutions.

The regeneration efficiency can be calculated using equation 3.3 (P. Zhang et al., 2008) as follows

$$\eta = \frac{\alpha'}{\alpha} x100\% \quad (3.3)$$

Where, α' is the saturated absorption capacity of regeneration aqueous serinol and α is the saturated absorption capacity of fresh aqueous serinol.

CHAPTER 4: RESULTS AND DISCUSSION

4.1 Introduction

In this chapter, molecular interaction of serinol, MDEA, water with CO_2 using COSMO-RS are discussed in terms of σ – profiles and σ – potentials. For further investigation, the ability of aqueous serinol in capturing CO_2 at high pressure between 1034.31 kPa to 2068.43 kPa with temperature range from 313.15 K to 353.15 K and concentration of 1M, 2M and 3M aqueous serinol were measured experimentally. The density and viscosity of aqueous serinol were also measured at concentration of 1M, 2M and 3M and at temperature range from 298.15 K to 333.15 K. Then, Henry's law constant of CO_2 in 1M and 3M aqueous serinol were investigated using N_2O analogy at high pressure between 1034.31 kPa to 2068.43 kPa with temperature at 313.15 K and 333.15K. Finally, the regeneration performance of 3M aqueous serinol at elevated pressure between 1034.31 kPa to 2068.43 kPa at fixed temperature of 313.15 K were evaluated.

4.2 COSMO-RS

4.2.1 Qualitative prediction of solvents using σ – profiles and σ – potentials

The structures of the serinol, MDEA, water and CO_2 according to the COSMO energy are shown in Figure 4.1 to Figure 4.4. Water and MDEA are selected for the purpose of validation of the theoretical approach. This visualization is a beneficial tool for molecular design that allow the identification of structures of molecule either aid or hinder absorption of CO_2 (Jones, Connolly, Klamt, & Diedenhofen, 2005). The areas of strongly positive molecular polarity are colored blue. The regions of strongly negative molecular polarity are colored red while neutral regions of the molecules in which σ close to zero are colored green (Thormann, Klamt, Hornig, & Almstetter, 2006).

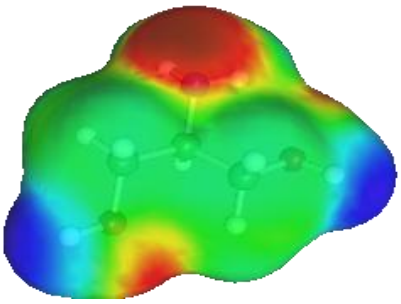

Figure 4.1: Screening charge density for serinol

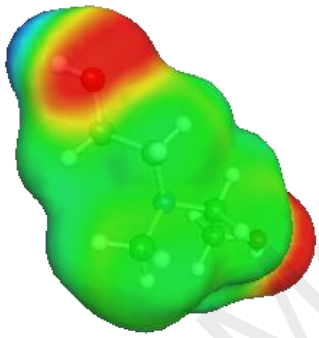

Figure 4.2: Screening charge density for MDEA

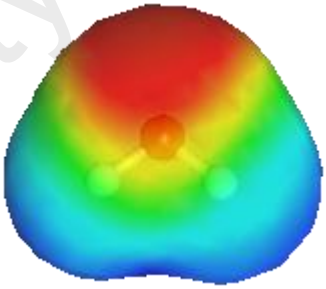

Figure 4.3: Screening charge density for water

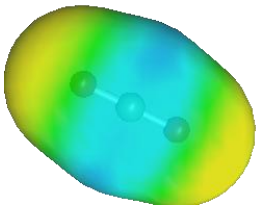

Figure 4.4: Screening charge density for CO_2

Figure 4.5 illustrates the σ-profile for serinol, MDEA, water and CO_2. σ-profile is divided into 3 regions which are hydrogen bond donor region (σ<-0.0082 e/Å^2), nonpolar region (-0.0082< σ< 0.0082 e/Å^2) and hydrogen bond acceptor region (σ>0.0082 e/Å^2) (Banerjee & Khanna, 2006).The σ-profile can estimate the electronic interactions and the hydrogen bond of the COSMO-RS model. In Figure 4.5, serinol presents a peak at +0.012e/Å^2 within the hydrogen bond acceptor region originated from the amino group, which displays its capability as a hydrogen bond acceptor. Besides, serinol shows a peak at -0.016 e/Å^2 within the hydrogen bond donor region, which corresponds to a hydrogen atom from the hydroxyl group. A peak at -0.002 e/Å^2 within the non-polar region is due to the 3 carbon atom bonded acting as a backbone of serinol.

In the other hand, MDEA shows the highest peak at -0.002 e/Å^2 within the non-polar region due to 4 carbon atom bonded in between nitrogen atoms. The higher number of bonded carbon atoms implies an increase scattering of the charge densities around the non-polar area (Palomar, Torrecilla, Ferro, & Rodriguez, 2008). Whereas a peak at +0.016 e/Å^2 in the hydrogen bond acceptor region attributed to the amino group. Additionally, MDEA presents a peak at -0.014 e/Å^2 within the hydrogen bond donor due to the oxygen atom of the hydroxyl group.

Based on σ-profile of serinol and MDEA, a larger scattering of screening charge density around the hydrogen bond acceptor region designates the capability of serinol and MDEA to behave as bases. Therefore, it is expected that any compound containing hydrogen bond donors groups is able to develop intermolecular interactions with serinol and MDEA. In addition, water is a polar solvent. The sigma profile for water is symmetric and wide. This indicates a favorable electrostatic interaction of water with itself, which explains its high surface tension and boiling point.

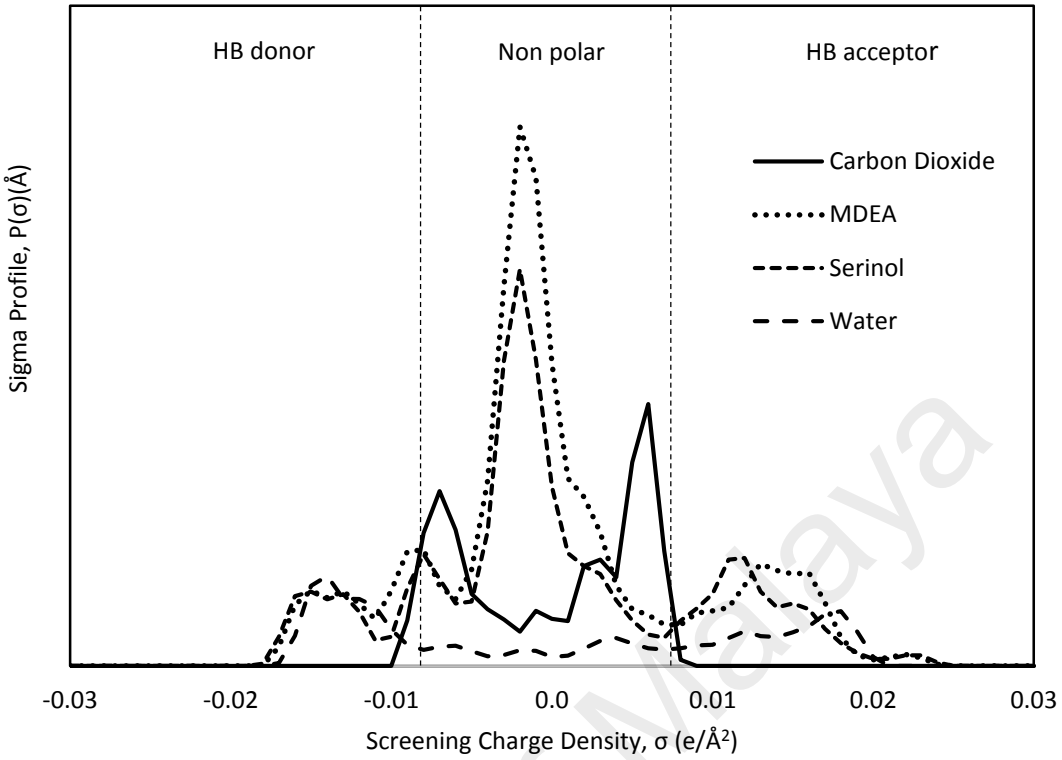

Figure 4.5: σ-profile for serinol, MDEA, water and carbon dioxide

The σ – potential in Figure 4.6 explains the behavior of serinol, MDEA, water and CO_2 based on HB-affinity and hydrophobicity (Mehler, Klamt, & Peukert, 2002). MDEA, serinol and water present negative at both $\sigma<-0.0082$ e/Å^2 and $\sigma>0.0082$ e/Å^2 which mark affinity at hydrogen bond acceptor and hydrogen bond donor regions. This shows that serinol and MDEA have good affinity towards hydrogen-bond donors due to the values of σ – potential which turns negative competitively faster outside the region of sigma cutoff for hydrogen bonding. While the values of σ – potential for serinol and MDEA are close to the negative part of the non-polar region, water has positive value in this region. This indicates the attempt of the non-polar molecule to move into serinol and MDEA, but not into water. Hydrophobicity is a characteristic, which arises from the strong and stable hydrogen bond interactions in water. CO_2 displays a positive value at $\sigma<-0.0082$ e/Å^2 and $\sigma>0.0082$ e/Å^2 corresponds to no affinity to hydrogen bond acceptor and hydrogen bond donor. The σ – profile and σ – potential of CO_2 with serinol, MDEA and water were

plotted together in order to illustrate the interactions between these solvents and CO_2. It can be observed that the σ – profile and σ – potential of serinol and CO_2 are complementary which indicates mutual interactions between them.

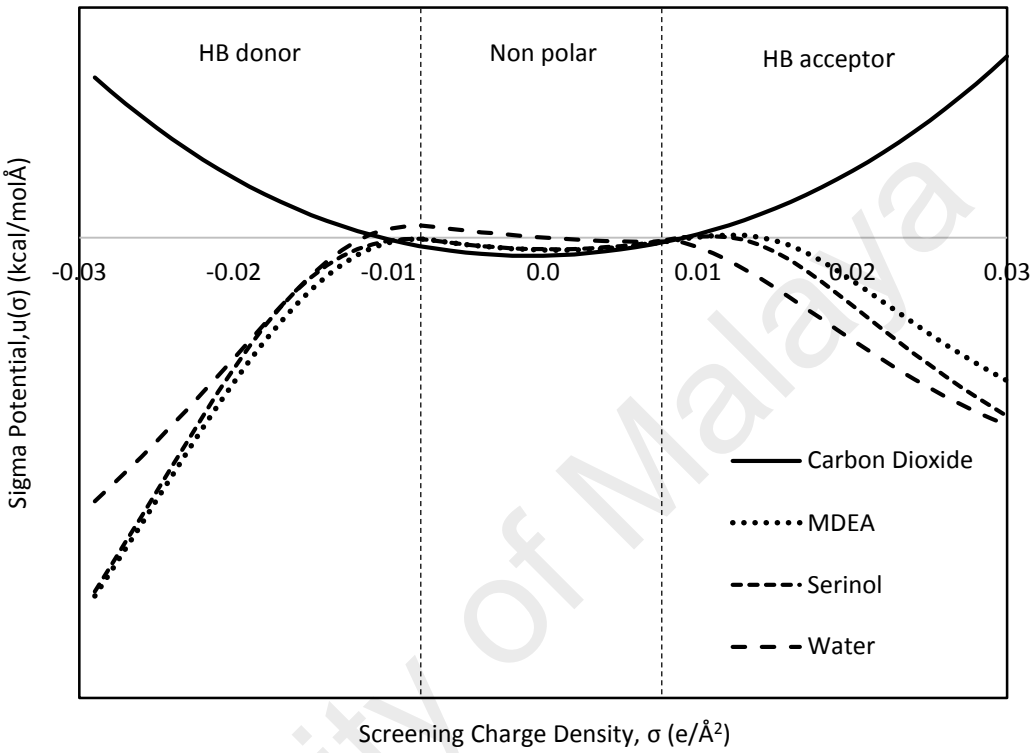

Figure 4.6: σ-potential for serinol, MDEA, water and carbon dioxide

COSMO-RS interprets the results of quantum chemical calculations into something more familiar to the practitioners of chemical engineering. COSMO-RS method provides a visualization of the screening charge density of the molecular structures of solvents through σ – profile. Particularly, σ – profile provides the main chemical information necessary to predict the possible hydrogen-bonding and electrostatic interaction between serinol and CO_2. According to σ – profile, serinol is capable to capture CO_2 due to comparable σ – profile with MDEA except for a small difference in peak height. This small difference in peak height is due to the amino group is located between the two hydroxyl groups which form steric hindrance around it (Bougie & Iliuta, 2014). The σ – profiles of serinol and CO_2 being complementary in nature, show the solubility of CO_2 in

serinol. In addition, the σ – potential measures the affinity of serinol and MDEA to CO_2. The overall negative sigma value of serinol suggests stability due to hydrogen bonding. This is because the negative value of the sigma potential designates hydrogen bonding interaction. The higher negative value of serinol leads to a hydrogen bonding between acceptor parts of serinol and the donor parts of CO_2. It is good to compare σ – profile and σ – potential of serinol and MDEA with CO_2 as MDEA remained the benchmark for current industrial standard solvent to capture CO_2 especially at high pressure. Therefore, for further investigations, experimental methods should be conducted to validate and examine the potential of serinol in absorption of CO_2 at different concentrations, pressures and temperatures.

4.3 CO_2 absorption capacities at high pressure

4.3.1 Validation of CO_2 absorption measurement

A few runs for CO_2 absorption using 2M MDEA at 313.15 K were conducted to confirm the accuracy of the measurements and to validate the experimental set up apparatus for this study. These data were compared with literature data as shown Figure 4.7 and it is found that both literature and experimental data has deviation of 1.386% in the solubility of CO_2 by using average absolute deviation equation 4.1 (Aziz, Yusoff, & Aroua, 2012).

$$AAD = \frac{1}{N}\sum_{I=1}^{N}\frac{|X_{exp,i}-X_{lit,i}|}{X_{lit,i}} x\ 100 \quad (4.1)$$

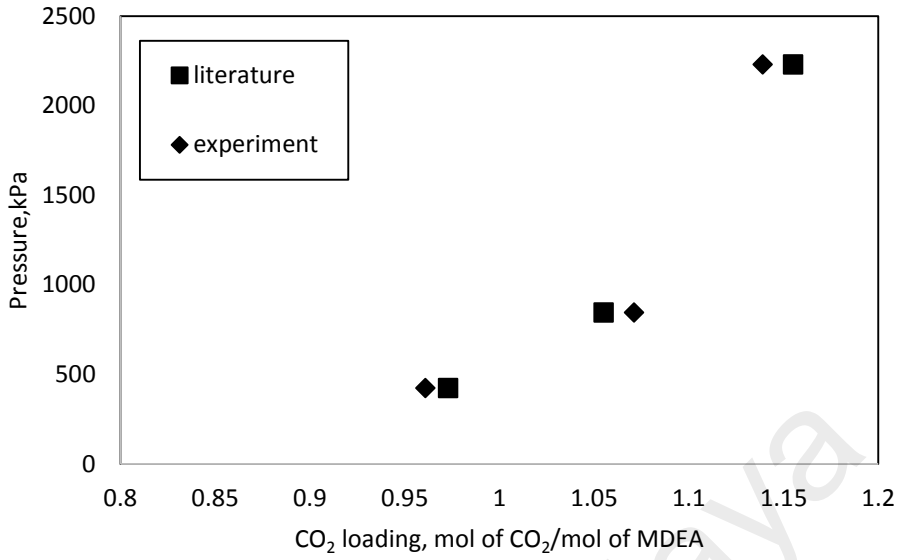

Figure 4.7: Comparison of CO_2 loading at 313.15 K in 2M MDEA between literature data (Aziz et al., 2012) and experimental data

4.3.2 Temperature effect on solubility

Figure 4.8 to Figure 4.11 display the effect of temperature on CO_2 solubility at partial pressure of CO_2 from 1034.31 kPa to 2068.43 kPa and concentration of aqueous serinol from 1M to 3M. All figures illustrate CO_2 solubility decreases with increases in temperature. The decrement in CO_2 solubility of aqueous serinol as temperature increases indicated more CO_2 was present in a solution at a lower temperature compared to a solution with a higher temperature. However, as the temperature approaches 353.15 K, the differences in the CO_2 solubility at concentration 1M and 2M of aqueous serinol became smaller. Based on the viscosity of aqueous serinol in Figure 4.23, as the temperature approaches 333.15 K, the differences in the viscosities became smaller particularly at concentration 1M and 2M of aqueous serinol. This will give effect to CO_2 loading within these temperature and concentration ranges.

The process of dissolving of CO_2 in solution is an exothermic process while the process of breaking the CO_2 molecules from solution is an endothermic process. When heat is added into the solution, this heat energy decreases the attractive forces between

the CO_2 gas and the solution molecules. This caused more motion molecules which break intermolecular bonds and escaped from solution. Thus, reducing CO_2 solubility in the solution.

Moreover according to Van't Hoff's law of dynamic equilibrium, as the temperature in the system increased, the system will be shifted to the new equilibrium condition which is more towards heat of absorption. As the absorption of CO_2 in aqueous serinol solution is an exothermic process, the solubility of CO_2 decreases as the temperature increases.

These experimental results show a complete agreement with the previous work by Shen and coworkers (Keh Perng Shen & Meng Hui Li, 1992).It was reported that solubility of CO_2 in MDEA aqueous solution increased as temperature decreased. The solubility of CO_2 data obtained from [bmim][PF_6] system also has good agreement as reported by Shiflett and coworker (Shiflett & Yokozeki, 2005). As the temperature increased from 283.15 K to 348.15 K, the absorption of CO_2 in ionic liquid decreased.

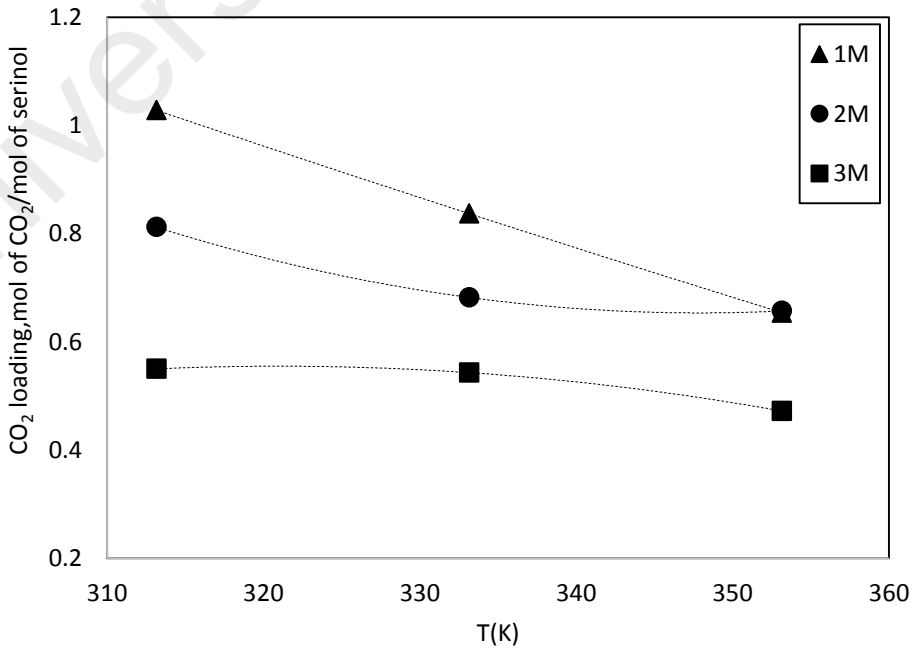

Figure 4.8: The effect of temperature on the CO_2 absorption for 1M, 2M and 3M systems at 1034.31 kPa

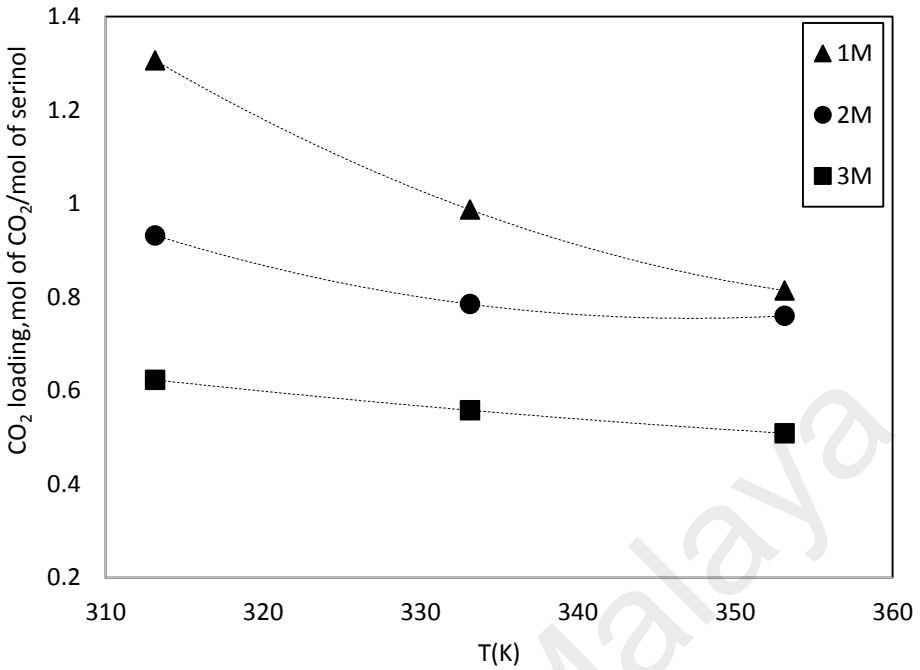

Figure 4.9: The effect of temperature on the CO_2 absorption for 1M, 2M and 3M systems at 1378.95 kPa

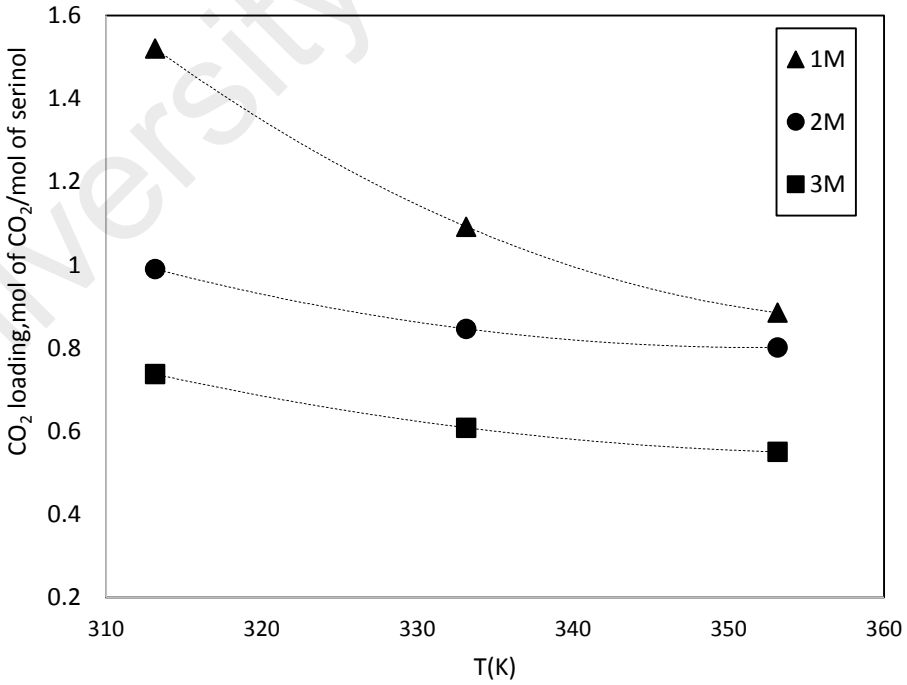

Figure 4.10: The effect of temperature on the CO_2 absorption for 1M, 2M and 3M systems at 1723.69 kPa

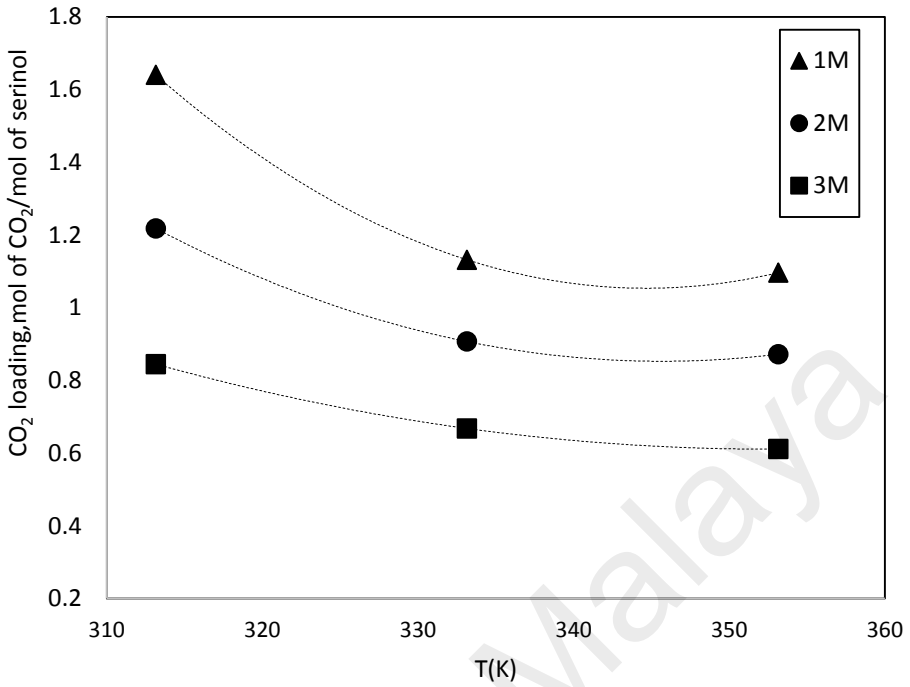

Figure 4.11: The effect of temperature on the CO_2 absorption for 1M, 2M and 3M systems at 2068.43 kPa

4.3.3 Pressure effect on solubility

Figure 4.12 to Figure 4.14 illustrate the effect of pressure on the CO_2 absorption at temperature of system from 313.15 K to 353.15 K and the concentration of aqueous serinol from 1M to 3M. The partial pressure of CO_2 has positive effect on the CO_2 solubility. All figures demonstrate that the CO_2 solubility increased with pressure at each temperature. At temperature system of 353.15 K, the differences in the CO_2 solubility became smaller at lower pressure particularly for concentration 1M and 2M of aqueous serinol. Based on the viscosity of aqueous serinol in Figure 4.23, as the temperature approaches 333.15 K, the differences in the viscosities became smaller particularly at concentration 1M and 2M of aqueous serinol. This will give effect to CO_2 loading within these temperature and concentration ranges.

The increasing trend can be explained by Le Chatelier principle. According to this principle, as the CO_2 partial pressure increases, the system will shift to a new equilibrium condition, which will absorb more CO_2 in order to counteract the effect of increasing CO_2 partial pressure. This will result in a higher CO_2 loading.

The observed trend was expected as a similar trend has been reported in numerous research paper on alkanolamine solutions as shown in the work of Tontiwachwuthikul et al. (1991), Tong et al. (2012) and Khan et al.(2016) (Khan, Halder, & Saha, 2016; Tong, Trusler, Maitland, Gibbins, & Fennell, 2012; Tontiwachwuthikul, Meisen, & Lim, 1991). Tontiwachwuthikul and coworkers reported that the solubility of CO_2 in aqueous 2-amino-2-methyl-1-propanol which is a sterically hindered amines increased with increasing CO_2 partial pressure introduced in the system.

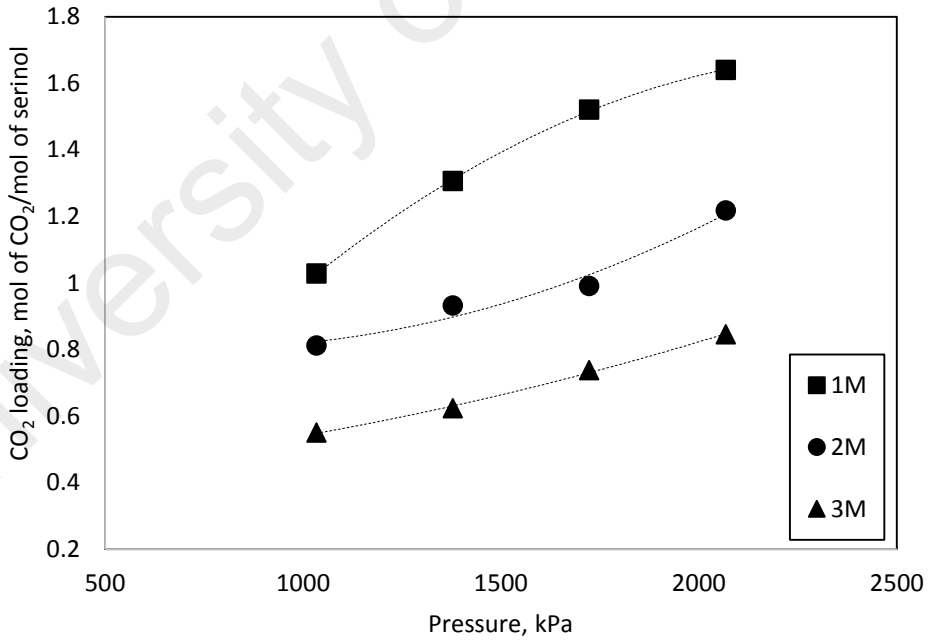

Figure 4.12: The effect of pressure on the CO_2 absorption for 1M, 2M and 3M systems at 313.15 K

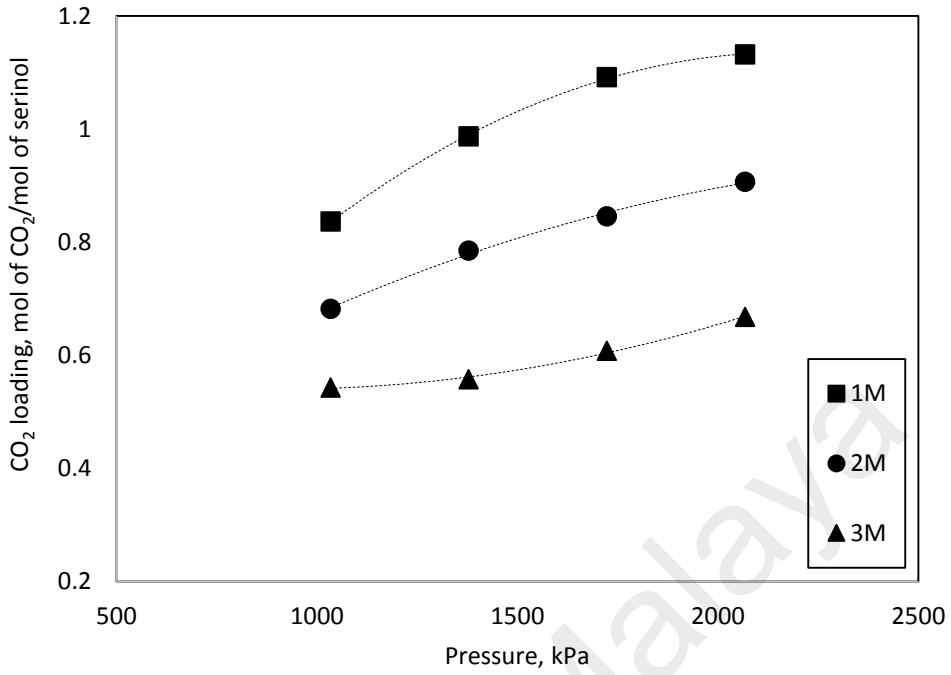

Figure 4.13: The effect of pressure on the CO_2 absorption for 1M, 2M and 3M systems at 333.15 K

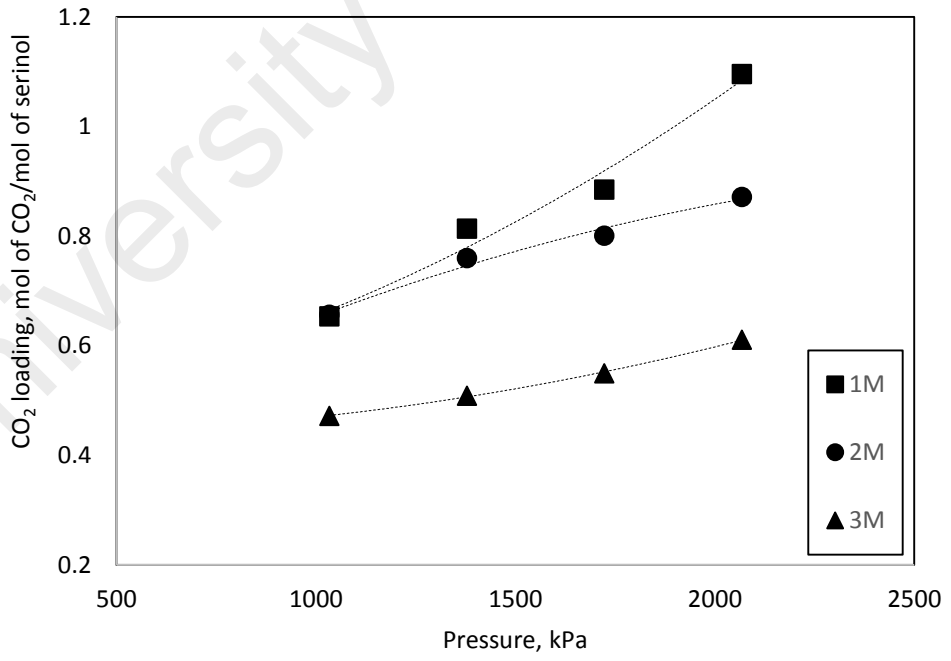

Figure 4.14: The effect of pressure on the CO_2 absorption for 1M, 2M and 3M systems at 353.15 K

4.3.4 Concentration effect on solubility

Figure 4.15 to Figure 4.17 show the effect of concentration on the CO_2 absorption for pressure range from 1034.31 kPa to 2068.43 kPa and temperature from 313.15 K to 353.15 K. Each concentration displays an increasing trend with increasing increment of partial pressure from 1034.31 kPa to 2068.43 kPa. This indicates that at a constant temperature, higher pressures result in higher CO_2 loading. At a given partial pressure of CO_2, higher concentrations of aqueous serinol give lower amounts of absorbed CO_2 per mole of serinol. In addition, at temperature system of 353.15 K, the differences in the CO_2 solubility became smaller at lower pressure particularly for concentration 1M and 2M of aqueous serinol. Based on the viscosity of aqueous serinol in Figure 4.23, as the temperature approaches 333.15 K, the differences in the viscosities became smaller particularly at concentration 1M and 2M of aqueous serinol. This will give effect to CO_2 loading within these temperature and concentration ranges.

Liu et al. analyzed the CO_2 solubility into 1-dimethylamino-2-propanol solution using molar concentrations over the range of 1M to 5M (H. Liu, Gao, Idem, Tontiwachwuthikul, & Liang, 2017). It was found that the CO_2 solubility of 5M 1-dimethylamino-2-propanol decreased drastically in comparison with that of 1M molar concentration. This is in agreement when comparing the trend reported by Maneeintr et al. where the CO_2 loading of aqueous solution of 2-(diethylamino) ethanol decreased as the solution concentration increased (Maneeintr, Phumkokrux, Boonpipattanapong, Assabumrungrat, & Charinpanitkul, 2017).

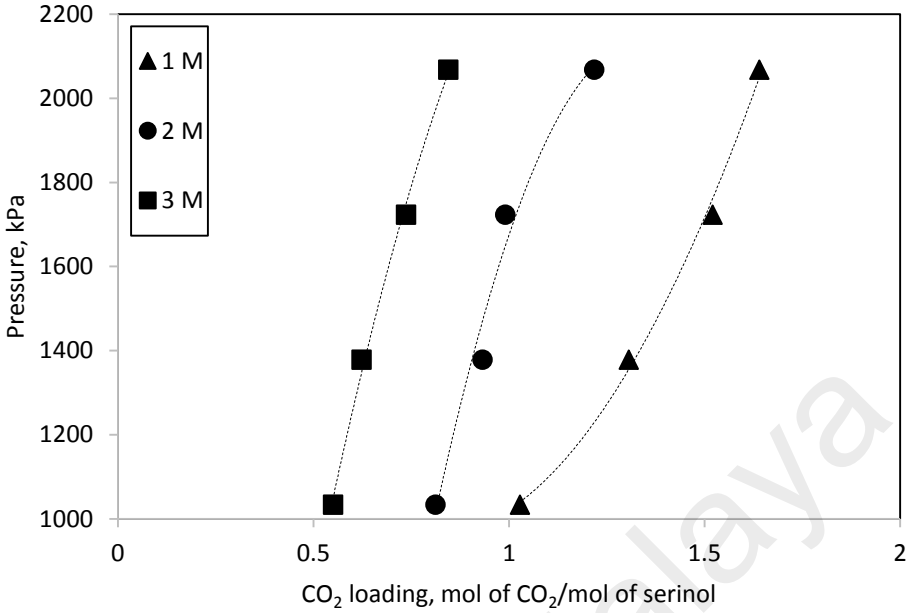

Figure 4.15: The effect of concentration on the CO_2 absorption for pressure from 1034.31 kPa to 2068.43 kPa at 313.15 K

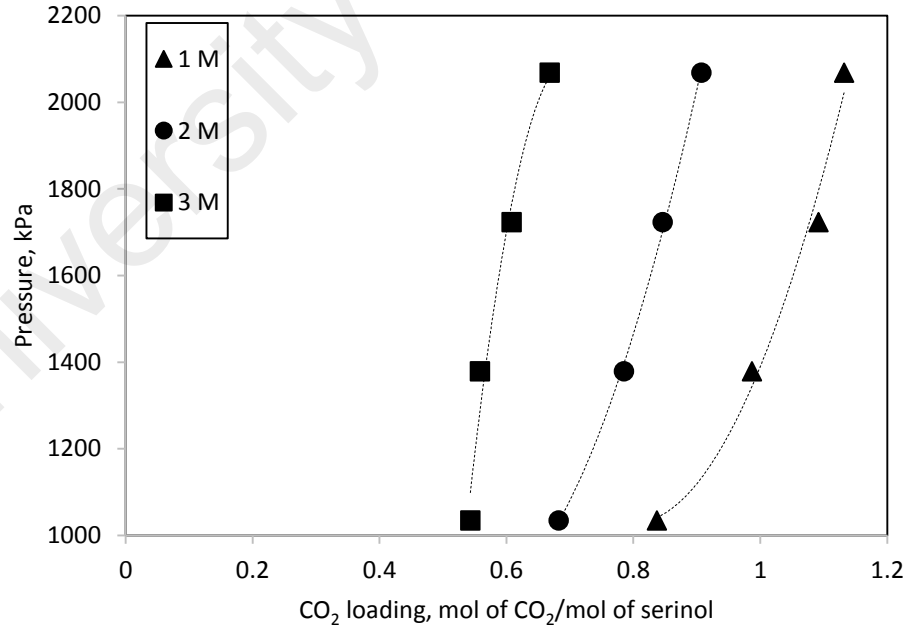

Figure 4.16: The effect of concentration on the CO_2 absorption for pressure from 1034.31 kPa to 2068.43 kPa at 333.15 K

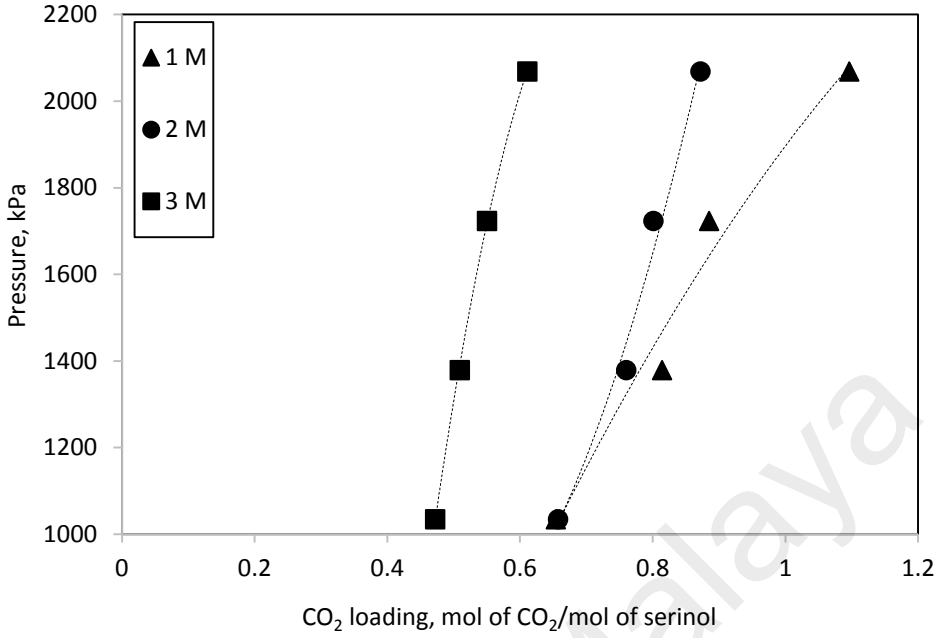

Figure 4.17: The effect of concentration on the CO_2 absorption for pressure from 1034.31 kPa to 2068.43 kPa at 353.15 K

4.3.5 Comparison with literature data

Comparison of the results of this work with the data reported in the literature was made at solution concentration of 3M, temperature of 313.15 K and CO_2 partial pressures up to 2900 kPa as shown in Figure 4.18 and Figure 4.19. 3M of solution concentration is selected due to higher concentration of alkanolamines solvent will reduce the energy cost of regeneration which crucial for the overall efficiency of CO_2 absorption (Yan, He, Ai, Wang, & Zhang, 2013). It is clear that the solubility of CO_2 followed the sequence: [bmim][Tf_2N]<glycerol<serinol< MDEA< MEA. Based on σ-profile in Figure 4.5, MDEA has a larger distribution of the charge densities around the hydrogen bond acceptor area than serinol. This indicates the capability of MDEA to absorb more CO_2 than serinol. MEA has a high reactivity towards CO_2 and a high absorbing capacity of CO_2. However, there are disadvantages that need to take account such as corrosivity of MEA and its damaging effect on the equipment (Kumar, Cho, & Moon, 2014). Other than

this, the formation of a stable carbamate and the high energy requirement for regeneration are other adverse factors to be considered (B. T. Zhao et al., 2012).

Glycerol and [bmim][Tf_2N] do not have amine group which reduces its ability to absorb more CO_2. The CO_2 solubility in ionic liquid depends strongly on the choice of anion. The CO_2 solubility being highest in the ionic liquids with fluoroalkyl groups in the anion ([Tf_2N]) and the lowest in the ionic liquids with nonfluorinated inorganic anions ([DCA])(Babamohammadi, Sh, & Aroua, 2015). Even though serinol has low solubility of CO_2 as compared to MEA but the molecular structure of serinol introduces steric hindrance to amino groups, which can lowers the stability of carbamate formation in CO_2-amine reactions. This is considered a great advantage for CO_2 regeneration performance.

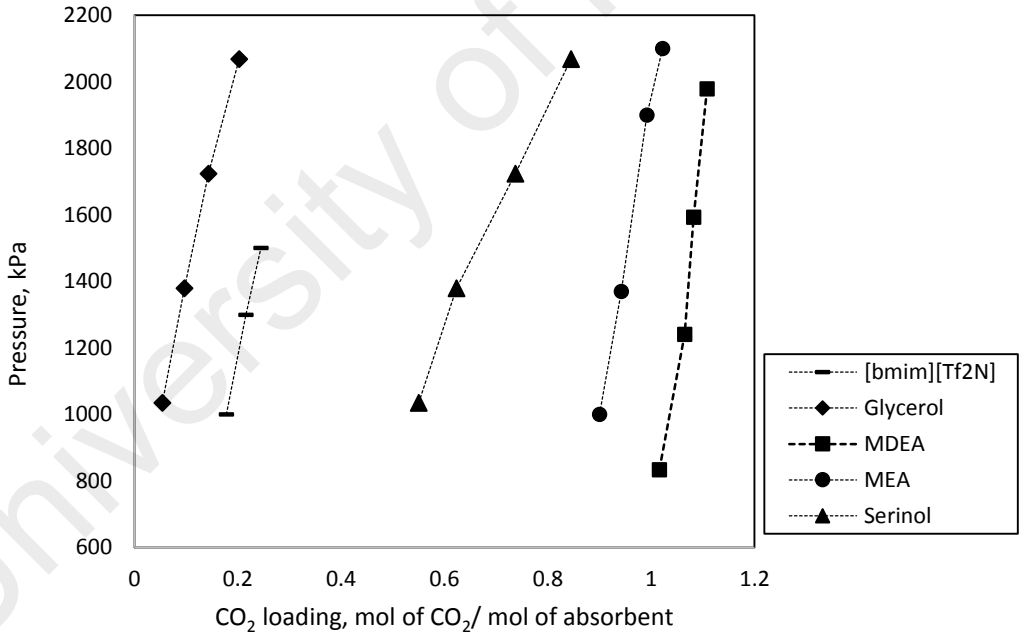

Figure 4.18: Comparison for CO_2 loading, mol of CO_2/mol of absorbent between this work (serinol) , glycerol, MEA (K. P. Shen & M. H. Li, 1992), MDEA (K. P. Shen & M. H. Li, 1992) and [bmim][Tf_2N] (Bahadur, Osman, Coquelet, Naidoo, & Ramjugernath, 2015)

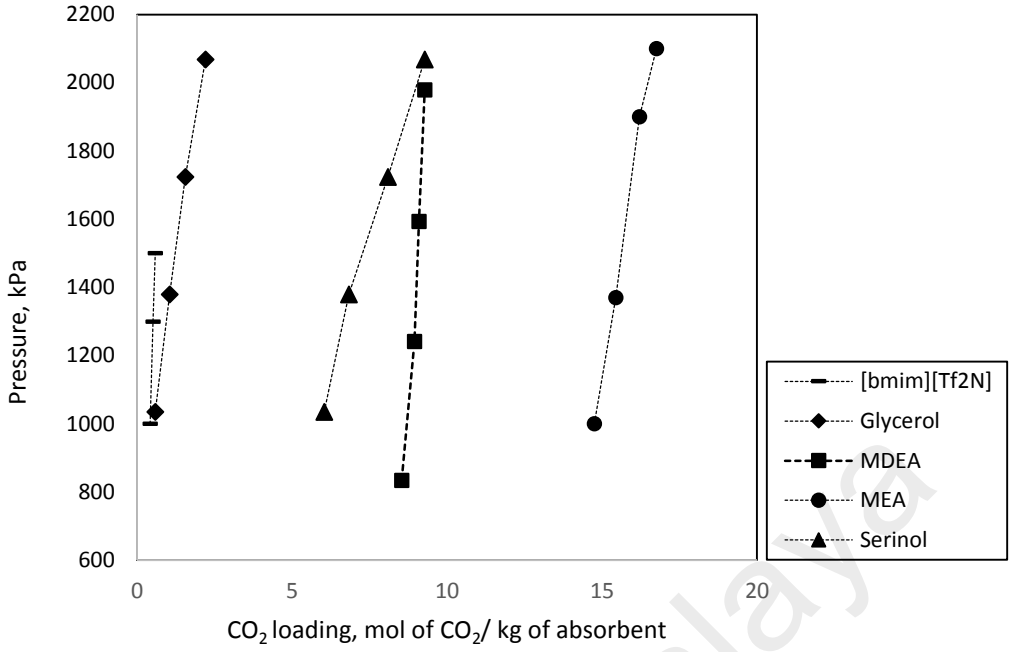

Figure 4.19: Comparison for CO_2 loading, mol of CO_2/kg of absorbent between this work (serinol) , glycerol, MEA (K. P. Shen & M. H. Li, 1992), MDEA (K. P. Shen & M. H. Li, 1992) and [bmim][Tf_2N] (Bahadur et al., 2015)

4.4 Density

4.4.1 Validation of the density measurement

A few runs for density measurement of aqueous serinol were conducted to confirm the accuracy of the measurements and to validate the experimental set up apparatus for this study. These data were compared with the reported literature data (Bougie & Iliuta, 2014) as shown in Table 4.1 and plotted in Figure 4.20. It was found that both literature and experimental data has deviation of 0.293 % by using average absolute deviation equation 4.1.

Table 4.1: Comparison of density at 313.15 K of aqueous serinol solution for literature data(Bougie & Iliuta, 2014) and experimental data

Concentration (mol/L)	Literature	Experiment
	ρ (g/cm^3)	ρ (g/cm^3)
0.882	1.005	1.003
1.762	1.019	1.023
2.721	1.033	1.037
3.434	1.045	1.043

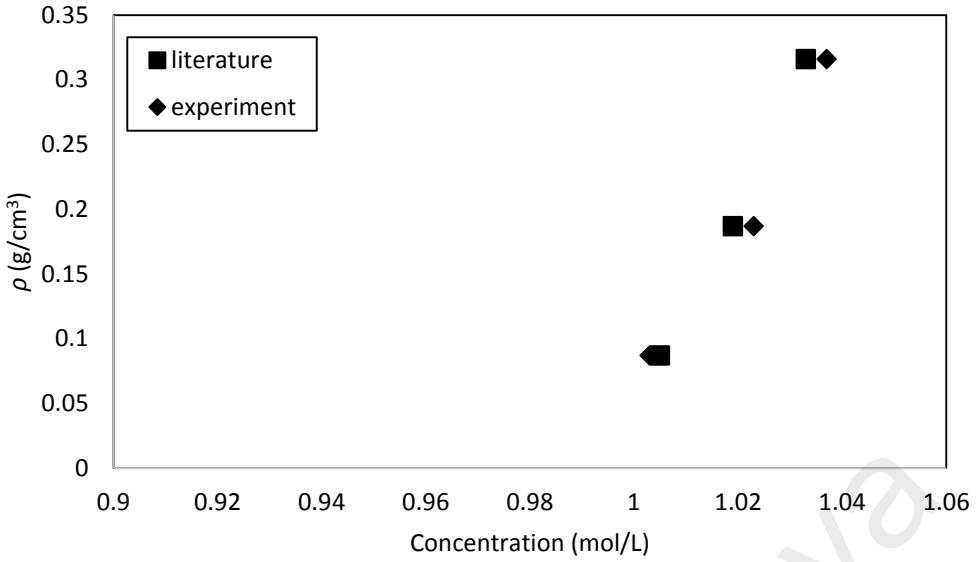

Figure 4.20: Comparison of density at 313.15 K of aqueous serinol for literature data(Bougie & Iliuta, 2014) and experimental data

4.4.2 Density of aqueous serinol solution

Figure 4.21 and Table 4.2 show the density measurements of aqueous serinol in concentration of 1M, 2M and 3M and at temperature range from 298.15 K to 333.15 K. The density of aqueous serinol decreases with increases in temperature. The concentration of aqueous serinol highly influenced the density of the systems. The sequence followed the order of 3M > 2M > 1M. This has been verified by the density of 3M was higher than that of 2M and 1M throughout the range of the temperatures.

The decrement of density measurements of aqueous serinol as the temperature increased indicated that the kinetic energy of molecules increased and this caused more motion of molecules that occupy a larger volume. The volume of the system increased as more spaces were fill up by the expansion. Therefore, increased in volume led to decrease of density. The observed trend was expected as similar trend has been reported by Sobrino and coworkers (Sobrino et al., 2016). It was reported that density increased when temperature decreased for MDEA-water and MEA-water mixtures.

Table 4.2: Density of aqueous serinol solutions for concentration 1M, 2M and 3M from temperature 298.15 K to 333.15 K

Temperature (K)	ρ (g/cm^3)		
	1 M	2 M	3 M
298.15	1.0121 ± 0.0001	1.0286 ± 0.0001	1.0427 ± 0.0001
303.15	1.0110 ± 0.0001	1.0271 ± 0.0001	1.0410 ± 0.0001
313.15	1.0072 ± 0.0001	1.0231 ± 0.0001	1.0367 ± 0.0001
323.15	1.0028 ± 0.0001	1.0185 ± 0.0001	1.0318 ± 0.0001
333.15	0.9978 ± 0.0001	1.0134 ± 0.0001	1.0266 ± 0.0001

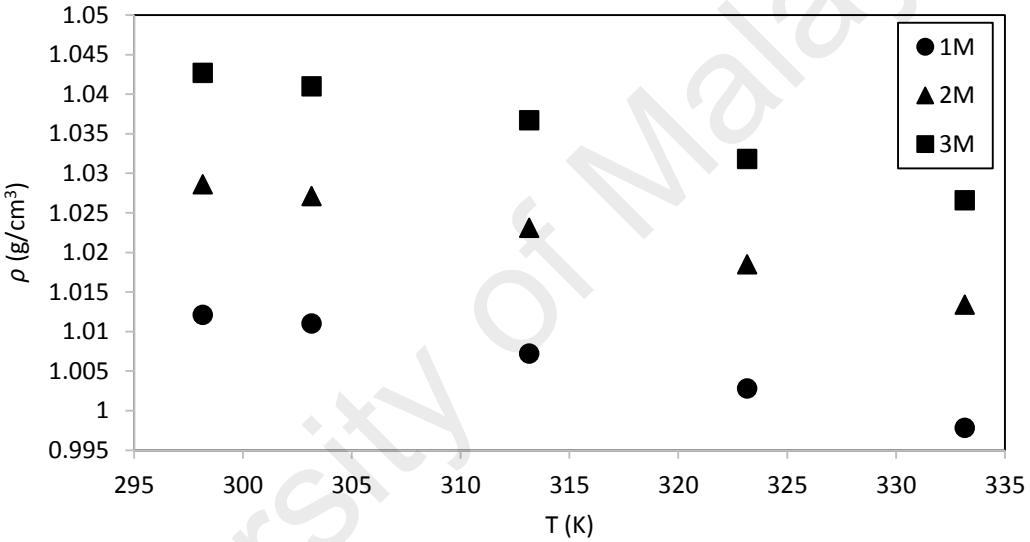

Figure 4.21: Density of aqueous serinol solutions for concentration 1M, 2M and 3M from temperature 298.15 K to 333.15 K

4.4.3 Correlation of density

The following equation 4.2 was used to correlate the density of aqueous serinol with temperature from 298.15 K to 333.15 K(Rebolledo-Libreros & Trejo, 2006):

$$\rho(gcm^{-3}) = [\alpha(gcm^{-3}K^{-1}) \times T(K)] + \beta(gcm^{-3}) \quad (4.2)$$

The characteristic parameters, α and β were determined from gradient and y-intercept of plotting a linear graph of density versus temperature at different concentration. The values of α and β are summarized in Table 4.3. Based on Table 4.3, 3M of aqueous serinol

exhibited the highest value of β followed by 2M and 1M of aqueous serinol. For aqueous serinol, the β value increased as the concentration of aqueous serinol increased. The R^2 values for all concentrations of aqueous serinol are closed to unity which displayed that the correlation in equation 4.2 can be used to estimate the density in the temperature range from 298.15 K to 333.15 K.

Table 4.3: The correlated parameters for densities at concentration 1M, 2M and 3M of aqueous serinol

Concentration (M)	α ($gcm^{-3}K^{-1}$)	β (gcm^{-3})	R^2
1	-0.0004	1.1358	0.9907
2	-0.0004	1.1592	0.9945
3	-0.0005	1.1811	0.9964

4.5 Viscosity

4.5.1 Validation of the viscosity measurement

The viscosity of aqueous serinol was determined and these data were compared with the reported literature data (Bougie & Iliuta, 2014) in order to establish the accuracy of density meter calibration as shown in Table 4.4 and plotted in Figure 4.22. It was found that both literature and experimental data was good agreement between them with an average absolute deviation from equation 4.1 in the density of aqueous serinol of 4.68%.

Table 4.4: Comparison of viscosity at 313.15 K of aqueous serinol for literature data(Bougie & Iliuta, 2014) and experimental data

Concentration (mol/L)	Literature	Experiment
	μ (mPa.s)	μ (mPa.s)
0.882	0.800	0.720
1.762	0.983	0.910
2.721	1.275	1.260
3.434	1.588	1.590

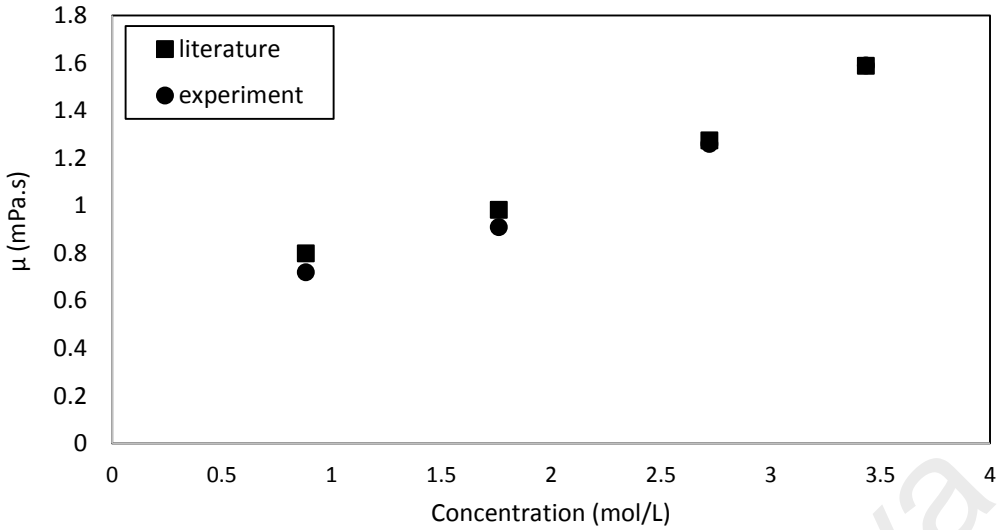

Figure 4.22: Comparison of viscosity at 313.15 K of aqueous serinol for literature data(Bougie & Iliuta, 2014) and experimental data

4.5.2 Viscosity of aqueous serinol

Figure 4.23 and Table 4.5 illustrate the viscosity measurements at temperature of system from 298.15 K to 333.15 K and concentration of aqueous serinol from 1M to 3M. At a fixed concentration, the viscosity decrease as the temperature increase. This showed that the viscosity of the solutions exhibited temperature-dependent behavior. However, as the temperature approaches 333.15 K, the difference in the viscosities became smaller. The impact of temperature on the viscosity is more significant at low temperature range (Nookuea et al., 2017). Moreover, it can be seen that from this figure, at a fixed temperature, the higher the concentration of aqueous serinol, the higher the viscosity by followed the order of 3M > 2M > 1M.

Increasing the temperature of the system caused adding heat energy to the molecules of the solution. This causes the molecules absorbed the required energy to overcome the intermolecular forces between them. Thus, the molecules move further apart and this reduces the viscosity of the solution. This similar trend has been reported by Leo and coworkers (Leo et al., 2016). In his work, at a fixed mixture composition of MDEA, MEA and PZ, as the temperature increased, the viscosity of the mixture decreased.

Table 4.5: Viscosity of aqueous serinol solutions for concentration 1M, 2M and 3M from temperature 298.15 K to 333.15 K

Temperature (K)	μ (mPa.s)		
	1 M	2 M	3 M
298.15	1.44 ± 0.01	1.83 ± 0.01	2.40 ± 0.01
303.15	1.11 ± 0.01	1.56 ± 0.01	1.92 ± 0.01
313.15	0.90 ± 0.01	1.20 ± 0.02	1.80 ± 0.01
323.15	0.78 ± 0.01	1.05 ± 0.00	1.50 ± 0.01
333.15	0.66 ± 0.01	0.81 ± 0.01	1.20 ± 0.01

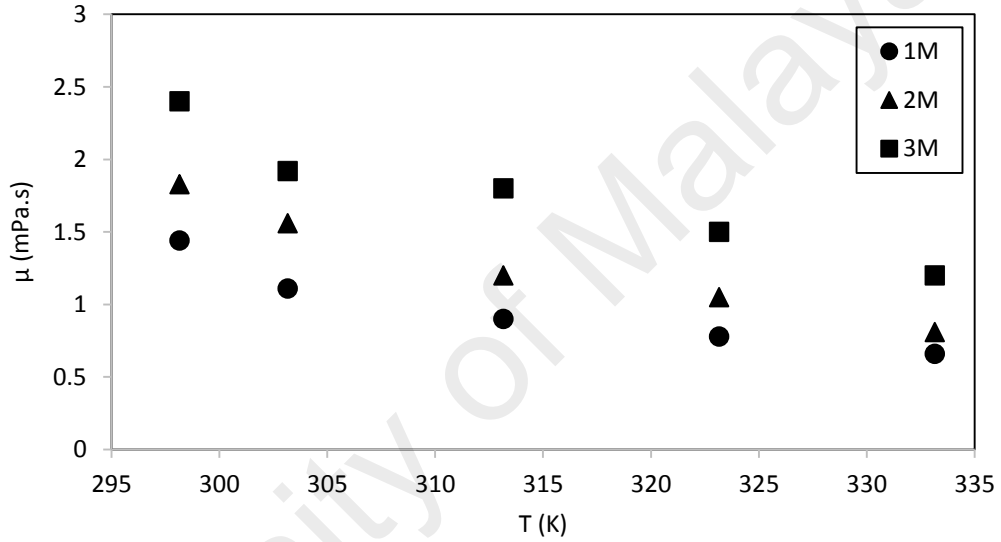

Figure 4.23: Viscosity of aqueous serinol solutions for concentration 1M, 2M and 3M from temperature 298.15 K to 333.15 K

4.5.3 Correlation of viscosity

The extended version of the Arrhenius equation was employed to correlate the temperature and the viscosity. The Arrhenius equation is expressed as in equation 4.3.

$$\ln \mu = \left(\frac{E_a}{RT}\right) + \ln \mu_\infty \tag{4.3}$$

Where;

μ = viscosity of the system (mPa.s)

E_a= activation energy (kJ/mol)

R= gas constant, 8.314 (kJ/kmol.K)

T= absolute temperature (K)

μ_∞= viscosity at infinite temperature (mPa.s)

A graph of ln μ versus 1/T was plotted for a temperature range of 298.15 K to 333.15K for all concentrations of aqueous serinol. The parameters E_a and μ_∞ were determined from the gradient and the y-intercept of the graph, respectively. The parameters are tabulated in Table 4.6. Table 4.6 shows that the activation energy value, E_a for aqueous serinol solution decreased as the concentration of solution increased and the values range between 14.732 kJ/mol and 18.438 kJ/mol.

Table 4.6: The correlated parameters for viscosities at concentration 1M, 2M and 3M of aqueous serinol

Concentration (M)	E_a(kJ/mol)	μ_∞ (x10^{-3} mPa.s)	R^2
1	17.197	1.287	0.9599
2	18.438	1.052	0.9891
3	14.732	6.042	0.9564

4.6 Physical solubility

4.6.1 Physical solubility of N_2O

It is well known that the physical solubility behavior of a gas in a solvent can be explained by Henry's law. Henry's law states that at a constant temperature, the amount of a given gas that dissolves in a liquid is directly proportional to the partial pressure of that gas in equilibrium with that liquid (Deng, Jiang, Liu, Zhang, & Ai, 2016). Henry's law constant can be defined as follows:

$$H_{N_2O} = \frac{P_{N_2O}}{x_{N_2O}} \tag{4.4}$$

Where H_{N2O} is Henry's law constant, P_{N2O} is the partial pressure of N_2O and x_{N2O} is mole fraction of solubility N_2O.

The physical solubility of N_2O in aqueous amine is dependent on the number of amine groups and the temperature of the system. The higher the number of amine groups present, the lower the physical solubility of N_2O in aqueous amine (Ma'mun & Svendsen, 2009). Table 4.7 showed the variation of Henry's law constant of N_2O in aqueous serinol of concentrations at 1M and 3M and at temperatures of 313.15 K and 333.15 K. A lower value of Henry's law constant corresponds to a higher solubility. These Henry's law constants were calculated to investigate the variation of Henry's law constant with temperature at the same concentration of aqueous amine. It was found that as the concentration of aqueous serinol increased, the physical solubility decreased at constant temperature. Furthermore, at constant concentration, the physical solubility decreased as the temperature increased.

Table 4.7: Henry's law constant of N_2O in aqueous serinol

Temperature (K)	Sample	H_{N2O}(kPa.m^3 .$kmol^{-1}$)
313.15	1M	842.7
	3M	1090.2
333.15	1M	3162.5
	3M	3410.0

Higher concentration of aqueous serinol increased the number amine molecules present in solution. This caused more amine molecules occupying the spaces between the water and the solute, which decreased the free spaces available for N_2O gas to dissolve in this solution as N_2O is not able to form chemical bonds with the amine molecule. According to Bougie et al., as the concentration of aqueous serinol solution increased, the density increased (Bougie & Iliuta, 2014). Therefore, higher concentration of the solution leads to increase in the density which reduced the available free spaces for N_2O to

dissolve in the solution. These discussions are in agreement with the trend in the results reported by Lee et al. (S. Lee et al., 2006). In his work, the physical solubility of aqueous sodium glycinate decreased as the concentration of the solution increased and the temperature of the system increased.

4.6.2 Comparison with literature data

Comparison with this work was made at concentration of 1M, temperature of 313.15K and 333.15 K as shown in Figure 4.24. This comparison explained how the Henry's law constant changed with temperature at the same concentration of aqueous serinol, MEA and MDEA. Based on Figure 4.24, the Henry's law constant of N_2O followed the sequence: serinol<MDEA<MEA. Henry's law constant of N_2O of aqueous serinol is the lowest which indicate higher solubility of N_2O in aqueous serinol than MDEA and MEA.

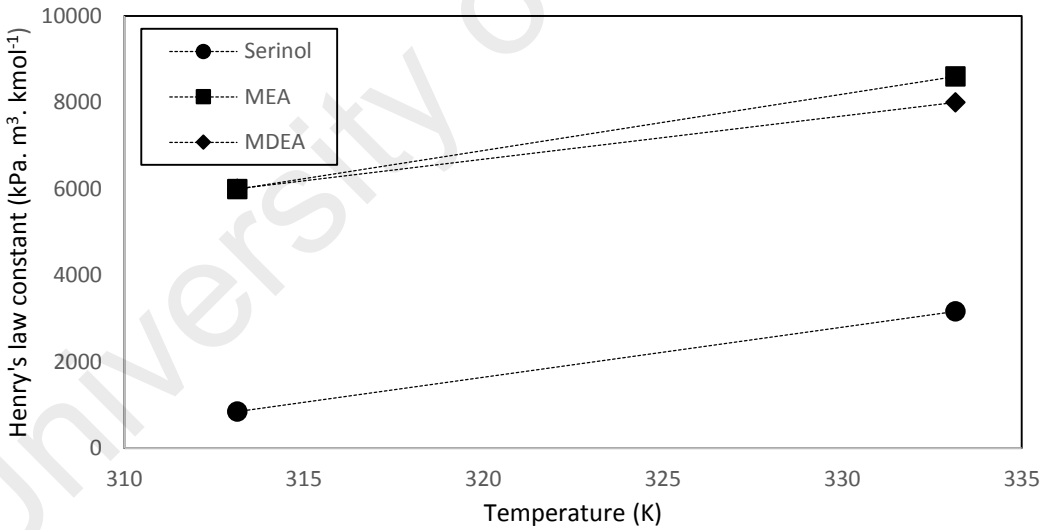

Figure 4.24: Comparison for Henry's law constant of N_2O between this work (aqueous serinol), MEA and MDEA(Penttilä et al., 2011)

4.6.3 Physical solubility of CO_2

The Henry's law constant of CO_2 in aqueous serinol can be determined by correlated the experimental solubility of N_2O in the same aqueous amines using equation 2.20. The Henry's law constant of CO_2 and H_2O in water can be calculated using equations 4.5 and 4.6 which was proposed by Versteeg and Van Swaaij (Versteeg & Van Swaalj, 1988).

The researchers have been used these equations extensively in many kind of solvents. Ahmady et al. and Kierzkowska-Pawlak et al. compared the estimated values obtained from equations 4.5 and 4.6 with the literature data of Henry's law constant of CO_2 and N_2O in water (Ahmady et al., 2011; Kierzkowska-Pawlak & Zarzycki, 2002). Their results were in good agreement with the calculated data thus confirmed the reliability of the technique. To evaluate the applicability of equation 2.20 in the calculation of physical solubility of CO_2 in aqueous serinol, the Henry's law constant of N_2O and CO_2 in water were measured. Table 4.8 shows the Henry's law constant of N_2O and CO_2 in water at 313.15 K.

$$H_{CO_2} = 2.8249 \times 10^6 \times \exp(-\frac{2044}{T}) \quad (4.5)$$

$$H_{N_2O} = 8.5460 \times 10^6 \times \exp(-\frac{2284}{T}) \quad (4.6)$$

Table 4.8: Henry's law constant of N_2O and CO_2 in water at 313.15 K

H_{N2O} (kPa.m^3 .kmol^{-1})	Reference	H_{CO2} (kPa.m^3 .kmol^{-1})	Reference
5810.7	Eq. 4.6	4133.0	Eq. 4.5
4382.9	This work	3614.6	This work

The Henry's law constant of CO_2 in aqueous serinol were calculated using equation 2.20, 4.5 and 4.6 and the results were tabulated in Table 4.9. Based on Table 4.9, the Henry's law constant of CO_2 in aqueous serinol increases as concentration of the solution and temperature of the system increases.

Table 4.9: Henry's law constant of CO_2 in aqueous serinol

Temperature (K)	Sample	H_{CO2}(kPa.m^3 .kmol^{-1})
313.15	1M	599.4
	3M	775.4
333.15	1M	2148.2
	3M	2316.4

4.7 Regeneration for CO_2 absorption

The regeneration of 3M of aqueous serinol for 4 different pressures at 313.15 K were illustrated in Figure 4.25. As shown in Figure 4.25, as the regeneration cycles increased, the CO_2 solubility decreased for each partial pressure. It is observed that the first cycle of regeneration of aqueous serinol gave the highest value of the solubility of CO_2 while the third cycle of regeneration gave the lowest value of CO_2 solubility. Figure 4.26 showed the regeneration efficiency of 3M aqueous serinol. It is observed that at constant pressure, the regeneration efficiency decreased as the number of regeneration cycles increased. The maximum decreased after three regeneration cycles is 41.41%.

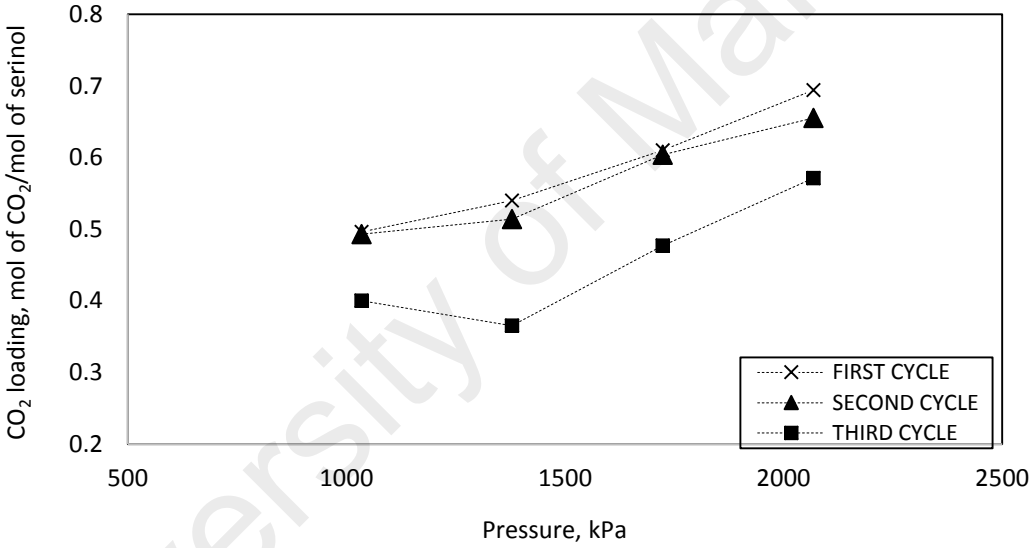

Figure 4.25: Effect of regeneration cycle on CO_2 loading of 3M aqueous serinol from CO_2 partial pressure range 1034.31 kPa to 2068.43 kPa at temperature 313.15 K

The reaction products between acid gas and alkanolamines gave a number of heat stable salts (HSS), which are difficult to regenerate under condition of regeneration. HSS are well-known product of degradation in the technologies of acid gas removal with alkanolamines (Bazhenov et al., 2014). These accumulated HSS may lead to reduction in the capacity of CO_2 absorption, regeneration efficiency, corrosion and foaming. These results show a complete agreement with the previous work by Zhang et al. (P. Zhang et al., 2008). It was reported that the regeneration efficiency of 2-amino-2-methyl-1-propanol decreased as the number of cycles increased.

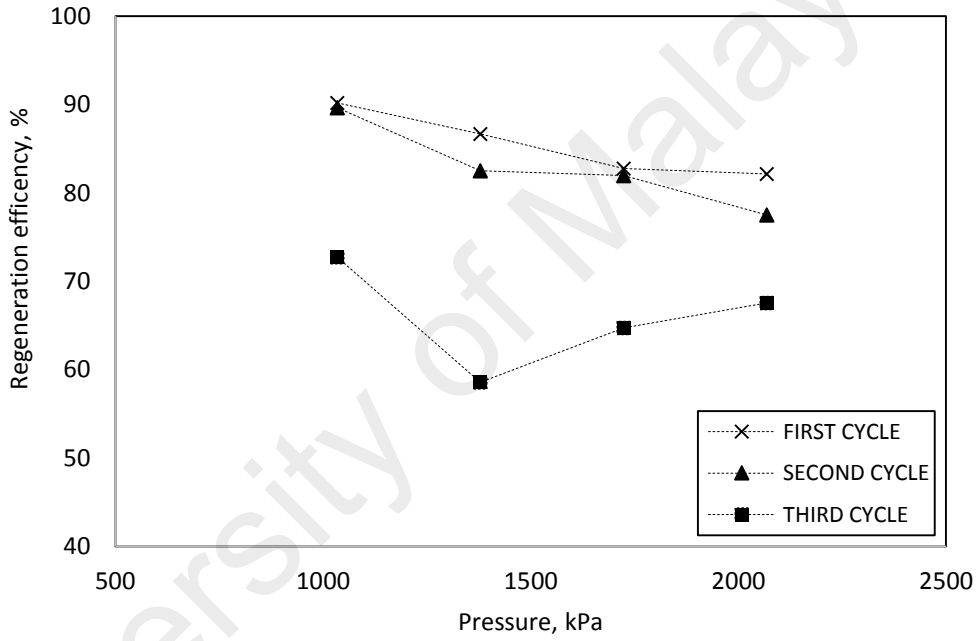

Figure 4.26: 3M of aqueous serinol regeneration efficiency from CO_2 partial pressure range 1034.31 kPa to 2068.43 kPa at temperature 313.15 K

CHAPTER 5: CONCLUSION AND RECOMMENDATIONS

5.1 Conclusion

The structure of serinol, MDEA, water and CO_2 were drawn and the geometry were optimized using TURBOMOLE software package at Hartree-Fock level of theory and 6-31G* basis set. Then, a *.cosmofile* was created and imported to the COSMOthermX software package. Using this approach, a 3D polarized charged distribution on the molecular surface of individual component were generated. Based on qualitative prediction by COSMO-RS, the σ – profiles and σ - potential of serinol and CO_2 are complementary in nature and showed solubility of CO_2 in serinol. The σ – profile for serinol shows peaks at the right-hand side of the dashed line which designated the existence of a hydrogen-bond acceptor while in the σ – potential, the values of σ – potential are negative at left-hand side of the dashed line which designated affinity for a hydrogen-bond donor. Thus, it is possible to predict that serinol is able to develop intermolecular interaction with CO_2.

To confirm the potential of serinol in capturing of CO_2, experimental methods for solubility of CO_2 in aqueous serinol were conducted at temperature ranging from 313.15K to 353.15 K and CO_2 partial pressures ranging from 1034.31 kPa to 2068.43 kPa at serinol concentration from 1M to 3M. As expected in literature, the solubility of CO_2 in aqueous serinol increased with pressure and decreased with temperature. Furthermore, the CO_2 loading (mol CO_2/ mol of serinol) decreased with increasing aqueous serinol concentration. 1M aqueous serinol showed the highest CO_2 solubility up to 1.64 mol of CO_2/mol of serinol at 313.15 K and 2068.43 kPa. When comparing with [bmim][Tf_2N], glycerol, MEA and MDEA, serinol showed lower performance than MEA and MDEA but higher performance than glycerol and [bmim][Tf_2N].

For physical properties of aqueous serinol, the density and viscosity measurements were conducted at concentration of 1M, 2M and 3M aqueous serinol for temperature range from 298.15 K to 333.15 K. The density and viscosity of aqueous serinol increased with increased in concentration and decreased in temperature.

Moreover, Henry's law constants for CO_2 in aqueous serinol were also calculated using N_2O analogy at concentration of 1M and 3 M for temperature at 313.15 K and 333.15 K. Henry's law constant of N_2O and CO_2 in aqueous serinol increased with increased in temperature and concentration. 599.4 kPa.m^3/kmol was the lowest Henry's law constant of CO_2 at 1M of aqueous serinol and temperature at 313.15 K.

For regeneration of 3M aqueous serinol for 4 different pressures at temperature of 313.15 K, the CO_2 solubility decreased as the regeneration cycles increased whereas the regeneration efficiency decreased as the number of regeneration cycle increased. For most part, experimental results confirmed serinol appeared as the potential solvent for CO_2 absorption especially at high pressures.

5.2 Recommendations

These outcomes could be practical in the study of the rate constant of a reaction and absorption kinetic for amine gas treatment in future work. These comprehensive studies can provide more detail description on the CO_2 absorption in aqueous serinol. In the industry, absorption of CO_2 is conducted in mixtures of other gases. So, a study on the solubility of CO_2 in gas mixtures with aqueous serinol at same parameters would be beneficial. The absorption of CO_2 can be conducted at low and high pressures. Since blend of alkanolamines can optimize the performance of separation for a gas mixture, a study on the effect of addition of serinol in MEA and MDEA aqueous solution for CO_2 absorption can be performed with same parameters. These results can be compared with the aqueous serinol.

REFERENCES

Abu-Zahra, M. R., Abbas, Z., Singh, P., & Feron, P. (2013). Carbon dioxide post-combustion capture: solvent technologies overview, status and future directions.

Ahmady, A., Hashim, M. A., & Aroua, M. K. (2011). Density, viscosity, physical solubility and diffusivity of CO2 in aqueous MDEA+[bmim][BF4] solutions from 303 to 333K. *Chemical Engineering Journal, 172*(2), 763-770.

Al-Lal, A. M., Garcia-Gonzalez, J. E., Llamas, A., Monjas, A., & Canoira, L. (2012). A new route to synthesize tert-butyl ethers of bioglycerol. *Fuel, 93*(1), 632-637.

Alaswad, A., Dassisti, M., Prescott, T., & Olabi, A. G. (2015). Technologies and developments of third generation biofuel production. *Renewable & Sustainable Energy Reviews, 51*, 1446-1460.

Amato, A., Hudak, B., D'Souza, P., D'Carlo, P., Noble, D., Scarborough, D., Lieuwen, T. (2011). Measurements and analysis of CO and O_2 emissions in $CH_4/CO_2/O_2$ flames. *Proceedings of the Combustion Institute, 33*, 3399-3405.

Amin, R., Jackson, A. T., & Kennaird, T. (2005). *The Cryocell: An Advanced Gas Sweetening Technology*.

Anantharaj, R., & Banerjee, T. (2010). Evaluation and comparison of global scalar properties for the simultaneous interaction of ionic liquids with thiophene and pyridine. *Fluid Phase Equilibria, 293*(1), 22-31.

Andirova, D., Cogswell, C. F., Lei, Y., & Choi, S. H. (2016). Effect of the structural constituents of metal organic frameworks on carbon dioxide capture. *Microporous and Mesoporous Materials, 219*, 276-305.

Aroonwilas, A., & Veawab, A. (2004). Characterization and comparison of the CO_2 absorption performance into single and blended alkanolamines in a packed column. *Industrial & engineering chemistry research, 43*(9), 2228-2237.

Aschenbrenner, O., & Styring, P. (2010). Comparative study of solvent properties for carbon dioxide absorption. *Energy & Environmental Science, 3*(8), 1106-1113.

Azhgan, M., Farsi, M., & Eslamloueyan, R. (2016). Solubility of carbon dioxide in aqueous solution of 1,5diamino-2-methylpentane: Absorption and desorption property. *International Journal of Greenhouse Gas Control, 51*, 409-414.

Aziz, N., Yusoff, R., & Aroua, M. K. (2012). Absorption of CO_2 in aqueous mixtures of N-methyldiethanolamine and guanidinium tris(pentafluoroethyl)trifluorophosphate ionic liquid at high-pressure. *Fluid Phase Equilibria, 322*, 120-125.

Babamohammadi, S., Sh, A., & Aroua, M. (2015). *A review of CO_2 capture by absorption in ionic liquid-based solvents*.

Bahadur, I., Osman, K., Coquelet, C., Naidoo, P., & Ramjugernath, D. (2015). Solubilities of carbon dioxide and oxygen in the ionic liquids methyl trioctyl ammonium bis(trifluoromethylsulfonyl)imide, 1-butyl-3-methyl imidazolium bis(trifluoromethylsulfonyl)imide, and 1-butyl-3-methyl imidazolium methyl sulfate. *J Phys Chem B, 119*(4), 1503-1514.

Banerjee, T., & Khanna, A. (2006). Infinite dilution activity coefficients for trihexyltetradecyl phosphonium ionic liquids: Measurements and COSMO-RS prediction. *Journal of Chemical and Engineering Data, 51*(6), 2170-2177.

Bashirnezhad, K., Bazri, S., Safaei, M. R., Goodarzi, M., Dahari, M., Mahian, O., Wongwises, S. (2016). Viscosity of nanofluids: A review of recent experimental studies. *International Communications in Heat and Mass Transfer, 73*, 114-123.

Bazhenov, S., Vasilevsky, V., Rieder, A., Unterberger, S., Grushevenko, E., Volkov, V., Volkov, A. (2014). Heat Stable Salts (HSS) Removal by Electrodialysis: Reclaiming of MEA Used in Post-combustion CO_2-Capture. *Energy Procedia, 63*, 6349-6356.

Bernard, S. M., Samet, J. M., Grambsch, A., Ebi, K. L., & Romieu, I. (2001). The potential impacts of climate variability and change on air pollution-related health effects in the United States. *Environmental Health Perspectives, 109*, 199-209.

Bougie, F., & Iliuta, M. C. (2014). Solubility of CO_2 in and Density, Viscosity, and Surface Tension of Aqueous 2-Amino-1,3-propanediol (Serinol) Solutions. *Journal of Chemical and Engineering Data, 59*(2), 355-361.

Bucklin, R., & Schendel, R. (1984). Comparison of fluor solvent and selexol processes. *Energy Prog.;(United States), 4*(3).

Budinis, S., Krevor, S., Dowell, N. M., Brandon, N., & Hawkes, A. (2018). An assessment of CCS costs, barriers and potential. *Energy Strategy Reviews, 22*, 61-81.

Burghoff, B., Goetheer, E. L. V., & de Haant, A. B. (2008). COSMO-RS-based extractant screening for phenol extraction as model system. *Industrial & engineering chemistry research, 47*(12), 4263-4269.

Centi, G., Perathoner, S., & Rak, Z. S. (2003). Reduction of greenhouse gas emissions by catalytic processes. *Applied Catalysis B-Environmental, 41*(1-2), 143-155.

Chiang, C.-Y., Lee, D.-W., & Liu, H.-S. (2017). Carbon dioxide capture by sodium hydroxide-glycerol aqueous solution in a rotating packed bed. *Journal of the Taiwan Institute of Chemical Engineers, 72*(Supplement C), 29-36.

Choi, S., Park, J., Han, C., & Yoon, E. S. (2008). Optimal design of synthesis gas production process with recycled carbon dioxide utilization. *Industrial & engineering chemistry research, 47*(2), 323-331.

Chong, F. K., Eljack, F. T., Atilhan, M., Foo, D. C. Y., & Chemmangattuvalappil, N. G. (2014). Ionic Liquid Design for Enhanced Carbon Dioxide Capture - A Computer Aided Molecular Design Approach. In P. S. Varbanov, J. J. Klemes, P. Y. Liew,

J. Y. Yong, & P. Stehlik (Eds.), *Pres 2014, 17th Conference on Process Integration, Modelling and Optimisation for Energy Saving and Pollution Reduction, Pts 1-3* (Vol. 39, pp. 253-258).

Cleary, J., Roulet, N. T., & Moore, T. R. (2005). Greenhouse gas emissions from Canadian peat extraction, 1990-2000: A life-cycle analysis. *Ambio, 34*(6), 456-461.

Constantinescu, D., Rarey, J., & Gmehling, J. (2009). Application of COSMO-RS Type Models to the Prediction of Excess Enthalpies. *Industrial & engineering chemistry research, 48*(18), 8710-8725.

Conway, W., Bruggink, S., Beyad, Y., Luo, W., Melián-Cabrera, I., Puxty, G., & Feron, P. (2015). CO_2 absorption into aqueous amine blended solutions containing monoethanolamine (MEA), N,N-dimethylethanolamine (DMEA), N,N-diethylethanolamine (DEEA) and 2-amino-2-methyl-1-propanol (AMP) for post-combustion capture processes. *Chemical Engineering Science, 126*, 446-454.

Conway, W., Wang, X., Fernandes, D., Burns, R., Lawrance, G., Puxty, G., & Maeder, M. (2013). Toward the Understanding of Chemical Absorption Processes for Post-Combustion Capture of Carbon Dioxide: Electronic and Steric Considerations from the Kinetics of Reactions of $CO_{2(aq)}$ with Sterically hindered Amines. *Environmental Science & Technology, 47*(2), 1163-1169.

Dantas, T. L. P., Luna, F. M. T., Silva, I. J., de Azevedo, D. C. S., Grande, C. A., Rodrigues, A. E., & Moreira, R. (2011). Carbon dioxide-nitrogen separation through adsorption on activated carbon in a fixed bed. *Chemical Engineering Journal, 169*(1-3), 11-19.

Dantas, T. L. P., Luna, F. M. T., Silva, I. J., Torres, A. E. B., de Azevedo, D. C. S., Rodrigues, A. E., & Moreira, R. (2011). Carbon dioxide-nitrogen separation through pressure swing adsorption. *Chemical Engineering Journal, 172*(2-3), 698-704.

deMontigny, D., Tontiwachwuthikul, P., & Chakma, A. (2001). Parametric studies of carbon dioxide absorption into highly concentrated monoethanolamine solutions. *Canadian Journal of Chemical Engineering, 79*(1), 137-142.

Deng, D. S., Jiang, Y. T., Liu, X. B., Zhang, Z. L., & Ai, N. (2016). Investigation of solubilities of carbon dioxide in five levulinic acid-based deep eutectic solvents and their thermodynamic properties. *Journal of Chemical Thermodynamics, 103*, 212-217.

Diedenhofen, M., Eckert, F., & Klamt, A. (2003). Prediction of infinite dilution activity coefficients of organic compounds in ionic liquids using COSMO-RS. *Journal of Chemical & Engineering Data, 48*(3), 475-479.

Diedenhofen, M., & Klamt, A. (2010). COSMO-RS as a tool for property prediction of IL mixtures-A review. *Fluid Phase Equilibria, 294*(1-2), 31-38.

Dinca, C., Slavu, N., & Badea, A. (2018). Benchmarking of the pre/post-combustion chemical absorption for the CO_2 capture. *Journal of the Energy Institute, 91*(3), 445-456.

Durmaz, T. (2018). The economics of CCS: Why have CCS technologies not had an international breakthrough? *Renewable and Sustainable Energy Reviews, 95*, 328-340.

Eckert, F., & Klamt, A. (2003). Prediction of halocarbon thermodynamics with COSMO-RS. *Fluid Phase Equilibria, 210*(1), 117-141.

El-Gendy, N. S., Hamdy, A., & Abu Amr, S. S. (2014). An Investigation of Biodiesel Production from Wastes of Seafood Restaurants. *International Journal of Biomaterials, 2014*, 17.

El Doukkali, M., Iriondo, A., Arias, P. L., Requies, J., Gandarias, I., Jalowiecki-Duhamel, L., & Dumeignil, F. (2012). A comparison of sol-gel and impregnated Pt or/and Ni based gamma-alumina catalysts for bioglycerol aqueous phase reforming. *Applied Catalysis B-Environmental, 125*, 516-529.

Fan, J.-L., Xu, M., Li, F., Yang, L., & Zhang, X. (2018). Carbon capture and storage (CCS) retrofit potential of coal-fired power plants in China: The technology lock-in and cost optimization perspective. *Applied Energy, 229*, 326-334.

Feng, B., Liu, W. Q., Li, X., & An, H. (2006). Overcoming the problem of loss-in-capacity of calcium oxide in CO_2 capture. *Energy & Fuels, 20*(6), 2417-2420.

Feron, P. H. M. (2010). Exploring the potential for improvement of the energy performance of coal fired power plants with post-combustion capture of carbon dioxide. *International Journal of Greenhouse Gas Control, 4*(2), 152-160.

Figueroa, J. D., Fout, T., Plasynski, S., McIlvried, H., & Srivastava, R. D. (2008). Advancesn in $CO_{(2)}$ capture technology - The US Department of Energy's Carbon Sequestration Program. *International Journal of Greenhouse Gas Control, 2*(1), 9-20.

Flowers, B. S., Mittenthal, M. S., Jenkins, A. H., Wallace, D. A., Whitley, J. W., Dennis, G. P., Bara, J. E. (2017). 1,2,3-Trimethoxypropane: A Glycerol-Derived Physical Solvent for CO_2 Absorption. *Acs Sustainable Chemistry & Engineering, 5*(1), 911-921.

Freire, M. G., Carvalho, P. J., Santos, L., Gomes, L. R., Marrucho, I. M., & Coutinho, J. A. P. (2010). Solubility of water in fluorocarbons: Experimental and COSMO-RS prediction results. *Journal of Chemical Thermodynamics, 42*(2), 213-219.

Gainar, I., & Anitescu, G. (1995). The solubility of CO_2, N_2 and H_2 in a mixture of dimethylether polyethylene glycols at high pressures. *Fluid Phase Equilibria, 109*(2), 281-289.

Gielen, D. J., Moriguchi, Y., & Yagita, H. (2002). CO_2 emission reduction for Japanese petrochemicals. *Journal of Cleaner Production, 10*(6), 589-604.

Glasscock, D. A., Critchfield, J. E., & Rochelle, G. T. (1991). CO_2 Absroption Desorption In Mixtures of Methyldiethanolamine with Monoethanolamine or Diethanolamine. *Chemical Engineering Science, 46*(11), 2829-2845.

Gómez, C. L., Echeverri, D. A., Inciarte, H. C., & Rios, L. A. (2019). Efficient processing of bioglycerol to a novel biobased polyunsaturated monomer. *Journal of Chemical Technology & Biotechnology, 94*(2), 634-640.

Hizaddin, H. F., Hashim, M. A., & Anantharaj, R. (2013). Evaluation of Molecular Interaction in Binary Mixture of Ionic Liquids plus Heterocyclic Nitrogen Compounds: Ab Initio Method and COSMO-RS Model. *Industrial & engineering chemistry research, 52*(50), 18043-18058.

Hong, S. M., Kim, S. H., & Lee, K. B. (2013). Adsorption of Carbon Dioxide on 3-Aminopropyl-Triethoxysilane Modified Graphite Oxide. *Energy & Fuels, 27*(6), 3358-3363.

Huck, J. M., Lin, L. C., Berger, A. H., Shahrak, M. N., Martin, R. L., Bhown, A. S., Smit, B. (2014). Evaluating different classes of porous materials for carbon capture. *Energy & Environmental Science, 7*(12), 4132-4146.

Irani, V., Maleki, A., & Tavasoli, A. (2019). CO2 absorption enhancement in graphene-oxide/MDEA nanofluid. *Journal of Environmental Chemical Engineering, 7*(1), 102782.

Jansen, D., Gazzani, M., Manzolini, G., Dijk, E. v., & Carbo, M. (2015). Pre-combustion CO_2 capture. *International Journal of Greenhouse Gas Control, 40*(Supplement C), 167-187.

Jones, R., Connolly, P. C., Klamt, A., & Diedenhofen, M. (2005). Use of surface charges from DFT calculations to predict intestinal absorption. *Journal of chemical information and modeling, 45*(5), 1337-1342. f

Kamimura, Y., Shimomura, M., & Endo, A. (2014). Simple template-free synthesis of high surface area mesoporous ceria and its new use as a potential adsorbent for carbon dioxide capture. *Journal of Colloid and Interface Science, 436*, 52-62.

Kanniche, M., & Bouallou, C. (2007). CO_2 capture study in advanced integrated gasification combined cycle. *Applied Thermal Engineering, 27*(16), 2693-2702.

Karnakar, K., Murthy, S. N., Ramesh, K., Reddy, K. H. V., Nageswar, Y. V. D., Chandrakala, U.,Prasad, R. B. N. (2012). A novel one-pot synthesis of spiro indoline-3,4 '-pyrazolo 3,4-e 1,4 thiazepine diones using recyclable bioglycerol-based sulfonic acid functionalized carbon catalyst. *Tetrahedron Letters, 53*(27), 3497-3501.

Kassim, M. A., Sairi, N. A., Yusoff, R., Ramalingam, A., Alias, Y., & Aroua, M. K. (2016). Experimental densities and viscosities of binary mixture of 1-butyl-3-methylimidazolium bis(trifluoromethylsulfonyl)imide or glycerol with sulfolane and their molecular interaction by COSMO-RS. *Thermochimica Acta, 639*, 130-147.

Kemper, J., Ewert, G., & Grunewald, M. (2011). Absorption and regeneration performance of novel reactive amine solvents for post-combustion CO_2 capture. In J. Gale, C. Hendriks, & W. Turkenberg (Eds.), *10th International Conference on Greenhouse Gas Control Technologies* (Vol. 4, pp. 232-239). Amsterdam: Elsevier Science Bv.

Kessel, D. G. (2000). Global warming - facts, assessment, countermeasures. *Journal of Petroleum Science and Engineering, 26*(1-4), 157-168.

Khan, A. A., Halder, G. N., & Saha, A. K. (2016). Comparing CO_2 removal characteristics of aqueous solutions of monoethanolamine, 2-amino-2-methyl-1-propanol, methyldiethanolamine and piperazine through absorption process. *International Journal of Greenhouse Gas Control, 50*, 179-189.

Kierzkowska-Pawlak, H., & Zarzycki, R. (2002). Solubility of carbon dioxide and nitrous oxide in water+ methyldiethanolamine and ethanol+ methyldiethanolamine solutions. *Journal of Chemical & Engineering Data, 47*(6), 1506-1509.

Kim, B.-S., & Harriott, P. (1987). Critical entry pressure for liquids in hydrophobic membranes. *Journal of Colloid and Interface Science, 115*(1), 1-8.

Kimura, H., & Tsuto, K. (1993). Catalytic synthesis ofdl-serine and glycine from glycerol. *Journal of the American Oil Chemists' Society, 70*(10), 1027-1030.

Klamt, A. (2003). Prediction of the mutual solubilities of hydrocarbons and water with COSMO-RS. *Fluid Phase Equilibria, 206*(1–2), 223-235.

Klamt, A. (2016). COSMO-RS for aqueous solvation and interfaces. *Fluid Phase Equilibria, 407*, 152-158.

Klamt, A., & Eckert, F. (2000). COSMO-RS: a novel and efficient method for the a priori prediction of thermophysical data of liquids. *Fluid Phase Equilibria, 172*(1), 43-72.

Klamt, A., & Eckert, F. (2004). Prediction of vapor liquid equilibria using COSMOtherm. *Fluid Phase Equilibria, 217*(1), 53-57.

Klamt, A., Eckert, F., & Hornig, M. (2001). COSMO-RS: A novel view to physiological solvation and partition questions. *Journal of Computer-Aided Molecular Design, 15*(4), 355-365.

Knudsen, J. N., Andersen, J., Jensen, J. N., & Biede, O. (2011). Evaluation of process upgrades and novel solvents for the post combustion CO_2 capture process in pilot-scale. *Energy Procedia, 4*(Supplement C), 1558-1565.

Kothandaraman, A. (2010). *Carbon dioxide capture by chemical absorption: a solvent comparison study*. Massachusetts Institute of Technology.

Koytsoumpa, E. I., Bergins, C., & Kakaras, E. (2018). The CO_2 economy: Review of CO_2 capture and reuse technologies. *The Journal of Supercritical Fluids, 132*, 3-16.

Ku, A. Y., Kulkarni, P., Shisler, R., & Wei, W. (2011). Membrane performance requirements for carbon dioxide capture using hydrogen-selective membranes in integrated gasification combined cycle (IGCC) power plants. *Journal of Membrane Science, 367*(1-2), 233-239.

Kumar, S., Cho, J. H., & Moon, I. (2014). Ionic liquid-amine blends and $CO_{(2)}$BOLs: Prospective solvents for natural gas sweetening and CO_2 capture technology-A review. *International Journal of Greenhouse Gas Control, 20*, 87-116.

Laboratory, D. N. D. o. E. N. E. T. (2011). Advanced Carbon Dioxide Capture R&D Program. *Technology Update, U.S.*

Lapkin, A. A., Peters, M., Greiner, L., Chemat, S., Leonhard, K., Liauw, M. A., & Leitner, W. (2010). Screening of new solvents for artemisinin extraction process using ab initio methodology. *Green Chemistry, 12*(2), 241-251.

Lee, C. S., Aroua, M. K., Daud, W., Cognet, P., Peres-Lucchese, Y., Fabre, P. L., Latapie, L. (2015). A review: Conversion of bioglycerol into 1,3-propanediol via biological and chemical method. *Renewable & Sustainable Energy Reviews, 42*, 963-972.

Lee, S., Song, H.-J., Maken, S., Shin, H.-C., Song, H.-C., & Park, J.-W. (2006). Physical solubility and diffusivity of N_2O and CO_2 in aqueous sodium glycinate solutions. *Journal of Chemical & Engineering Data, 51*(2), 504-509.

Leo, C. Y., Shamiri, A., Aroua, M. K., Aghamohammadi, N., Aramesh, R., Natarajan, E., Akbari, V. (2016). Correlation and measurement of density and viscosity of aqueous mixtures of glycerol and N-methyldiethanolamine, monoethanolamine, piperazine and ionic liquid. *Journal of Molecular Liquids, 221*(Supplement C), 1155-1161.

Leung, D. Y. C., & Lee, Y. T. (2000). Greenhouse gas emissions in Hong Kong. *Atmospheric Environment, 34*(26), 4487-4498.

Levitt, C. J., Pedersen, M. S., & Sorensen, A. (2015). Examining the efforts of a small, open economy to reduce carbon emissions: The case of Denmark. *Ecological Economics, 119*, 94-106.

Li, B. Y., Duan, Y. H., Luebke, D., & Morreale, B. (2013). Advances in CO_2 capture technology: A patent review. *Applied Energy, 102*, 1439-1447.

Li, L., Zhao, N., Wei, W., & Sun, Y. H. (2013). A review of research progress on CO_2 capture, storage, and utilization in Chinese Academy of Sciences. *Fuel, 108*, 112-130.

Li, X. F., Wang, S. J., & Chen, C. H. (2013). Experimental study of energy requirement of CO_2 desorption from rich solvent. In T. Dixon & K. Yamaji (Eds.), *Ghgt-11* (Vol. 37, pp. 1836-1843). Amsterdam: Elsevier Science Bv.

Li, Z. S., Zhang, T., & Cai, N. S. (2008). Experimental study of O_2-CO_2 production for the oxyfuel combustion using a Co-based oxygen carrier. *Industrial & engineering chemistry research, 47*(19), 7147-7153.

Liao, C. H., & Li, M. H. (2002). Kinetics of absorption of carbon dioxide into aqueous solutions of monoethanolamine plus N-methyldiethanolamine. *Chemical Engineering Science, 57*(21), 4569-4582.

Lin, B. Q., & Lei, X. J. (2015). Carbon emissions reduction in China's food industry. *Energy Policy, 86*, 483-492.

Liu, H., Gao, H., Idem, R., Tontiwachwuthikul, P., & Liang, Z. (2017). Analysis of CO_2 solubility and absorption heat into 1-dimethylamino-2-propanol solution. *Chemical Engineering Science, 170*, 3-15.

Liu, L., Chakma, A., & Feng, X. (2004). Preparation of hollow fiber poly(ether block amide)/polysulfone composite membranes for separation of carbon dioxide from nitrogen. *Chemical Engineering Journal, 105*(1-2), 43-51.

Ludwig, H. M., & Zhang, W. S. (2015). Research review of cement clinker chemistry. *Cement and Concrete Research, 78*, 24-37.

Luis, P. (2015). Use of monoethanolamine (MEA) for CO_2 capture in a global scenario: Consequences and alternatives. *Desalination*.

Luis, P., Van Gerven, T., & Van der Bruggen, B. (2012). Recent developments in membrane-based technologies for CO_2 capture. *Progress in Energy and Combustion Science, 38*(3), 419-448.

Lv, B., Guo, B., Zhou, Z., & Jing, G. (2015). Mechanisms of CO_2 Capture into Monoethanolamine Solution with Different CO_2 Loading during the Absorption/Desorption Processes. *Environmental Science & Technology, 49*(17), 10728-10735.

Lyadov, A. S., & Khadzhiev, S. N. (2017). Bioglycerol as an Alternative Raw Material for Basic Organic Synthesis. *Russian Journal of Applied Chemistry, 90*(11), 1727-1737.

Ma, J., Sun, N., Zhang, X., Zhao, N., Xiao, F., Wei, W., & Sun, Y. (2009). A short review of catalysis for CO_2 conversion. *Catalysis Today, 148*(3), 221-231.

Ma'mun, S., & Svendsen, H. F. (2009). Solubility of N_2O in aqueous monoethanolamine and 2-(2-Aminoethyl-amino)ethanol solutions from 298 to 343 K. *Energy Procedia, 1*(1), 837-843.

Mallesham, B., Sudarsanam, P., & Reddy, B. M. (2014). Production of Biofuel Additives from Esterification and Acetalization of Bioglycerol over SnO_2-Based Solid Acids. *Industrial & engineering chemistry research, 53*(49), 18775-18785.

Mandal, B. P., Guha, M., Biswas, A. K., & Bandyopadhyay, S. S. (2001). Removal of carbon dioxide by absorption in mixed amines: modelling of absorption in aqueous MDEA/MEA and AMP/MEA solutions. *Chemical Engineering Science, 56*(21-22), 6217-6224.

Maneeintr, K., Phumkokrux, N., Boonpipattanapong, P., Assabumrungrat, S., & Charinpanitkul, T. (2017). Measurement of Solubility and Physical Properties of

Aqueous Solution of 2-(Diethylamino)ethanol for CO_2 Capture. *Energy Procedia, 142*, 3625-3630.

Mangas-Sánchez, J., & Adlercreutz, P. (2015). Highly efficient enzymatic biodiesel production promoted by particle-induced emulsification. *Biotechnology for Biofuels, 8*, 58.

Maul, P. R., Metcalfe, R., Pearce, J., Savage, D., & West, J. M. (2007). Performance assessments for the geological storage of carbon dioxide: Learning from the radioactive waste disposal experience. *International Journal of Greenhouse Gas Control, 1*(4), 444-455.

Mavroudi, M., Kaldis, S. P., & Sakellaropoulos, G. P. (2003). Reduction of CO_2 emissions by a membrane contacting process. *Fuel, 82*(15-17), 2153-2159.

McCann, N., Maeder, M., & Attalla, M. (2008). Simulation of Enthalpy and Capacity of CO_2 Absorption by Aqueous Amine Systems. *Industrial & engineering chemistry research, 47*(6), 2002-2009.

McGlashan, N. R., & Marquis, A. J. (2008). Simultaneous removal of CO_2, SO_2, and NO_x from flue gas by liquid phase dehumidification at cryogenic temperatures and low pressure. *Proceedings of the Institution of Mechanical Engineers Part a-Journal of Power and Energy, 222*(A1), 31-45.

Meerman, J. C., Hamborg, E. S., van Keulen, T., Ramirez, A., Turkenburg, W. C., & Faaij, A. P. C. (2012). Techno-economic assessment of CO_2 capture at steam methane reforming facilities using commercially available technology. *International Journal of Greenhouse Gas Control, 9*, 160-171.

Mehler, C., Klamt, A., & Peukert, W. (2002). Use of COSMO-RS for the prediction of adsorption equilibria. *AIChE journal, 48*(5), 1093-1099.

Melero, J. A., Iglesias, J., & Morales, G. (2009). Heterogeneous acid catalysts for biodiesel production: current status and future challenges. *Green Chemistry, 11*(9), 1285-1308.

Metz, B., Davidson, O., Coninck, H. d., Loos, M., & Meyer, L. (2005). *IPCC special report on carbon dioxide capture and storage*: Cambridge University Press, New York, NY (United States); Intergovernmental Panel on Climate Change, Geneva (Switzerland). Working Group III.

Mohanty, S., Banerjee, T., & Mohanty, K. (2010). Quantum Chemical Based Screening of Ionic Liquids for the Extraction of Phenol from Aqueous Solution. *Industrial & engineering chemistry research, 49*(6), 2916-2925.

Monteiro, J. G. M. S., & Svendsen, H. F. (2015). The N_2O analogy in the CO_2 capture context: Literature review and thermodynamic modelling considerations. *Chemical Engineering Science, 126*(Supplement C), 455-470.

Mores, P., Rodriguez, N., Scenna, N., & Mussati, S. (2012). CO_2 capture in power plants: Minimization of the investment and operating cost of the post-combustion process

using MEA aqueous solution. *International Journal of Greenhouse Gas Control, 10*, 148-163.

Mortazavi-Manesh, S., Satyro, M., & Marriott, R. A. (2011). A semi-empirical Henry's law expression for carbon dioxide dissolution in ionic liquids. *Fluid Phase Equilibria, 307*(2), 208-215.

Mu, T. C., Rarey, J., & Gmehling, J. (2007). Performance of COSMO-RS with sigma profiles from different model chemistries. *Industrial & engineering chemistry research, 46*(20), 6612-6629.

Murshed, S. M. S., & Estellé, P. (2017). A state of the art review on viscosity of nanofluids. *Renewable and Sustainable Energy Reviews, 76*, 1134-1152.

Mustapha, S., Okonkwo, P., & Waziri, S. (2013). Improvement of carbon dioxide absorption technology using conductor-like screening model for real solvents (COSMO-RS) method. *Journal of Environmental Chemistry and Ecotoxicology, 5*(4), 96-105.

Nookuea, W., Wang, F., Yang, J., Tan, Y., Li, H., Thorin, E., Yan, J. (2017). Viscosity Data of Aqueous MDEA–[Bmim][BF4] Solutions Within Carbon Capture Operating Conditions. *Energy Procedia, 105*, 4581-4586.

Norstebo, V. S., Midthun, K., & Bjorkvoll, T. (2012). Analysis of carbon capture in an industrial park-A case study. *International Journal of Greenhouse Gas Control, 9*, 52-61.

Notz, R., Tonnies, I., McCann, N., Scheffknecht, G., & Hasse, H. (2011). CO_2 Capture for Fossil Fuel-Fired Power Plants. *Chemical Engineering & Technology, 34*(2), 163-172.

Nunes, A. V. M., Carrera, G. V. S. M., Najdanovic-Visak, V., & Nunes da Ponte, M. (2013). Solubility of CO_2 in glycerol at high pressures. *Fluid Phase Equilibria, 358*(Supplement C), 105-107.

Nwaoha, C., Saiwan, C., Supap, T., Idem, R., Tontiwachwuthikul, P., Al-Marri, M. J., & Benamor, A. (2017). Regeneration Energy Analysis of Aqueous Tri–Solvent Blends Containing 2–Amino–2–Methyl–1–Propanol (AMP), Methyldiethanolamine (MDEA) and Diethylenetriamine (DETA) for Carbon Dioxide (CO_2) Capture. *Energy Procedia, 114*(Supplement C), 2039-2046.

Nwaoha, C., Saiwan, C., Tontiwachwuthikul, P., Supap, T., Rongwong, W., Idem, R., Benamor, A. (2016). Carbon dioxide (CO_2) capture: Absorption-desorption capabilities of 2-amino-2-methyl-1-propanol (AMP), piperazine (PZ) and monoethanolamine (MEA) tri-solvent blends. *Journal of Natural Gas Science and Engineering, 33*, 742-750.

Olajire, A. A. (2010). CO_2 capture and separation technologies for end-of-pipe applications – A review. *Energy, 35*(6), 2610-2628.

Oner, C., & Altun, S. (2009). Biodiesel production from inedible animal tallow and an experimental investigation of its use as alternative fuel in a direct injection diesel engine. *Applied Energy, 86*(10), 2114-2120.

Palomar, J., Ferro, V. R., Torrecilla, J. S., & Rodriguez, F. (2007). Density and molar volume predictions using COSMO-RS for ionic liquids. An approach to solvent design. *Industrial & engineering chemistry research, 46*(18), 6041-6048.

Palomar, J., Torrecilla, J. S., Ferro, V. R., & Rodriguez, F. (2008). Development of an a priori ionic liquid design tool. 1. Integration of a novel COSMO-RS molecular descriptor on neural networks. *Industrial & engineering chemistry research, 47*(13), 4523-4532.

Pan, Z. J., & Connell, L. D. (2009). Comparison of adsorption models in reservoir simulation of enhanced coalbed methane recovery and CO_2 sequestration in coal. *International Journal of Greenhouse Gas Control, 3*(1), 77-89.

Park, J., Park, J. S., Kim, H. P., Kim, J. S., Kim, S. C., Choi, J. G., Park, H. S. (2007). NO emission behavior in oxy-fuel combustion recirculated with carbon dioxide. *Energy & Fuels, 21*(1), 121-129.

Patil, Y. P., Tambade, P. J., Jagtap, S. R., & Bhanage, B. M. (2010). Carbon dioxide: a renewable feedstock for the synthesis of fine and bulk chemicals. *Frontiers of Chemical Engineering in China, 4*(2), 213-235.

Pazuki, G. R., Pahlevanzadeh, H., & Mohseni Ahooei, A. (2006). Solubility of CO_2 in aqueous ammonia solution at low temperature. *Calphad, 30*(1), 27-32.

Penttilä, A., Dell'Era, C., Uusi-Kyyny, P., & Alopaeus, V. (2011). The Henry's law constant of N2O and CO2 in aqueous binary and ternary amine solutions (MEA, DEA, DIPA, MDEA, and AMP). *Fluid Phase Equilibria, 311*, 59-66.

Pires, J. C. M., Martins, F. G., Alvim-Ferraz, M. C. M., & Simoes, M. (2011). Recent developments on carbon capture and storage: An overview. *Chemical Engineering Research & Design, 89*(9), 1446-1460.

Powell, C. E., & Qiao, G. G. (2006). Polymeric CO_2/N_2 gas separation membranes for the capture of carbon dioxide from power plant flue gases. *Journal of Membrane Science, 279*(1-2), 1-49.

Putnam, R., Taylor, R., Klamt, A., Eckert, F., & Schiller, M. (2003). Prediction of infinite dilution activity coefficients using COSMO-RS. *Industrial & engineering chemistry research, 42*(15), 3635-3641.

Puxty, G., Rowland, R., Allport, A., Yang, Q., Bown, M., Burns, R., Attalla, M. (2009). Carbon Dioxide Postcombustion Capture: A Novel Screening Study of the Carbon Dioxide Absorption Performance of 76 Amines. *Environmental Science & Technology, 43*(16), 6427-6433.

Puxty, G., Wei, S. C.-C., Feron, P., Meuleman, E., Beyad, Y., Burns, R., & Maeder, M. (2014). A Novel Process Concept for the Capture of CO_2 and SO_2 Using a Single Solvent and Column. *Energy Procedia, 63*, 703-714.

Ramazani, R., Samsami, A., Jahanmiri, A., Van der Bruggen, B., & Mazinani, S. (2016). Characterization of monoethanolamine plus potassium lysinate blend solution as a new chemical absorbent for CO_2 capture. *International Journal of Greenhouse Gas Control, 51*, 29-35.

Ramdin, M., de Loos, T. W., & Vlugt, T. J. H. (2012). State-of-the-Art of CO_2 Capture with Ionic Liquids. *Industrial & engineering chemistry research, 51*(24), 8149-8177.

Ramesh, K., Murthy, S. N., Karnakar, K., Nageswar, Y. V. D., Vijayalakhshmi, K., Devi, B., & Prasad, R. B. N. (2012). A novel bioglycerol-based recyclable carbon catalyst for an efficient one-pot synthesis of highly substituted imidazoles. *Tetrahedron Letters, 53*(9), 1126-1129.

Ravagnani, A., Ligero, E. L., & Suslick, S. B. (2009). CO_2 sequestration through enhanced oil recovery in a mature oil field. *Journal of Petroleum Science and Engineering, 65*(3-4), 129-138.

Rebolledo-Libreros, M. E., & Trejo, A. (2006). Density and Viscosity of Aqueous Blends of Three Alkanolamines: N-Methyldiethanolamine, Diethanolamine, and 2-Amino-2-methyl-1-propanol in the Range of (303 to 343) K. *Journal of Chemical & Engineering Data, 51*(2), 702-707.

Rivera-Tinoco, R., & Bouallou, C. (2010). Comparison of absorption rates and absorption capacity of ammonia solvents with MEA and MDEA aqueous blends for CO_2 capture. *Journal of Cleaner Production, 18*(9), 875-880.

Romano, M. C., Chiesa, P., & Lozza, G. (2010). Pre-combustion CO_2 capture from natural gas power plants, with ATR and MDEA processes. *International Journal of Greenhouse Gas Control, 4*(5), 785-797.

Rufford, T. E., Smart, S., Watson, G. C. Y., Graham, B. F., Boxall, J., Diniz da Costa, J. C., & May, E. F. (2012). The removal of CO_2 and N_2 from natural gas: A review of conventional and emerging process technologies. *Journal of Petroleum Science and Engineering, 94-95*, 123-154.

Saha, A. K., Bandyopadhyay, S. S., & Biswas, A. K. (1993). Solubility and diffusivity of nitrous oxide and carbon dioxide in aqueous solutions of 2-amino-2-methyl-1-propanol. *Journal of Chemical and Engineering Data, 38*(1), 78-82.

Scheffknecht, G., Al-Makhadmeh, L., Schnell, U., & Maier, J. (2011). Oxy-fuel coal combustion-A review of the current state-of-the-art. *International Journal of Greenhouse Gas Control, 5*, S16-S35.

Schreiber, A., Zapp, P., & Kuckshinrichs, W. (2009). Environmental assessment of German electricity generation from coal-fired power plants with amine-based carbon capture. *International Journal of Life Cycle Assessment, 14*(6), 547-559.

Schurer, G., & Peukert, W. (2005). Prediction of thermodynamic properties from pure compound information: Characterization of fullerenes. *Applied Surface Science, 252*(3), 512-518.

Shamiri, A., Shafeeyan, M. S., Tee, H. C., Leo, C. Y., Aroua, M. K., & Aghamohammadi, N. (2016). Absorption of CO_2 into aqueous mixtures of glycerol and monoethanolamine. *Journal of Natural Gas Science and Engineering, 35*(Part A), 605-613.

Shen, K. P., & Li, M. H. (1992). Solubility of Carbon Dioxide in Aqueous Mixtures of Monoethanolamine with Methyldiethanolamine. *Journal of Chemical and Engineering Data, 37*(1), 96-100.

Shen, K. P., & Li, M. H. (1992). Solubility of carbon dioxide in aqueous mixtures of monoethanolamine with methyldiethanolamine. *Journal of Chemical and Engineering Data, 37*(1), 96-100.

Shiflett, M. B., & Yokozeki, A. (2005). Solubilities and Diffusivities of Carbon Dioxide in Ionic Liquids: [bmim][PF6] and [bmim][BF4]. *Industrial & engineering chemistry research, 44*(12), 4453-4464.

Soares, J. L., Oberziner, A. L. B., Jose, H. J., Rodrigues, A. E., & Moreira, R. (2007). Carbon dioxide adsorption in Brazilian coals. *Energy & Fuels, 21*(1), 209-215.

Sobrino, M., Concepcion, E. I., Gomez-Hernandez, A., Martin, M. C., & Segovia, J. J. (2016). Viscosity and density measurements of aqueous amines at high pressures: MDEA-water and MEA-water mixtures for CO_2 capture. *Journal of Chemical Thermodynamics, 98*, 231-241.

Sumon, K. Z., & Henni, A. (2011). Ionic liquids for CO_2 capture using COSMO-RS: Effect of structure, properties and molecular interactions on solubility and selectivity. *Fluid Phase Equilibria, 310*(1-2), 39-55.

Supekar, S. D., & Skerlos, S. J. (2014). Market-Driven Emissions from Recovery of Carbon Dioxide Gas. *Environmental Science & Technology, 48*(24), 14615-14623.

Svendsen, H. F., Hessen, E. T., & Mejdell, T. (2011). Carbon dioxide capture by absorption, challenges and possibilities. *Chemical Engineering Journal, 171*(3), 718-724.

Takht Ravanchi, M., & Sahebdelfar, S. (2014). Carbon dioxide capture and utilization in petrochemical industry: potentials and challenges. *Applied Petrochemical Research, 4*(1), 63-77.

Thormann, M., Klamt, A., Hornig, M., & Almstetter, M. (2006). COSMO s im: Bioisosteric Similarity Based on COSMO-RS σ Profiles. *Journal of chemical information and modeling, 46*(3), 1040-1053.

Tong, D., Trusler, J. P. M., Maitland, G. C., Gibbins, J., & Fennell, P. S. (2012). Solubility of carbon dioxide in aqueous solution of monoethanolamine or 2-amino-2-methyl-1-propanol: Experimental measurements and modelling. *International Journal of Greenhouse Gas Control, 6*, 37-47.

Tontiwachwuthikul, P., Meisen, A., & Lim, C. J. (1991). Solubility of CO_2 In 2-Amino-2-Methyl-1-Propanol Solutions. *Journal of Chemical and Engineering Data, 36*(1), 130-133.

Torralba-Calleja, E., Skinner, J., & Gutiérrez-Tauste, D. (2013). CO_2 Capture in Ionic Liquids: A Review of Solubilities and Experimental Methods. *Journal of Chemistry, 2013*.

Versteeg, G. F., & Van Swaalj, W. (1988). Solubility and diffusivity of acid gases (carbon dioxide, nitrous oxide) in aqueous alkanolamine solutions. *Journal of Chemical and Engineering Data, 33*(1), 29-34.

Vijay, M., Prasad, R. B. N., & Devi, B. (2013). Bioglycerol-based Sulphonic Acid Functionalized Carbon: An Efficient and Recyclable, Solid Acid Catalyst for the Regioselective Azidolysis of Epoxides in Aqueous Acetonitrile. *Journal of Oleo Science, 62*(10), 849-855.

Wambach, J., Baiker, A., & Wokaun, A. (1999). CO_2 hydrogenation over metal/zirconia catalysts. *Physical Chemistry Chemical Physics, 1*(22), 5071-5080.

Wang, C. A., Zhang, X. M., Liu, Y. H., & Che, D. F. (2012). Pyrolysis and combustion characteristics of coals in oxyfuel combustion. *Applied Energy, 97*, 264-273.

Yadav, G. D., & Chandan, P. A. (2014). A green process for glycerol valorization to glycerol carbonate over heterogeneous hydrotalcite catalyst. *Catalysis Today, 237*, 47-53.

Yamada, H., Shimizu, S., Okabe, H., Matsuzaki, Y., Chowdhury, F. A., & Fujioka, Y. (2010). Prediction of the Basicity of Aqueous Amine Solutions and the Species Distribution in the Amine-H_2O-CO_2 System Using the COSMO-RS Method. *Industrial & engineering chemistry research, 49*(5), 2449-2455.

Yan, S. P., He, Q. Y., Ai, P., Wang, Y. Y., & Zhang, Y. L. (2013). Regeneration performance of concentrated CO_2-rich alkanolamine solvents: The first step study of a novel concept for reducing regeneration heat consumption by using concentration swing absorption technology. *Chemical Engineering and Processing, 70*, 86-94.

Yang, Q., Puxty, G., James, S., Bown, M., Feron, P., & Conway, W. (2016). Toward Intelligent CO_2 Capture Solvent Design through Experimental Solvent Development and Amine Synthesis. *Energy & Fuels, 30*(9), 7503-7510.

Yeh, A. C., & Bai, H. L. (1999). Comparison of ammonia and monoethanolamine solvents to reduce CO_2 greenhouse gas emissions. *Science of the Total Environment, 228*(2-3), 121-133.

Yu, H. (2018). Recent developments in aqueous ammonia-based post-combustion CO_2 capture technologies. *Chinese Journal of Chemical Engineering, 26*(11), 2255-2265.

Yu, Y. S., Li, Y., Lu, H. F., Yan, L. W., & Zhang, Z. X. (2011). Performance improvement for chemical absorption of CO_2 by global field synergy optimization. *International Journal of Greenhouse Gas Control, 5*(4), 649-658.

Yuan, Y., & Rochelle, G. T. (2018). CO_2 absorption rate in semi-aqueous monoethanolamine. *Chemical Engineering Science, 182*, 56-66.

Zanganeh, K. E., & Shafeen, A. (2007). A novel process integration, optimization and design approach for large-scale implementation of oxy-fired coal power plants with CO_2 capture. *International Journal of Greenhouse Gas Control, 1*(1), 47-54.

Zareie-kordshouli, F., Lashani-zadehgan, A., & Darvishi, P. (2016). Comparative evaluation of CO_2 capture from flue gas by Emim Ac ionic liquid, aqueous potassium carbonate (without activator) and MEA solutions in a packed column. *International Journal of Greenhouse Gas Control, 52*, 305-318.

Zhang, P., Shi, Y., Wei, J., Zhao, W., & Ye, Q. (2008). Regeneration of 2-amino-2-methyl-1-propanol used for carbon dioxide absorption. *Journal of Environmental Sciences, 20*(1), 39-44.

Zhang, X. P., Zhang, X. C., Dong, H. F., Zhao, Z. J., Zhang, S. J., & Huang, Y. (2012). Carbon capture with ionic liquids: overview and progress. *Energy & Environmental Science, 5*(5), 6668-6681.

Zhao, B. T., Su, Y. X., Tao, W. W., Li, L. L., & Peng, Y. C. (2012). Post-combustion CO_2 capture by aqueous ammonia: A state-of-the-art review. *International Journal of Greenhouse Gas Control, 9*, 355-371.

Zhao, Y. S., Huang, Y., Zhang, X. P., & Zhang, S. J. (2015). A quantitative prediction of the viscosity of ionic liquids using S sigma-profile molecular descriptors. *Physical Chemistry Chemical Physics, 17*(5), 3761-3767.

LIST OF PUBLICATIONS AND PAPERS PRESENTED

1. Abdul Samat, N. F. N., Yusoff, R. B., Aroua, M. K., Ramalingam, A., & Kassim, M. A. (2019). Solubility of CO_2 in aqueous 2‑amino‑1, 3‑propanediol (Serinol) at elevated pressures. *Journal of Molecular Liquids, 277*, 207-216.